Order Number 9510711

Boron acid complexation reactions: Equilibria, thermodynamics and metal ion binding

Ricatto, Pascal John, Ph.D.

City University of New York, 1994

U·M·I
300 N. Zeeb Rd.
Ann Arbor, MI 48106

BORON ACID COMPLEXATION REACTIONS: EQUILIBRIA, THERMODYNAMICS AND METAL ION BINDING

by

Pascal John Ricatto

A Dissertation submitted to the Graduate Faculty in Chemistry in partial fulfillment of the requirements for the degree of Doctor of Philosophy, The City University of New York.

1994

This manuscript has been read and accepted for the Graduate Faculty in Chemistry in satisfaction of the dissertation requirement for the degree of Doctor of Philosophy.

August 30, 1994
Date

Chair of Examining Committee

August 30, 1994
Date

Executive Officer

Supervisory Committee

The City University of New York

1994

Abstract

BORON ACID COMPLEXATION REACTIONS:
EQUILIBRIA, THERMODYNAMICS AND METAL ION BINDING

by

Pascal John Ricatto

Adviser: Professor Richard Pizer

The application of both ^{1}H and ^{11}B NMR to the study of boron acid complexation reactions is demonstrated in this work. Variable temperature FTNMR is shown to be a reliable technique for the determination of thermodynamic parameters ($\Delta H°$ and $\Delta S°$) for the complexation reactions of borate with a wide range of ligands. Results for the reactions of aliphatic diols with various borate ions show that all of these reactions are quite similar. The reactions are all exothermic with an average value of $\Delta H° \sim -20$ kJ / mol. All of the entropy changes are quite negative ($\Delta S° \sim -60$ J / mol K) and this can be attributed to the loss of ligand configurational entropy on complexation.

Results for reactions of borate ion with α-hydroxy carboxylic acids and dicarboxylic acids show that the large increase in K_1 for α-hydroxy carboxylic acids compared with K_1 for the reaction of borate with diols is entirely due to a much more favorable $\Delta H°$. The second complexation reaction here is emphatically different from the first. K_2 is much smaller than K_1 and extremely large differences in both $\Delta H°$ and $\Delta S°$ are observed.

The results for these systems as well as those presented for the

formation of mixed ligand complexes show the important effect the first ligand has on subsequent bis complex formation. Many of these results can be explained by the significant differences found in boron - oxygen bonds of the various borates as determined by AM1 calculations.

The synergic binding of both Ca^{2+} and Sr^{2+} is demonstrated in the ternary M^{2+} / borate / tartrate system. Ca^{2+} and Sr^{2+} show a large preference for coordination to 1:2 borotartrate complexes (BT_2^{5-}) compared with 1:1 complexes (BT^{3-}) or free tartrate (T^{2-}). Stability constants for these synergic interactions were determined for both the BT_2^{5-} (*l* - tartrate) and BT_2^{5-} (*meso* - tartrate) complexes. On the other hand, Mg^{2+} binds preferentially to free tartrate, T^{2-}, and shows little if any interaction with the borotartrate complex ions. A terdentate metal ion binding site on the BT_2^{5-} complex is proposed which is consistent with both our experimental results and molecular mechanics (MM2) calculations.

Dedication

This thesis is dedicated to my father and mother, John and Carol Ricatto, who worked so hard in their lives so that my sister and I would not have to.

Acknowledgment

I would like to express my gratitude to Professor Richard Pizer who served as my mentor for both my Masters and Ph.D. research. It was his friendship and guidance that led me to pursue my doctorate. Without his support, I certainly would not have undertaken such a challenge. Not only is he is an extremely competent scientist, more importantly, he is truly a man of his word.

I would like to thank Professors Thomas Strekas and Gary Mennitt for their interest in this research and for serving on my Thesis Committee. I would also like to acknowledge Professors Gary Mennitt and Herman Zieger for their expert advice in the area of NMR spectroscopy. My deepest thanks to the entire staff of the Chemistry Department. I have always felt they were behind me. I would like to thank Professor B.J. Haske for turning me on to chemistry as an undergraduate at Dowling College.

Special thanks to Dr. Cherryl Tihal for her patience and guidance during my frustrating early days in the laboratory. She was like a second mentor to me. I would also like to thank Sal Atzeni, Shiming Wo, Rosemary Mollica, Joanne Fromkin and Dr. Warren Hirsch for their friendship and support.

I am most grateful to all of my family and friends for their understanding and support throughout my studies (I am currently finishing 23rd grade). Special thanks to my sister, Pattie, who has always been in my corner.

Finally, no one deserves more credit for this Thesis coming to completion than my wife Pam whose love and incredible patience has enabled me to focus on this project. She is the most unselfish person I know. Besides, without her I would still be typing!!

Contents

List of Tables

List of Figures

CHAPTER 1

Introduction to Boron Acid Chemistry

1.1 Historical Perspective

As early as 1835 Biot discovered that boric acid ($B(OH)_3$) altered the optical rotation of tartaric acid solutions. In 1842, Biot [1] reported that a solution of boric acid became acidic to litmus upon the addition of sugars. These experimental observations led Thomson [2] to study the interaction of boric acid and hydroxy compounds quantitatively using phenolphthalein as an acid-base indicator. Magnanini [3-5] established that solutions of boric acid and polyhydroxy compounds exhibit conductivities greater than those expected for the sum of the conductivities of the individual solutions. It was not until 1898, however, that van't Hoff [6] suggested that these unusual characteristics of boric acid / polyhydroxy compound solutions might be explained by the formation of a complex between the two species. This was the first structural interpretation which was offered for the observed experimental results.

In the early part of this century Boeseken [7-14] and coworkers studied the interaction of boric acid with a variety of structural and geometric isomers of polyhydroxybenzenes, cyclic diols and sugars by conductivity measurements. In all cases, only ligands with an appropriately oriented diol linkage produced an increase in the conductivity of the solution. Boeseken concluded that the hydroxyl groups must be adjacent and cis in order for coordination to boric acid to occur. These results found widespread application in the determination of the geometric orientation of hydroxyl groups in carbohydrates as well as to distinguish between "α" and "β" isomers of sugars [8,14].

Remarkable as it may seem, Hermans [15] proposed the scheme shown below for the reaction of boric acid with a 1,2 diol based only on the changes in acidity, optical rotation and conductivity already mentioned. The structures of the complexes { (1:1) and (1:2) } are shown to be tetrahedral and this was later proven to be correct.

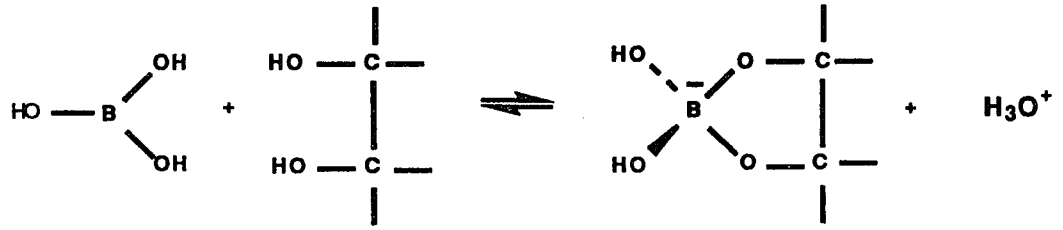

(1:1)

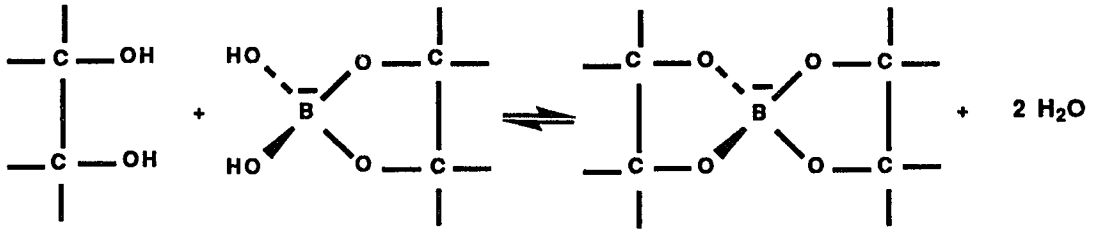

(1:2)

Additional evidence for a tetrahedral boron center in these complexes was found in 1942 when Boeseken [14] showed that α - hydroxycarboxylic acids also caused decreases in pH when added to solutions of boric acid. Boeseken concluded that formation of the complex was accompanied by the release of a proton which could only occur if the coordination number of the boron center was increased from three (in boric acid) to four (in the tetrahedral complex).

Boeseken and Hermans [15] isolated and characterized crystals precipitated from a solution of boric acid and catechol. The isolated compound was characterized correctly as the potassium salt of a monovalent polyatomic anion having a four-coordinate boron atom connected to two fixed catechol ligands via four boron - oxygen bonds. Meulenhoff [16] isolated and characterized a similar bis complex from a solution of boric acid and salicylic acid using an optically active base. Meulenhoff then used the optical activity of the 1:2 complex of boric acid with salicylic acid to prove that the boron atom must be a chiral center and, therefore, necessarily of tetrahedral rather than trigonal geometry.

Despite all the evidence presented in the literature, the structures of the borate ion and the boric acid / polyol complexes were not determined directly until the advent of modern spectroscopic techniques. Edwards [17] conducted the first Raman study of the structure of the aqueous borate ion. He compared the Raman spectrum of borate with the I.R. spectrum of crystalline teepelite, a mineral which is known to contain a boron tetrahedrally coordinated to four oxygen atoms from X-ray crystallographic studies. He found that the number, shapes, and positions of the bands in the Raman spectrum of the boronate mineral were in good agreement with those of the aqueous borate ion. The Raman spectrum of the aqueous borate ion also contains the correct number of active lines expected for a tetrahedral ion based on group theory, and the spectrum also resembles that of the tetrahedral BF_4^- ion.

Larsson and Nunziata [18,19] used the decrease in I.R. stretching frequency in boric acid complexes compared with free boric acid to show the decrease in bond order upon conversion from trigonal boric acid to the tetrahedral complex. Raman studies of boric acid complexes conducted by

Oertel [20] also verify that the complex is a chelate system with a tetrahedrally coordinated boron center.

The thermodynamics of ionization of boric acid was studied as early as 1912 by Arrhenius. In a comparison of the free energy and enthalpy of ionization of a series of acids, Arrhenius found boric acid was exceptional in its behavior. He states that " ... boric acid ... behaves quite differently from other acids" [21].

Two other important thermodynamic studies should be mentioned here. Manov, Delollis and Acree [22] reported the ionization constant and thermodynamic parameters for boric acid at 298K and $\mu = 0$. The results are as follows: $pK_a = 9.2$, $\Delta H° = +14$ kJ / mol and $\Delta S° = -13$ J / mol K. Edwards and Sederstrom [23] reported the ionization constant, $\Delta H°$ and $\Delta S°$ for the ionization of phenylboronic acid under the same conditions; $pK_a = 8.84$, $\Delta H° = +7.9$ kJ / mol and $\Delta S° = -14$ J / mol K. Edwards then used the unusual negative entropy values found for boric acid and phenylboronic acid as further evidence for the expansion of the coordination number upon ionization for the boron acids. He compared the entropy of ionization of the two boron acids with the value given by Pitzer [24] for the entropy of ionization of neutral Bronsted-Lowry acids and found the entropies for the boron acids to be much more negative.Using all the evidence described above, Edwards [23] was the first to conclude that boric acid was not a Bronsted-Lowry acid, but rather a Lewis acid reacting as described in the next section.

1.2 General Characteristics of Boron Acids

Boron acids ($RB(OH)_2$) are weak monobasic acids which act not as proton donors, but, rather, as Lewis acids, accepting hydroxide ions in aqueous solution. The vacant p orbital on the trigonal (sp^2) boron center accepts electrons to form a coordinate covalent bond with the electron donor (OH^-). This reaction is best illustrated using the simplest unsubstituted boron acid, boric acid ($B(OH)_3$), as shown below:

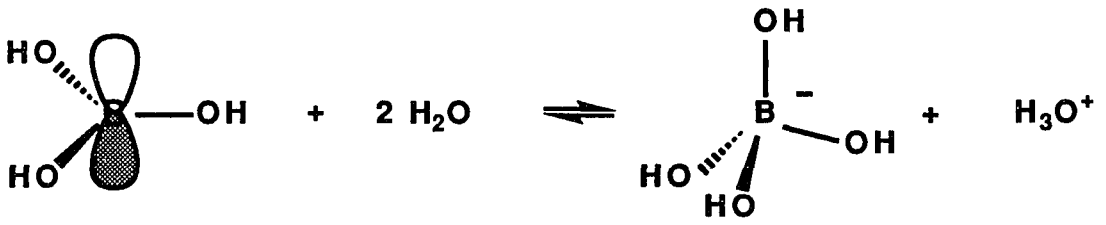

The reaction products are the tetrahedral (sp^3) borate anion ($B(OH)_4^-$) and hydronium ion (H_3O^+). The three coordinate boron center in the unionized boron acid has a formal charge of zero, while the four coordinate boron center in borate has a formal charge of negative one. The reaction thus leads to an expansion of the coordination number from three to four as well as a net decrease in formal charge on the boron center.

Boron acids then decrease the pH of aqueous solutions by addition of hydroxide ion. Variation of the substituent groups bonded to boron

(CH_3 , ϕ ...) can change the acidity of the substituted boron acid relative to that of boric acid. This idea can be illustrated nicely using the three boron acids most frequently used in this laboratory - methylboronic acid ($CH_3B(OH)_2$), phenylboronic acid ($\phi B(OH)_2$) and boric acid ($B(OH)_3$). Methylboronic acid is less acidic than boric acid while phenylboronic acid is more acidic than boric acid. One theory proposed to explain these variations stems from the existence of backbonding [25] in the unionized form of the various boron acids. Backbonding stabilizes the trigonal boron compound but is necessarily lost in the tetrahedral anion. If a substituent group causes an increase in backbonding, it stabilizes the trigonal acid form. If a substituent group causes a decrease in backbonding, it destablizes the trigonal acid and makes the compound more acidic. The I.R. and Raman studies previously discussed [18 -20] offer some experimental verification of these ideas. Furthermore, NMR studies [25,26] along with force constant calculations [25] indicate the presence of multiple bonding in trigonal boron acids which also helps to validate the proposed backbonding interaction.

Both trigonal boron acids ($RB(OH)_2$) and their tetrahedral conjugate bases ($RB(OH)_3^-$) can react with suitable bidentate oxygen donor ligands such as polyols, α - hydroxy carboxylic acids, dicarboxylic acids or 1,2-benzene diols to form the same 1:1 cyclic, anionic product (BL^-) shown schematically in Figure 1.1. Formation of the 1:1 complex (BL^-) from a trigonal boron acid (HB) is both an addition and a substitution reaction which occurs with a change in coordination number (from 3 to 4), hybridization (from sp^2 to sp^3) and formal charge (from 0 to -1) on the boron center. Formation of the 1:1 complex

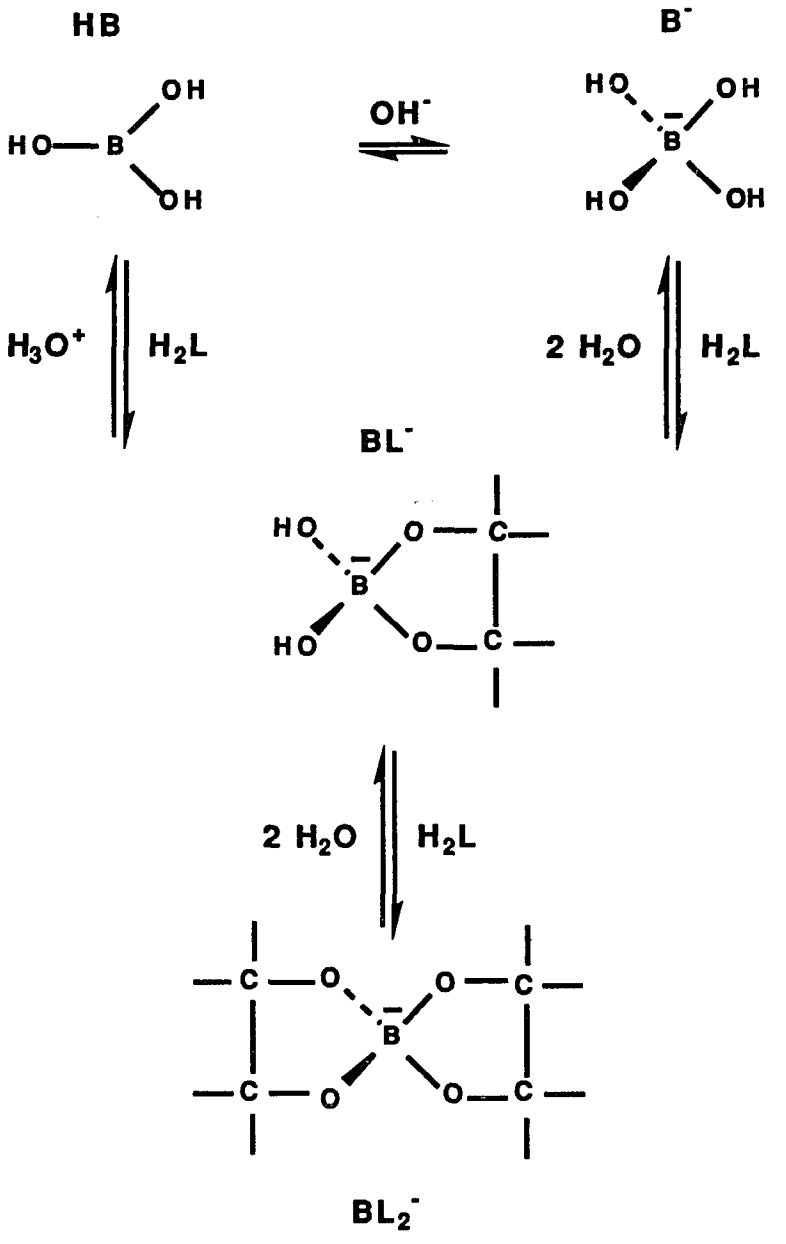

Figure 1.1 : The reaction of boric acid (HB) and its conjugate base borate (B^-) with a fully protonated ligand (H_2L) to produce the same 1:1 complex (BL^-). The 1:1 complex can then further react with a second molecule of ligand to form the 1:2 complex (BL_2^-).

(BL^-) from the tetrahedral borate ion (B^-) is a substitution reaction in which the bidentate ligand replaces two hydroxyl groups on the boron center, releasing two water molecules. This condensation reaction occurs with no change in coordination number, hybridization or formal charge. These two fundamentally different complex formation reactions are, however, coupled thermodynamically through the ionization reaction of the boron acid, and stability constants and thermodynamic parameters can be interconverted from one form of the reaction to the other simply by using the appropriate Born-Haber cycle.

Although unidentate complexes (such as the one shown below) can form, they are very unstable and rapidly hydrolyze back to starting materials if they do not undergo ring closure to form bidentate complexes stabilized by the chelate effect [27].

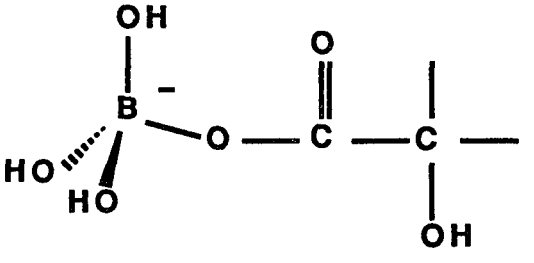

1:1 bidentate complexes (BL^-) of boric acid can undergo reaction with a second ligand (H_2L) to form the 1:2 complex (BL_2^-) as shown in Figure

1.1(bottom). The formation of the 1:2 complex (BL_2^-) from the 1:1 complex is strictly a substitution reaction in which the bidentate ligand replaces the two remaining hydroxyl groups on the boron center, releasing two water molecules. Just as in formation of the 1:1 complex (BL^-) from borate (B^-) discussed above, there is no change in the coordination number, hybridization or formal charge on the boron center in this condensation process.

Boric acid is necessarily the only boron acid capable of forming 1:2 complexes because it is the only acid with four coordination sites available for ligand bond formation. Substituted boron acids have one of their coordination sites blocked, making it impossible for the 1:1 complex to go on to form a 1:2 complex.

1.3 Kinetics of Boron Acid Complex Reactions

Kustin and Pizer [28] carried out the first kinetic investigation of boron acid complexation reactions with bidentate chelating ligands. The reactions of boric acid with tartaric acid and the tartrate anion were studied in acidic solution using the temperature - jump technique. In this work only the formation of the 1:1 complex was studied and it was proposed that complexation occurred via attack of ligand oxygen donor atom on the empty p orbital of the boron center followed by rapid ring closure with the loss of a water molecule. This study also showed the importance of ligand acidity and donor atom protonation on reaction rate. Pizer et al. also studied the reactions of phenylboronic acid with oxalic acid [29], malonic acid [30] and lactic acid [31]. The results for these systems further demonstrated the importance of ligand acidity as well as donor atom protonation on reaction rate. A comparison of rates between the oxalic acid system and the malonic acid system shows the oxalic acid system to be appreciably faster, showing that chelate ring size is another important factor which affects relative rate constants [30]. In this continuing investigation Babcock and Pizer conducted a comprehensive study [32] of the dynamics of boron acid complexation reactions in which a variety of bidentate chelating ligands were studied with a series of boron acids under the same experimental conditions in order to determine what role substituent effects play on the kinetics and stability constants of 1:1 boron acid - ligand complexes. The main conclusion of this work is that the reactions of trigonal boron acids with fully protonated ligands are characterized by a mechanism that involves proton transfer in a rate limiting ring closure step. Correlations of rate constants with acidities of the boron acid and ligand are direct consequences of such a

mechanism. Included in this treatise is the study of 1:1 complex formation of boron acids with catechol and subsitituted catechols [33] studied in this laboratory a few years earlier.

The only temperature - jump study which includes both the formation of the 1:1 (BL^-) and 1:2 (BL_2^-) complexes was conducted by Pizer and Selzer [34]. This study of the boric acid/lactic acid system showed that the forward rate constant for the formation of the 1:2 complex from the 1:1 was three orders of magnitude greater than that for the formation of the 1:1 complex from trigonal boric acid. This suggests that four-coordinate borates are more labile toward substitution than trigonal boron species. This result is further supported by the fact that *meta* -nitrophenylboronate anion reacts faster than *meta* - nitrophenylboronic acid [32].

These studies laid the groundwork for an excellent and comprehensive investigation of the reaction of substituted boron acids with polyols in basic solution carried out by Pizer and Tihal [35,36]. By studying the complexation reactions of polyols in basic medium, Pizer and Tihal were able to show that trigonal boron acids are quite unreactive with polyols, making the principal kinetic pathway to complex formation the reaction between the four-coordinate boronate anion ($RB(OH)_3^-$) and fully protonated ligand (H_2L). The ratio of forward rate constants for the reactions of $RB(OH)_3^-$ and $RB(OH)_2$ with polyols may be > 10^6 for the methylboronic acid / poloyol systems. This study also shows the importance of proton transfer as discussed in terms of an associative transition state between the four - coordinate boronate and the fully protonated polyol.

The result of these comprehensive studies demonstrates the influence of

ligand donor atom protonation, ligand geometry and orientation, chelate ring size and the importance of the acidities of both boron acid and ligand on the dynamics of complex formation. The conclusions arrived at are important not only for boron acid complexation reactions but also for the more general class of complexation reactions of polyoxoanions.

1.4 The Determination of Stability Constants and Thermodynamic Parameters

Since this thesis primarily deals with questions of stability constant determination, thermodynamics and the relationship between thermodynamic stability and structure, a comprehensive review of the literature important to these areas is contained in this section.

Although the early contributions of Antikainen [37] can not be ignored, the first quantitative determination of stability constants for both the formation of the 1:1 and 1:2 borate complexes of polyols was made by Edwards and coworkers [38]. Edwards used a pH titration method to determine stability constants for the complexation reactions between borate and a series of ten polyols and sugars. This work is the first to identify borate as the reactive species in complex formation with polyols at high pH. Edwards et al. determined stability constants for the formation of both complexes using the equilibria:

$$B^- + P \rightleftharpoons BP^- + 2\,H_2O$$

$$K_1 = \frac{[BP^-]}{[B^-]\,[P]}$$

$$BP^- + P \rightleftharpoons BP_2^- + 2\,H_2O$$

$$K_2 = \frac{[BP_2^-]}{[BP^-]\,[P]}$$

Quite remarkably, the values determined in this study have stood up very well, considering the large number of re-determinations (Table 1.1) using increasingly more sophisticated techniques over the years. One example of this is a comparison of K_1 and K_2 from Edwards pH method for the borate / 1,2-ethanediol system which gives values of 1.85 and 0.1, respectively, with the values of 1.4 and 0.18 determined by ^{11}B and ^{1}H NMR in this laboratory [39 - 40] over thirty years later.

Because of the large number of determinations of stability constants in these systems, the results are most simply presented using a tabular format. Table 1.1 gives the system, K_1 and K_2 values, temperature, ionic strength and the reference for systems which are important to our work. K_1 represents the reaction of borate (B^-) with fully protonated ligand (H_2L) to form the 1:1 complex (BL^-) and K_2 represents the subsequent reaction of the 1:1 complex (BL^-) with a second molecule of H_2L to form the 1:2 complex (BL_2^-) as shown below:

$$B^- + H_2L \rightleftharpoons BL^- + 2\,H_2O \qquad K_1$$

$$BL^- + H_2L \rightleftharpoons BL_2^- + 2\,H_2O \qquad K_2$$

Table 1.1 shows that the largest number of studies has been conducted for the simple diols, 1,2-ethanediol and 1,2-propanediol. The lack of agreement among different workers in the field as well as between different studies by the same group [45,46] shows the obvious need for a systematic determination of stability constants and thermodynamic parameters (ΔG°, ΔH° and ΔS°) for these systems at constant temperature, ionic strength and solvent composition (% D_2O).

Table 1.1: Stability constants for various borate complexation reactions as compiled from the literature.

System	K_1	K_2	T (°C)	μ (M)	method	Reference
borate / 1,2-ethanediol	1.85	0.10	25	0.08	pH-change	38
	2.15	1.15	25	~0.1	"	41
	1.78	0.12	25	1.0	"	42
	1.82	0.18	25	0.006	"	43
	1.00	0.1	33	0.8	^{11}B NMR	44
	0.74	0.29	25	0.6	"	45
	3.0	0.40	25	0.25	"	46
	1.0	0.16	25	0.10	"	47,51
borate / 1,2-propanediol	3.10	1.60	25	0.08	pH-change	38
	4.05	3.85	25	~0.1	"	41
	3.2	1.48	25	0.006	"	43
	1.8	1.5	33	0.8	^{11}B NMR	44
	1.8	1.5	25	0.10	"	47
	2.2	0.55	25	0.6	"	45
	4.7	0.80	25	0.25	"	46
	4.4	0.57	25	3.0	"	48
borate / 1,2-benzenediol	9.38×10^3	1.95	25	0.1	pH-change	49,50
	1.05×10^4	---	25	0.1	"	33
borate / oxalic acid	1.7×10^8	~ 0	25	3.0	^{11}B NMR	51
borate / glycolic acid	1.4×10^5	20	25	3.0	^{11}B NMR	51
borate / lactic acid	1.71×10^6	66	25	0.1	pH-change	34
borate / *d* - tartrate *(2,3 diol linkage)*	11	1.7	25	0.1	^{11}B NMR	47
borate / *meso* - tartrate *(2,3 diol linkage)*	2.2	0.36	25	0.1	^{11}B NMR	47

Since the number of studies conducted for other classes of ligands (dicarboxylates, α - hydroxy carboxylic acids and catechols) is substantially less than for the simple diols, the need for a systematic determination of stability constants and thermodynamic parameters for these systems is also apparent so that complexation reactions for ligands of the same class, and more importantly, complexation reactions for ligands of different classes can be compared.

Although there have already been several reports (Table 1.2) of thermodynamic parameters for borate complexation reactions with these ligands in the literature, significant disagreement among the various studies is common and, as is the case with the stability constants, the thermodynamic parameters remain somewhat uncertain. The two techniques used in these studies have been the measurement by pH techniques of stability constants as a function of temperature (van't Hoff method) [52] and calorimetry. Table 1.2 gives the ligand, $\Delta H°$, $\Delta S°$, ionic strength and reference for borate / ligand systems which are either directly or indirectly related to this thesis. Borate / D - mannitol is included in Table 1.2 because it is the one system that is included in all five of the major thermodynamic studies (three van't Hoff and two calorimetric studies). In fact, it is the borate / D-mannitol system which shows the largest discrepancies in thermodynamic parameters, especially values of $\Delta S°$. These discrepancies are not surprising considering that D-mannitol has multiple binding sites which can not be distinguished by either potentiometric or calorimetric techniques. 2:1 complexes such as B_2L^{2-} can not be ruled out in systems with ligands that have multiple binding sites [56], but, again, these techniques can only account for such species through

Table 1.2: Thermodynamic parameters for complexations of borate ion (B^-) with fully protonated ligands (H_2L) in aqueous solution at 25°C.

$$(BL_{j-1})^- + H_2L \leftrightarrow (BL_j)^- + 2\,H_2O$$

Ligand (H_2L)	$\Delta H_j°$ (kJ/mol)		$\Delta S_j°$ (J/K mol)		μ (M)	method	Ref.
	j = 1	j = 2	j = 1	j = 2			
H_2E	-11.3	-8.2	-31	-26	~0.1	van't Hoff	41
	-15.1	-8.4	-45.6	-42.7	0.006	"	43
	-5.8	---	-15	---	1.0	calorimetry	53
H_2P	-12.6	-30.1	-30	-92	~0.1	van't Hoff	41
	-21.4	-19.3	-62.0	-61.5	0.006	"	43
	-9.3	-38.9	-22	-138	1.0	calorimetry	53
H_2Cat	-13.3	15.8	30	134	~0.1	van't Hoff	41
	-11.2	---	33	---	0.006	"	43
	-23	-24	80	84	0.1	"	49
	-23	-24	-1.7	0	0.1	"	50
D- mannitol	-33.6	-18.6	-54.3	36	~0.1	van't Hoff	41
	-23.0	-34.3	-19.3	-19.7	0.006	"	43
	-32	-32	-32	-13	~0.1	"	50,54
	-19.7	32.4	-7.9	-50	1.0	calorimetry	53
	-18.6	-19.9	-4.6	-27	0.05	"	55

where: H_2E = 1,2-ethanediol, H_2P = 1,2-propanediol and H_2Cat = 1,2-benzenediol (catechol).

approximation. The problems associated with the accurate determination of stability constants and, therefore, thermodynamic parameters for such ligands led us to confine our own ^{11}B studies to ligands with only one binding site at a particular pH. Therefore, polyols such as mannitol are not included in this thesis.

In general, a principle reason for the lack of agreement in thermodynamic parameters for these systems is that both techniques (van'tHoff and calorimetry) depend on accurate values of reaction stability constants, and, as shown in Table 1, different values in the literature exist.

One important contribution to the field, not yet mentioned, is a calorimetric determination conducted by Aruga [57] of thermodynamic parameters for borate complex formation with a series of sugars. Aruga is a noted contributor to the field of aqueous coordination chemistry using potentiometric and calorimetric techniques. In this work, ΔH° for 1:2 complex formation reactions is uniformly less negative than ΔH° for 1:1 complex formation. ΔS° for 1:2 complex formation reactions is also uniformly much less negative than ΔS° for 1:1 complex formation. These results by a noted worker in the field using a very different experimental technique are completely in line with our own results for diols and α-hydroxy carboxylic acids using variable temperature ^{11}B NMR [40].

Excluding the work of Aruga [57] previously mentioned, most of the thermodynamic determinations cited in this section offer little or no discussion of the relationship between reaction thermodynamics and structure. In many cases, results are presented only in terms of their agreement or disagreement with the literature, or with respect to results for a series of ligands in the same

class. In the work presented in this thesis, we specifically studied the reactions of borate with simple ligands from different classes (diols, α-hydroxy carboxylic acids and dicarboxylic acids) as well as the formation of mixed ligand complexes with the hope of explaining some of the unusual thermodynamic trends seen in these reactions. Lastly, as far as we can tell, no thermodynamic studies of simple α-hydroxy carboxylic acids or dicarboxylic acids with boric acid have been previously reported.

1.5 The Application of ^{11}B NMR to Boron Acid Chemistry in Aqueous Solution

Over the past thirty years or so, the application of ^{11}B NMR to the study of a wide range of boron containing species in solution has been very extensive [57]. It is safe to say that NMR spectroscopy, ^{11}B coupled with ^{1}H and ^{13}C, is the diagnostic method of choice in the field today. Table 1.3 contains the fundamental physical parameters [58] of the ^{11}B nucleus, the important aspects of which are discussed briefly here.

^{11}B has a natural abundance of 80% and a relative sensitivity of 0.17 giving it an absolute sensitivity of 0.13. Therefore the sensitivity of the ^{11}B signal is ~ 1 / 8 that of the ^{1}H signal. The signal intensity relative to ^{13}C is given by the receptivity with ^{11}B having a receptivity of 754. Thus, qualitative results for relatively dilute solutions (~ 0.05M in boron) can be obtained with only a dozen or so scans, and quantitative results can be obtained with a few thousand scans using a modern FTNMR.

The nuclear spin (I) for ^{11}B is 3 / 2. Using the quantum mechanical relationship for spin multiplicity (2 (I) + 1), we see that ^{11}B nucleus can exist in four discrete spin states in an external magnetic field ($\mathbf{B_o}$), namely m = -3 / 2, - 1 / 2, + 1 / 2 and + 3 / 2. In the case of transitions of any nuclear isotope, however, all transitions occur at a single frequency since all the energy separations are equal and transitions are only allowed between adjacent levels (i.e. the selection rule $\Delta m = \pm 1$ operates) [59]. The quadrupole nature ($I > 1/2$) of the ^{11}B nucleus does, however, significantly affect the ^{11}B resonance. The finite quadrupole moment of the ^{11}B nucleus shown in Table 1.3 necessarily

Table 1.3: Selected physical parameters of the ^{11}B nucleus important to ^{11}B FTNMR; as compiled in reference [58].

^{11}B NMR

Natural abundance :	**80%**
Relative sensitivity ($^{1}H = 1.00$) **:**	**0.17**
Absolute sensitivity :	**0.13**
Receptivity ($^{13}C = 1.00$) **:**	**754**
Frequency ($^{1}H = 100$ Hz) **:**	**32.084 Hz**
Nuclear spin (I) **:**	**3 / 2**
Quadrupole moment :	**3.6×10^{-30} M^2**
Linewidth :	**~ 15 - 70 Hz**

Reference : 0.15M Boric acid in 20% D_2O/ H_2O @ pH = 2.0

causes excited spin systems to relax back to the ground state very rapidly, via a spin - spin relaxation (T_2) mechanism. The consequences of this are two-fold, one good and one bad. First the good, the rapid T_2 dominated relaxation mechanism allows the sequential accumulation of scans using an FT instrument with very little delay between pulses. The down side of such a rapid relaxation is the effect it has on the Lorentzian line shapes of typical ^{11}B resonances, causing the line widths to be relatively broad (15 -70 Hz) and thus decreasing the resolution of the spectrum.

At this point, it is important to mention that although ^{11}B shows strong coupling to ^{1}H, ^{19}F and ^{31}P nuclei, as seen in the complex spectra of boron hydrides [57], none of the species studied in our work have any other element than oxygen or carbon directly bound to boron. Therefore, all of the resonances are singlets which dramatically simplifies each spectrum.

The first application of ^{11}B NMR to the study of these systems was a preliminary investigation by Kennedy and co-workers [60] in 1969. This work showed that the ^{11}B chemical shift of solutions of borax (~0.5M) was pH dependent. This is due to the rapid equilibration of boric acid with borate ions. Kennedy et al. followed up on this work with a series of publications in which both the interconversion of aqueous boron species as a function of pH [44] and the interaction of borate with diols [44] and sugars [61] was studied quantitatively using ^{11}B NMR spectroscopy. The interconversion of boric acid ($B(OH)_3$) to borate anion ($B(OH)_4^-$) was studied [44] at low enough concentrations of boric acid (> 0.10M) so that no polyborate formation could be detected. This study was conducted by following the dependence of the ^{11}B chemical shift (δ) and line width ($W_{1/2}$) of the composite boron peak

($B(OH)_3$ + $B(OH)_4^-$) as a function of pH. Figure 1.2 is reproduced from Kennedy's original work [44]. Figure 1.2 can best be described as an ^{11}B NMR titration curve in which the ionization of boric acid, shown as an insert in Figure 1.2, can be followed either by following the chemical shift (δ) or the line width ($W_{1/2}$) of the composite boron peak as a function of pH. The trigonal / tetrahedral interconversion on the boron center during ionization is rapid on the ^{11}B NMR time scale. Therefore, at no time are separate resonances seen for the interconverting species ($B(OH)_3$ + $B(OH)_4^-$). What is seen, however, is one peak that is a time weighted average in terms of chemical shift and line width of the two interconverting species with the maximum in line width as well as change in chemical shift ($\Delta\delta$) occurring close to the pK_a of boric acid (~9). Since the external reference in this work (methyl ether boron trifluoride) is different from the external standard used throughout this thesis (0.15M boric acid, pH = 2, 20% (v/v) D_2O), the discussion of intrinsic chemical shifts presented here will be given in terms of the difference in chemical shift between a particular resonance and the chemical shift of completely unionized boric acid ($\Delta\delta$). At pH = 2, well below the pK_a of boric acid, essentially all the boron nuclei are present in trigonal unionized boric acid ($B(OH)_3$), with an intrinsic $\Delta\delta$ of 0 and an intrinsic line width ($W_{1/2}$) of ~ 75 Hz. As the pH of the solution is raised from 2 to 12, the peak starts to walk up field (from left to right) while broadening due to chemical exchange is a maximum of ~ 140 Hz at a pH ~ 8.2. At a pH ~ 12 and above, well above the pK_a of boric acid, the chemical shift and line width are no longer functions of pH. At this pH the peak is essentially all borate with an intrinsic δ of -17.6 ppm and a much narrower intrinsic line

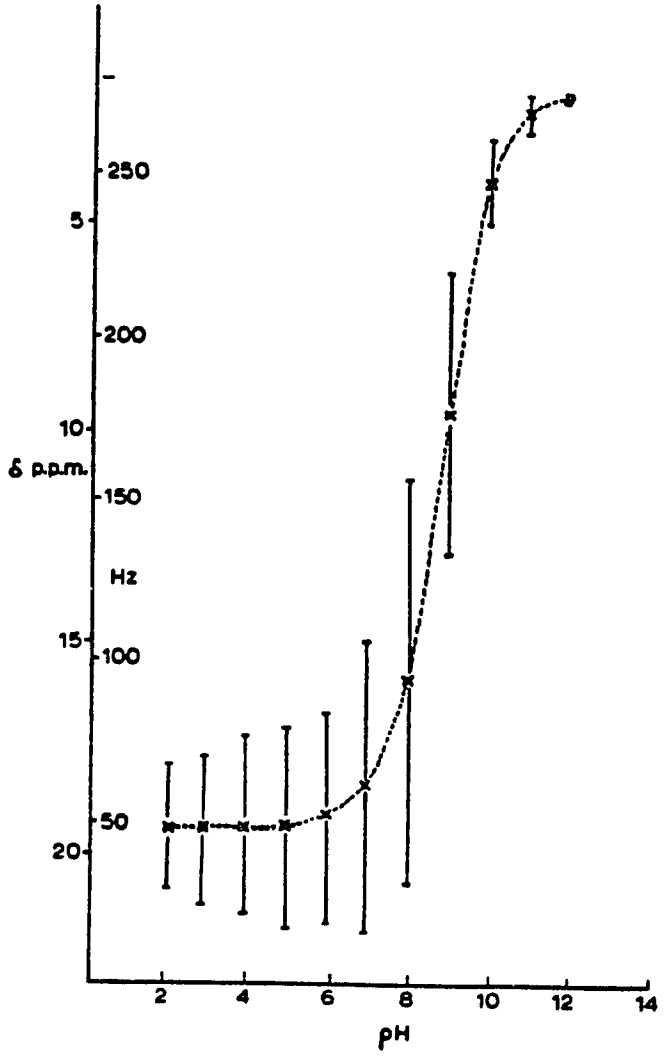

Figure 1.2 : ^{11}B NMR data at 12.83 MHz of solutions of boric acid (0.8M) at different pH values. The chemical shift at a given pH is shown by **X** and the line width at half height ($W_{1/2}$) is shown by a vertical bar. Methyl ether / boron trifluoride was used as the external reference at $\delta = 0$. Reproduced from reference [44].

width of ~ 15 Hz due to its T_d symmetry.

The chemical shift for boron species in our work, as well as the studies discussed here, fall into this range from 0 ppm for boric acid to -17.6 ppm for borate. 1:1 complexes typically have chemical shifts of -12 ppm while 1:2 complexes typically have chemical shifts of ~ -8 ppm relative to $B(OH)_3$. The ^{11}B NMR chemical shifts of these boron species give a fairly accurate picture of the electronic environment of the boron center, with upfield shifts corresponding to a more shielded environment. We will return to this point later.

Certainly no introduction to the application of ^{11}B NMR to the study of boric acid in aqueous solution would be complete without including the work of Peters, Kieboom, van Bekkum et al. Since their work is so closely related to the work presented in this thesis, and therefore will be referred to throughout this manuscript, only an overview of the contribution made by this group to the field is included here. Peters and co-workers published two excellent and comprehensive series of articles. One series [47,51,62-68] is an extensive investigation by ^{11}B, ^{13}C and ^{1}H NMR spectroscopy of borate complexes involving ligands ranging from diols to carbohydrates. Although stability constants for complex formation are reported (Sect. 1.4) in some of these studies, the principal subject of much of the work focuses on stereochemistry and the detailed determination of NMR coupling constants and chemical shifts for the various complexes. The second series [69-76] is one in which the "synergic" effect of borate on the metal ion sequestering ability of over twenty polyhydroxycarboxylates was studied using ^{11}B NMR and other experimental techniques. This work will be discussed in detail in Chapter 2.

Salentine [77] studied polyborate equilibria in aqueous solution using

high - field ^{11}B NMR. In this work, Salentine was able to calculate formation constants for the polyborates $B_3O_3(OH)_4^-$, $B_4O_5(OH)_4^{2-}$ and $B_5O_6(OH)_4^-$ as well as use variable - temperature ^{11}B NMR (5°C to 80°C) and concentration dependent spectra to support previous observations of the dissociation of polyborate complexes at high temperature or high dilution.

There are two kinetic studies which support our contention that ^{11}B NMR could be used to determine the exchange rate constant for the boron acid / borate interconversion directly. In the first study, Nolle and co-workers [78] measured the H_2O - D_2O solvent isotope effect on T_1 for ^{11}B and ^{10}B in both $B(OH)_3$ and $B(OH)_4^-$. From the ratios of T_1, the quadrupolar origin of the relaxation mechanism was inferred. In this work Nolle states that the broadening in the transition region of the ^{11}B line width for boric acid / borate interconversion as a function of pH could be used to calculate the exchange rate constant, but for reliable results, instead of the observed line widths, directly measured T_2 values should be used. In the second study, Blackborow [79] used resonance line broadening due to chemical exchange to deduce the rates and mechanism of exchange of some tertiary amine adducts of boron trichloride, thus showing the application of ^{11}B NMR to solution kinetics.

Finally, the application of ^{11}B NMR to biochemical systems has been substantial. With this in mind, we include here only two such studies. In the first study, Jordan and Adebodun [80] demonstrate the potential of ^{11}B NMR to the study of the active center of enzymes in solution by studying the transition state analog phenylboronic acid bound to chymotrypsin. In the second study, Baldwin and co-workers [81] use ^{11}B NMR spectroscopy to observe directly a tetrahedral boronic acid -β- lactamase complex.

1.6 Experimental Objectives of Thermodynamic Studies

The series of experiments and calculations undertaken here has two main objectives. The first object is to measure the stability constant (K_1 and K_2) and thermodynamic parameters ($\Delta G°$, $\Delta H°$ and $\Delta S°$) for the reaction of borate ion ($B(OH)_4^-$) with a series of ligands covering the complete range of ligand pK_a's in order to assess the effect of ligand variation on the stability and thermodynamics of 1:1 and 1:2 borate complex formation reactions. The series of ligands chosen covers the entire range of oxygen donor chelating ligands significant in borate coordination chemistry: polyols, 1,2 - benzenediols, α - hydroxy carboxylic acids and dicarboxylic acids. The stability and thermodynamics of mixed ligand 1:2 complexes were also investigated. All the thermodynamic parameters were determined from the temperature dependence of K_1 and K_2 as measured by ^{11}B FTNMR spectroscopy. The experiments discussed here were conducted in a systematic fashion in order to best elucidate (1) the effect of ligand variation on the ratio of successive stability constants (K_1 / K_2), (2) the dramatic differences in thermodynamic parameters for 1:2 complex formation compared with 1:1 complex formation found for some ligands, and (3) to use the thermodynamic results to gain some insight into the factors which affect the stability and reactivity of these complexes.

Second, theoretical calculations (AM1) [82] were conducted in collaboration with Dr. Sol Jacobson of the Hoechst Celanese Mitchell Technical Center. AM1 energy minimization calculations were conducted on all of the systems studied experimentally. In these studies, structural

parameters such as B - O bond length, O - B - O bond angle and charge density determinations on various atoms give valuable insight into the structural as well as electronic requirements of these complexes. The results of these calculations correlate nicely with the experimentally determined thermodynamic parameters previously discussed, giving a better understanding of the relationship between thermodynamics and structure for borate complexation reactions in aqueous solution.

CHAPTER 2

Introduction to Divalent Metal Ion Binding

2.1 Introduction

The isolation and / or synthesis of high affinity ligands for the complexation of metal cations (ionophores) is of major importance to industrial, environmental, biological as well as inorganic chemistry. In the chemistry of life a large number of natural substances are known to show strong, sometimes extreme, metal binding capabilities and thus have been used as models for synthetic ionophores [83]. One concept borrowed from a natural system [84] is the development of efficient host systems based on bringing together several bidentate coordination units in order to give podand or cage-like frameworks with preorganized coordination centers (as shown below). Macromolecular

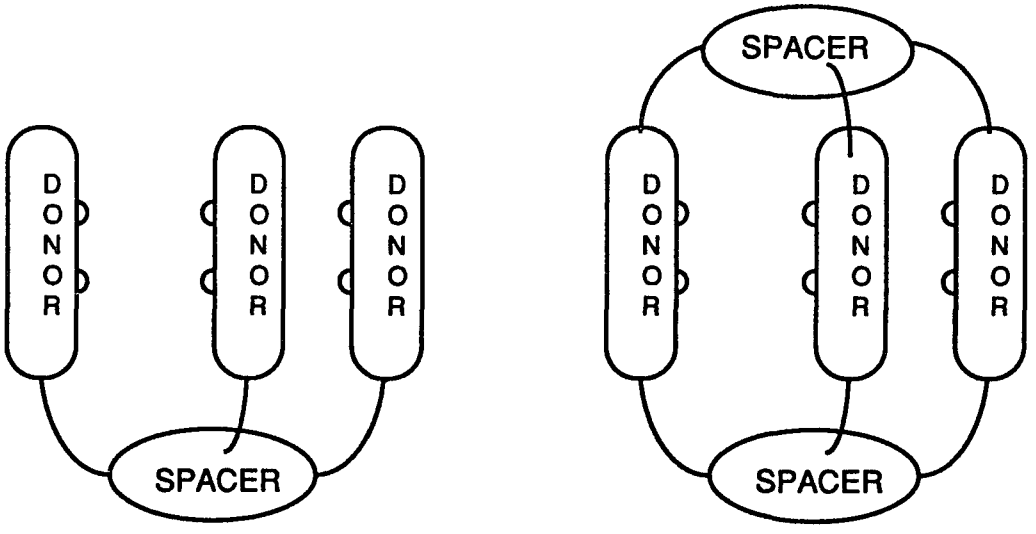

hosts of this kind typically exhibit high binding strengths combined with guest selectivities depending on the nature of the chelating donor units [85].

Research previously conducted in this laboratory in the area of metal ion coordination by macromolecular hosts had focused on the stability [86] and dynamics [87-89] of alkaline earth and lanthanide cryptates. The recent publication of a comprehensive series of articles by Peters and co-workers [69-76], in which metal ion binding by borate complexes was investigated using ^{11}B NMR , was of great interest in this laboratory because it brought together two previously separate areas of our work - namely, borate complexation chemistry and metal ion binding by macromolecular host compounds. It is the intent of this chapter to: (1) review important aspects of alkaline earth coordination by oxygen donor ligands; and (2) discuss those areas of Peters results which are important to this thesis. In this way, the ground work for the results reported in Chapter 6 is presented.

2.2 Alkaline Earth - Ligand Interactions

A comprehensive review of the crystal structures of alkaline earth metal ions by Einspahr and Bugg [90] has provided a wealth of information regarding the sterochemical principles governing Ca^{2+} and Mg^{2+} interactions with oxygen donor ligands. By studying the structural parameters of 150 different examples of M^{2+} - water, M^{2+} - carboxylate and M^{2+} - hydroxyl interactions and summarizing the results in the form of histograms, this review is able to characterize the distribution of M^{2+} - O bond distances, coordination numbers and modes of coordination most common in these systems. Figures 2.1 through 2.3 are reproduced from Einspar and Bugg's review article [91]. Figure 2.1 shows the three most commonly observed modes of coordination found in calcium - carboxylate interactions. The α mode is of of special interest to our work as it is the probable mode of coordination of Ca^{2+} to ligands with α - hydroxy carboxylic acid functions such as lactate or tartrate [92]. Figures 2.2 and 2.3 are histograms of the Ca - O and Mg - O distances in carboxylates broken down according to coordination mode and coordination number. Ca^{2+} - oxygen distances in various carboxylate complexes (Fig. 2.2) show a substantial range with many examples between 2.3 Å and 2.6 Å. Ca^{2+} is typically 7 or 8 coordinate in these systems with unidentate and α - coordination predominating over bidentate coordination. Mg^{2+} - Oxygen distances in various carboxylate complexes (Fig. 2.3) are not only much shorter but also fall into a much narrower range between 2.0 Å and 2.1 Å. No breakdown according to magnesium coordination is provided since almost all examples are six coordinate. Sr^{2+} - O distances in various carboxylate

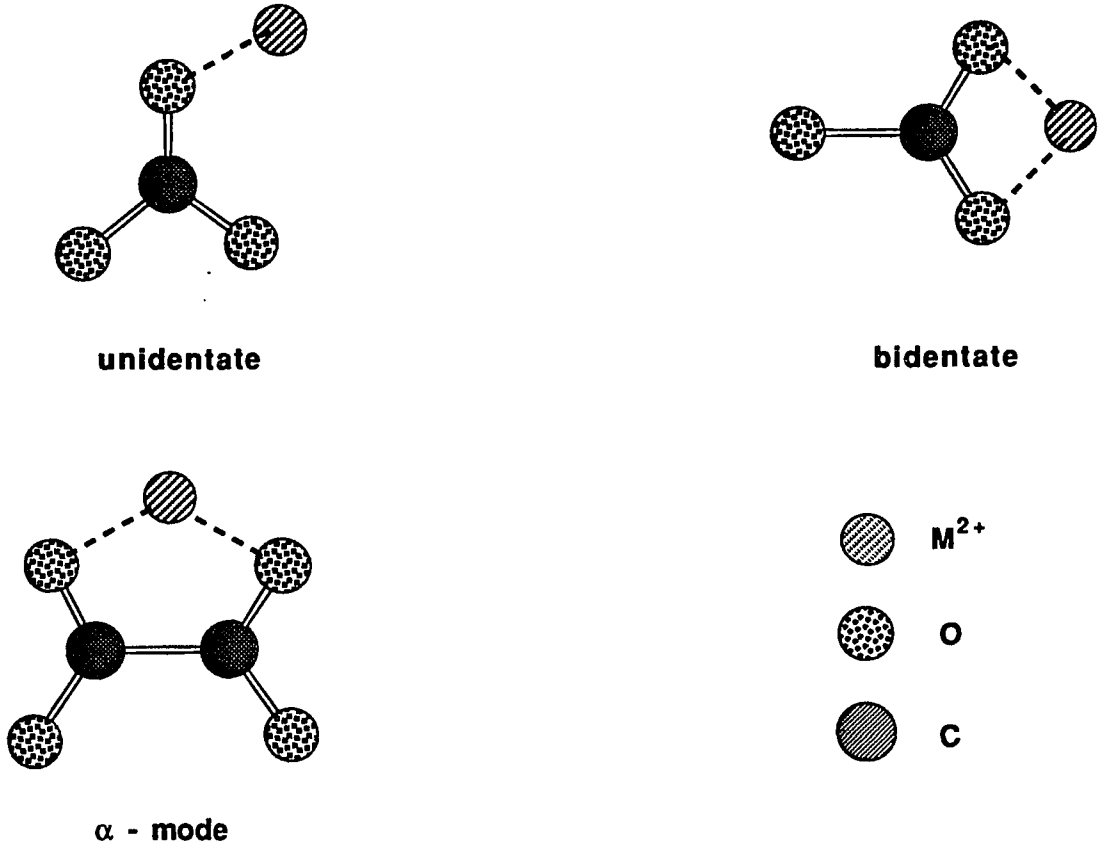

Figure 2.1: The three most commonly observed modes of coordination found in divalent cation (M^{2+})- carboxylate interactions [91].

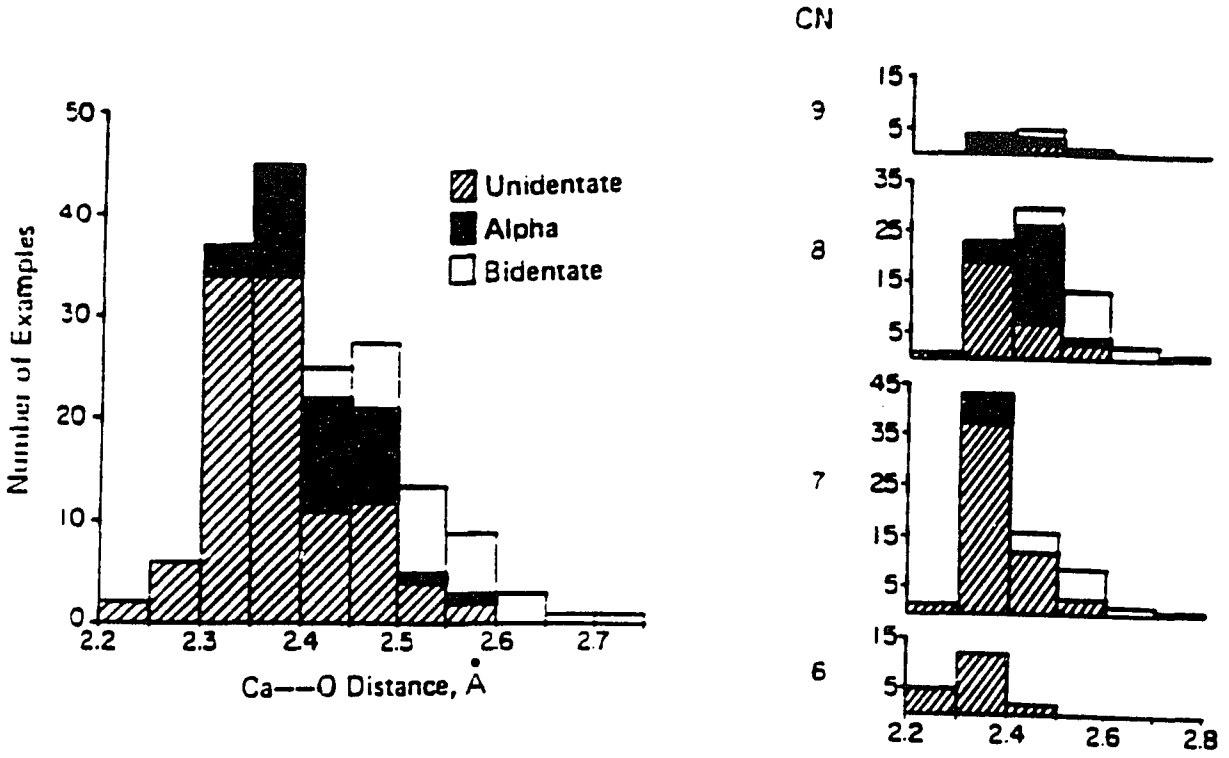

Figure 2.2: Histograms of Ca^{2+} - O distances in the calcium - carboxylate study compiled by Einspar and Bugg [91]. The overall distribution is shown in the histogram on the left; the four histograms on the right show the breakdown according to calcium coordination number.

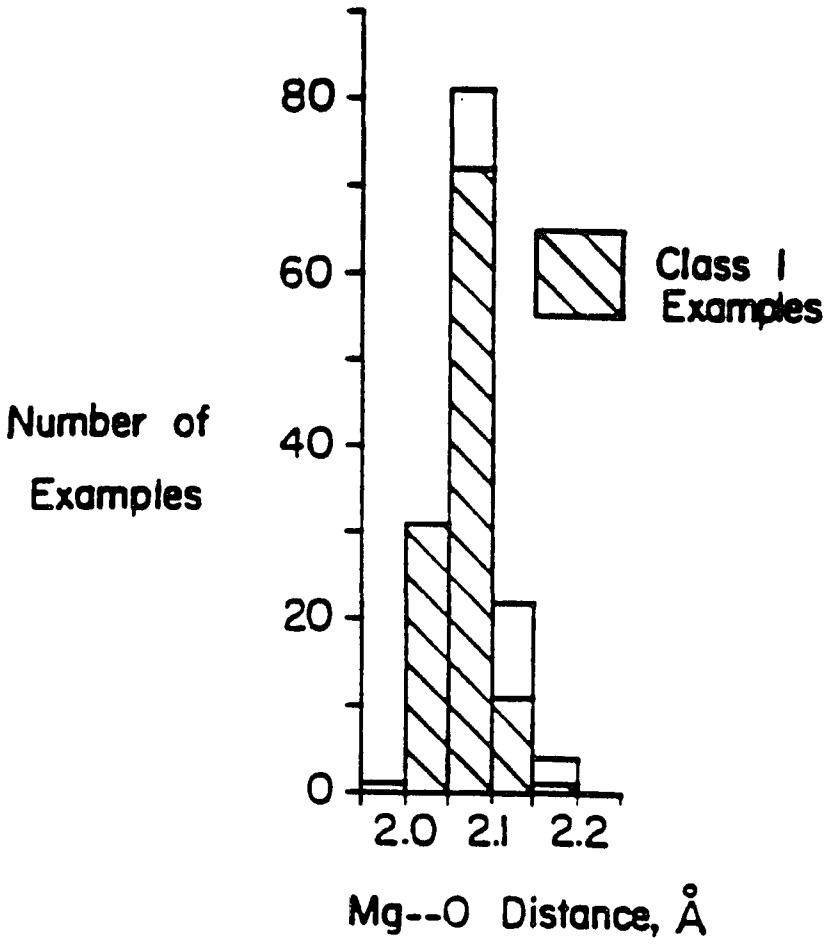

Figure 2.3: Histogram of the Mg^{2+} - O distances in the magnesium -water study compiled by Einspar and Bugg [91]. No breakdown according to magnesium coordination number is provided since almost all examples have coordination number six.

complexes are expected to be slightly longer and probably have an even greater distribution of distances compared with Ca^{2+} . We shall return to this discussion of metal - oxygen distances in carboxylate structures in Chapter 6 as it is important to our interpretation of the metal ion selectivity found for ternary alkaline earth complex ions in the M^{2+} / borate / tartrate system.

Ambady determined the crystal and molecular structures of strontium tartrate trihydrate and calcium tartrate tetrahydrate [92]. The important structural results are: (1) the tartrate ion behaves like a chelating agent towards both calcium and strontium; (2) in both structures the cation exhibits an 8- fold coordination. The coordination polyhedra in both cases are distorted dodecahedra. In the calcium structure, six of the coordination sites are occupied by tartrate oxygens, the remaining two being occupied by oxygens from water molecules. In the strontium structure, only five coordination sites are occupied by tartrate oxygens, with the remaining three sites being occupied by oxygens from water molecules. The average Ca^{2+} - O distance observed in the calcium structure is 2.47 Å; the average Sr^{2+} - O distance is 2.65 Å. The M^{2+} - O distances found in these binary systems (M^{2+} / tartrate) agree with the M^{2+} - O distances calculated for the ternary complexes (M^{2+} / borate/ tartrate) proposed in Chapter 6.

Recently, Doxsee and co-workers [93] characterized the calcium complex of phenacyl alcohol. Solution and solid - state structural data show a discrete complex of phenacyl alcohol with calcium chloride $[(C_6H_5COCH_2OH)_2Ca(H_2O)_3]Cl_2{\cdot}H_2O]$ in which phenacyl alcohol serves as a bidentate ligand with coordination of calcium to both the carbonyl oxygen and the hydroxyl group. The calcium ion is coordinated by two bidentate phenacyl alcohol molecules and three water molecules, providing an overall seven -

coordinate complex (~pentagonal bipyramidal), with two waters in the axial position and the two phenacyl alcohol units plus an additional water in the equatorial plane. The seven Ca^{2+} - O distances fall between 2.33 Å and 2.45 Å which is consistent with Figure 2.2. This study is included here because it shows the formation of discrete calcium complexes via α - mode (Fig. 2.1) coordination to bidentate oxygen donor ligands with Ca^{2+} - O distances consistent with those proposed in Chapter 6.

Shifting from crystal structure to aqueous solution phase chemistry, it is important to mention two studies here. Aruga determined the thermodynamic parameters ($\Delta H°$ and $\Delta S°$) for the association of Mg^{2+}, Ca^{2+}, Sr^{2+} and Ba^{2+} with malate ion using a calorimetric technique [94]. The results indicate that the stability order of the alkaline - earth metal complexes of malate ($Mg^{2+} < Ca^{2+} > Sr^{2+} > Ba^{2+}$) is determined by enthalpic factors. The thermodynamic results are interpreted to explain the "irregular" [95] position of magnesium in comparison with calcium due to the difficulty (less exothermic) of stable chelate bond formation by the smaller Mg^{2+} ion with polydentate ligands. Ligands classified as having an "irregular" stability order with respect to alkaline earth cation coordination have strict stereochemical requirements for chelate formation and, thus, preferentially coordinate to the divalent metal cation which best fits the binding site [94]. Hydroxycarboxylates, polycarboxylates and polyamino-carboxylates typically favor Ca^{2+} coordination for these reasons. In general, the more rigid the ligand, the more selective its interactions with cations become. The entropy data suggest the presence of different desolvation processes for each cation.

The second article, which also illustrates the importance of ligand

structure on alkaline earth binding, is a biochemical study conducted by Sadler and co-workers [95]. In this study the unusually strong binding of Ca^{2+} by the novel antibiotic squalestatin - 1 as compared with citrate (by more than one order of magnitude) is determined. The enhanced stability is attributed to the presence of a ring system which constrains the spatial orientation of the carboxylate and hydroxyl groups in the squalestatin -1 ligand as compared with the flexible citrate ligand.

2.3 Borate Complexes as Divalent Metal Ionophores

As mentioned previously, Peters and co-workers have published a comprehensive series of articles [69-76] in which the "synergic" effect of borate on the metal ion sequestering ability of over twenty polyhydroxycarboxylates was studied using ^{11}B, ^{13}C and ^{1}H NMR and other experimental techniques. This section is intended to be a review of that series of articles as they pertain to the work presented in this thesis.

The increased ability of polyhydroxycarboxylates to sequester Ca^{2+} in aqueous alkaline solution upon the addition of borate has been recognized for over fifty years [96]. Surprisingly enough, it was not until the first of Peters articles in 1978 that any detailed analysis of these interactions was reported [69]. In this work, Peters et al. studied the interaction between Ca^{2+} / $B(OH)_4^-$ and a host of polyhydroxycarboxylates including *l* - tartrate and *meso* - tartrate using ^{11}B NMR, calcium-ion-selective electrode measurements [97-98] and calcium sequestration capacities [99-100]. The important conclusions of this work are: (1) 1:2 borate complexes are shown to be the predominant calcium coordinating species, (2) ^{11}B NMR and calcium ion specific electrode results were combined in order to determine the "synergic effect" of each ligand system (The "synergic effect" as defined here is the increased metal ion coordinating ability of borate / polyhydroxycarboxylate systems over polyhydroxycarboxylates or borate used individually.), (3) The synergic effect is shown to be greatest for borate / ligand systems involving the diastereomeric ligands D-glucarate, L-idarate and D-mannarate which have two non-esterified hydroxyl groups α to both the 3,4- threo position occupied by the chelated borate and the terminal carboxylate groups in the 1:2 borate complex

(Figure 2.4a shows a non-stereospecific structure of such a 1:2 complex. Figure 2.4b shows the Fischer projection for each of the three diastereomers.), (4) Peters reports, contrary to our results (Chapter 6), no synergic effect in both the borate / D - tartrate and borate / *meso* - tartrate systems, therefore attributing the calcium coordinating properties of these systems entirely to that of the free tartrate ligand. (The Fischer projections of the simpler (threo) D - tartrate and (erytho) *meso* - tartrate ligands are given in Figure 2.4c.) and (5) Evidence is provided for the existence of the dicalcium species $Ca_2BL_2^-$ in the Ca^{2+} / borate / D - glucarate system.

The second study in the series [70] focusses on structural aspects of calcium coordination by the 1:2 borate complex in the Ca^{2+} / borate / glucarate system. ^1H, ^{11}B and ^{13}C NMR are used to determine the calcium coordination sites on both diastereomeric borate diesters of glucarate. Each borate diester is found to contain two Ca^{2+} coordinating sites consisting of two carboxylate groups, two borate ester ring oxygens, and, depending on the α - COH configurations, up to two α - hydroxy groups. The overall Ca^{2+} coordinating strength of both borate diester diastereoisomers of glucarate is found to be about equal. This article also employs two related crystallographic determinations as evidence for the proposed binding site on the 1:2 boro-glucarate complex. The solid state coordination site for the potassium salt of the borate diester of malic acid [101] and the sodium salt of the borate diester of tartaric acid [102] shown in Figure 2.5 both show the characteristic coordination site in these systems. In both cases the metal ion is coordinated to two carboxylate oxygens (one from each of the borate ester rings) and one borate ester ring oxygen.

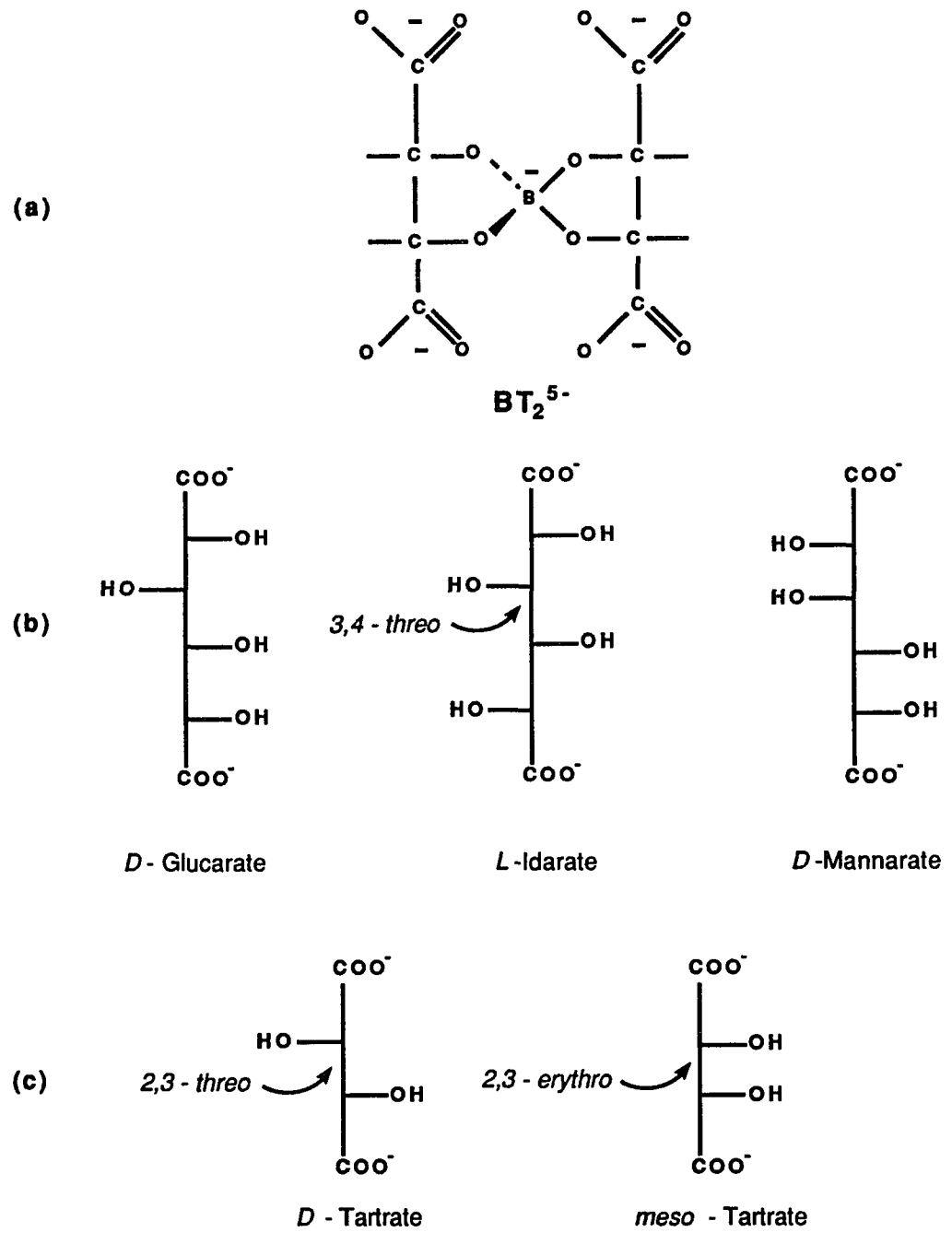

Figure 2.4: **(a)** Structure of the bis-borotartrate complex (BT^{5-}) in basic solution. **(b)** absolute configuration of *D* - glucarate, *L* - idarate and *D* - mannarate. **(c)** absolute configuration of *D*- and *meso* - tartrate.

(a)

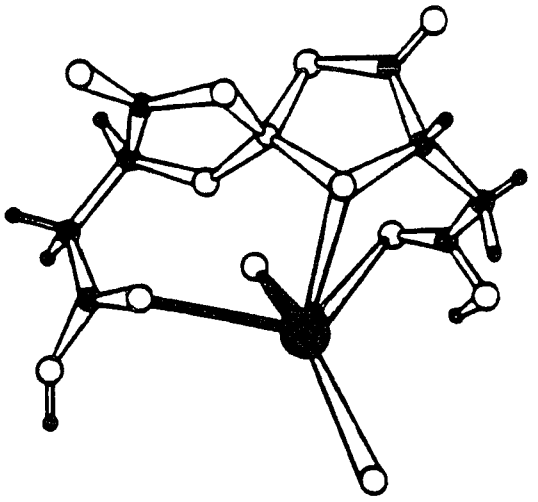

(b)

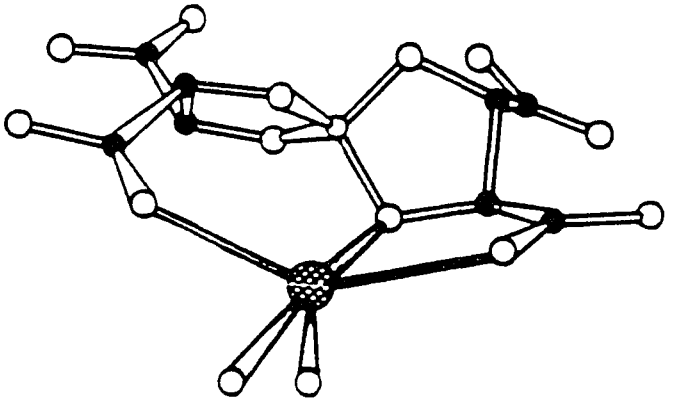

Figure 2.5: The solid state coordination site for; **(a)** the potassium salt of the borate diester of malic acid [101], and; **(b)** the sodium salt of the borate diester of tartaric acid [102].

The third article in the series [71], and the last which is directly related to the work presented in this thesis, is an ^{11}B NMR study of the divalent metal ion selectivity of the 1:2 borate diester of D-glucarate. The seven divalent cations which are coordinated by borate diesters of D-glucarate are Mg^{2+}, Ca^{2+}, Sr^{2+}, Ba^{2+}, Co^{2+}, Cd^{2+} and Ni^{2+}. The cations said to ionize the α - hydroxyl functions of D - glucarate and / or compete with borate for the diol functions are Cu^{2+}, Zn^{2+}, Pr^{3+} and Pb^{2+}. Al^{3+} and Fe^{3+} are said to be much more strongly coordinated by free D-glucarate than by its borate diesters. The authors classify the cations into three groups based on their observed interaction with borate diesters of D-glucarate and attempt to correlate the results with the charge / radius density (D) [103] and the polarizing ability (P) [104] of the particular cation. The classification goes as follows: Group (i). The monovalent cations Na^{+}, K^{+} and Ag^{+} {D < 160, P < 20} did not show preferential coordination to one of the borate ester or to the free D-glucarate. This is in agreement with the generally observed weak coordination of these cations by organic acyclic polyoxygen ligands [105].; Group (ii). Divalent cations with moderate polarizing abilities, Mg^{2+}, Ca^{2+}, Co^{2+}, Ni^{2+}, Sr^{2+}, Cd^{2+}, Ba^{2+} {190 < D < 280, 10 < P < 40}, showed preferential coordination to the 1:2 boro-glucarate complex; Group (iii). The polyvalent and strongly polarizing cations, Al^{3+}, Cu^{2+}, Zn^{2+}, Pr^{3+} and Pb^{2+} {D>280, P>40} induced dissociation of both the 1:1 and 1:2 borate complexes. Ionization of α-hydroxyl functions upon cation coordination and / or borate substitution is said to be responsible for these phenomena.

The very large size range (0.7 to 1.7 Å) [106] of divalent cat accommodated by the 1:2 borate complex of D-glucarate is rationalized in terms of a flexible cation coordination site. This can be understood by the

rotational freedom around C(1) - C(2) / C(6) - C(5) and C(2) - C(3) / C(5) - C(4) bonds, and the flexibility of the five - membered borate ester rings in the 1:2 borate complex of D - glucarate (Fig. 2.4). The qualitative results presented show little selectivity among the seven cations classified in group (ii). The *relationship between binding site flexibility and cation selectivity* is very important to our results and will be discussed in more detail in Chapter 6. The placement of the much smaller divalent cations Mg^{2+} , Co^{2+} and Ni^{2+} into the same classification (group (iii)) as the large divalent cations Ca^{2+} , Sr^{2+} , Ba^{2+} and Cd^{2+} is surprising and may be specific to the M^{2+} / borate / D-glucarate system due to the flexibility of the non-esterfied hydroxyl groups. This classification may not hold, for instance, in the metal coordinating ability of 1:2 borate esters of tartrate which have no non-esterified hydroxyl groups to participate in metal ion binding.

In order to further illustrate the differences between the aqueous coordination chemistry of Mg^{2+}, Co^{2+} and Ni^{2+} from Ca^{2+}, Sr^{2+}, Ba^{2+} and Cd^{2+}, the characteristic rate constants for substitution of inner sphere H_2O of various aqua ions can be compared. Mg^{2+} , Ni^{2+} , and Co^{2+} all have rate constants between 10^4 s^{-1} and 10^6 s^{-1}, while Ca^{2+} , Sr^{2+} . Ba^{2+} and Cd^{2+} all have rate constants greater than 10^8 s^{-1} [107]. Although we are using kinetic data to make a thermodynamic point, this illustration shows the danger of lumping cations, which behave very differently in aqueous solution, together based on an experimental result and one chosen physical parameter.

The rest of the series on synergic metal - ion binding by Peters and co-workers is much less related to our work and will only be mentioned briefly here. The synergic metal ion sequestration by borate / polyhydroxy-aminocarboxylate systems [72], borate / carbohydrate oxime systems [74] and

borate / bis (polyhydroxyalkyl) amines [76] was determined using ^{11}B NMR and other experimental techniques. The results show preferential binding of divalent cations which typically display strong coordination to nitrogen donor atoms such a Cu^{2+}, Ni^{2+} and Cd^{2+} . 1:2 borate complexes formed from (amino) polyhydroxy oxime ligands, for example, bind Cd^{2+} via two oxime (R_2C=N-OH), two amino and probably two borate ester ring oxygens, making the overall M^{2+} coordination by the 1:2 borate complex hexadentate [74].

Although the outstanding contributions by Peters and co-workers reviewed in this section are unparalleled and believed to be qualitatively correct (excluding the results for the Ca^{2+} / borate / tartrate systems), no quantitative determinations of stability constants for metal cation binding by borate diesters of polyhydroxy carboxylates are reported. The closest thing to a quantitative determination of stability constants for metal ion binding by borate diesters is given in the first article [69] in which Peters reports "although accurate fitting of the experimental data for these systems was not possible, this model gave log K_{CaBL2} and K_{Ca2BL2} values of 3.8 - 5.0 and 3.3 -3.6 respectively."

2.4 Aluminum Complexes as Divalent Metal Ionophores

Addition of Ca^{2+} to solutions of Al^{3+} and the aldarate ions (xylarate, D - arbinarate, D - glucarate and D - mannarate) results in the formation of new complexes that display slow exchange on the NMR time scale with the existing species [75]. The authors explain this result in terms of a shift of the Al^{3+} coordination site from an α - hydroxycarboxylate chelate to an adjacent diol function upon addition of Ca^{2+}. This behavior contrasts with that of the Ca^{2+} / borate / glucarate system [70-71] where the boron center is positioned at the deprotonated diol function prior to Ca^{2+} coordination. The differences between the borate and Al^{3+} systems are attributed to the higher metal - ion acidity of boron (III) compared with aluminum (III). In the case of Al^{3+}, "co - coordination of Ca^{2+} is required for the deprotonation of the diol functions on the glucarate ligands. The aluminum (III) complexes also differ from borate complexes in stoichiometry. Arabinarate and glucarate give predominantly 2:2 Al^{3+} / ligand complexes with tetrahedrally coordinated Al^{3+} which bind one and two Ca^{2+} ions, respectively, making the overall stoichiometry of the ternary systems 1:1:2 and 2:2:2 (Ca^{2+} / Al^{3+} / ligand). This contrasts with the stoichiometry (1:1:2) of the Ca^{2+} / borate / ligand systems previously discussed (Sect. 2.3). The proposed Ca^{2+} binding site in the Al^{3+} systems is, however, very similar to the borate systems, consisting of free carboxylate groups, Al^{3+} - bonded hydroxyl groups and free hydroxyl groups.

The final two articles in this series [108,109] are especially important to our work because they involve the Al^{3+} analog of our boro-tartrate complexes. *l* - (2R,3R) - Tartaric acid preferentially forms 1:3 and dinuclear 2:2 complexes

with octahedrally (1:3) and tetrahedrally (2:2) coordinated Al^{3+}. The tartrate ligands are again coordinated to the Al^{3+} center exclusively through α - hydroxycarboxylate groups in the absence of a second metal ion. Addition of the alkaline earth metal ions, Ca^{2+} , Sr^{2+} and Ba^{2+} to Al^{3+} / / -tartrate solutions shows preferential M^{2+} coordination by the 1:3 aluminum (III) tartrate complex at the expense of the 2:2 complex and the free tartrate in solution. Addition of Mg^{2+} to Al^{3+} / / -tartrate solutions, however, shows only a small preference for the 1:3 complex at the expense of the 2:2 complex with the amount of free tartrate remaining essentially unchanged.

The observed metal ion induced stoichiometry change (2:2 to 1:3) can be rationalized both on electrostatic and structural grounds. The charge on the 2:2 aluminum tartrate complex is -2 while the negative charge on the 1:3 complex is at least -3 and can go up to a maximum of -6, depending on the protonation of the three uncoordinated carboxylate groups. The 1:3 complex is therefore electrostatically more attractive to a divalent cation. Structurally the 2:2 aluminum (III) tartrate complex has all of its potential oxygen donor binding groups already coordinated to aluminum in the rigid dinuclear complex. The 1:3 aluminum (III) tartrate complex, on the other hand, has three flexible uncoordinated a - hydroxy carboxylate groups available for chelate formation with a divalent cation.

Qualitatively, the results show that the selectivity of these Al^{3+} / tartrate complexes for the alkaline earth cations is $Ba^{2+} \sim Sr^{2+} > Ca^{2+} >> Mg^{2+}$. This ordering is typically associated with anions of oxygenated inorganic or organic acids of large dimension [94].

Peters et al. [109] propose a six coordinate M^{2+} binding site on the 1:3 aluminum tartrate complex in which the alkaline earth cation is chelated to

three α - hydroxy carboxylate groups at one end of the ternary complex with the aluminum (III) in a similar octahedral coordination site on the opposite side of the complex. It is interesting to note that while addition of Ca^{2+} to Al^{3+} / glucarate solutions [75] induces a shift of the Al^{3+} coordination site in the 1:2 aluminum (III) gluconate complex from an α - hydroxycarboxylate chelate to the adjacent diol function, no such isomerism is observed here. This is because the much simpler tartrate ligand does not have enough hydroxyl groups to spare. By moving the Al^{3+} from the (1,2) α - hydroxycarboxylate position to the (2,3) diol position, the complex goes from having 3 α -hydroxy carboxylate (bidentate) groups which essentially form a pocket (with a hydrogen bonding network [109]) to having two groups of three carboxylates which are cut off from one another by the aluminum center. These results show a strong synergic effect for Ca^{2+} , Sr^{2+} and Ba^{2+} in the M^{2+} / Al^{3+} / tartrate system due to the podand-like structure of the 1:3 aluminum tartrate complex. The results presented here contradict the results previously published by the same workers for the M^{2+} / borate / tartrate system [69]. In that work, as mentioned previously, the authors claim that the system shows no synergy and that "the calcium - coordinating properties of this system are entirely due to *meso* - tartrate". Surprisingly, the results of the borate system are never compared with those of the aluminum system in the later article [109]. The authors may have felt that the chemistry of the boron center (bound by the octet rule) and that of the octehedral Al^{3+} center in the 1:3 aluminum - tartrate complex are too different to warrant such a comparison.

2.5 Experimental Objectives of Metal Ion Binding Studies

The series of metal ion binding experiments undertaken here (Chapter 6) has two main objectives. The first objective is to establish a quantitative technique to determine the stability constants for ternary M^{2+} / borate / ligand complexes. The analytical method employed couples ^{11}B NMR spectroscopy with a spectrophotometric competitive binding technique in order to quantify all of the significant interactions involved in this system of multiple equilibria. ^{11}B NMR is used to determine the stability constants for borate complex formation (both 1:1 and 1:2) as well as to determine quantitatively the interaction of each of the borate species ($B(OH)_4^-$, 1:1 and 1:2) with added divalent cation. Independent, competitive binding experiments are then used to determine the various association constants between divalent cations and free tartrate. The results are then combined in order to model each ternary M^{2+} / borate / tartrate system. The tartrate ligand was chosen because there is only one borate chelation site (2,3 diol position) on each borotatrate complex (1:1 and 1:2) at high pH. This allows for a much more accurate modeling of the system than would be possible for systems involving ligands that have multiple diol chelation sites. The success of this model in the quantitative determination of stability constants for M^{2+} binding by borotartrate complexes can then enable the achievement of our second objective.

The second objective of these metal ion binding studies is to determine the metal ion specificity of borotartrate complexes among the alkaline earth cations and to determine the effect absolute configurational changes on the ligand (*l* - vs. *meso* - tartrate) have on the metal ion binding properties of these systems. These metal ion specificity and ligand configurational studies should

give important evidence regarding the structural requirements for effective M^{2+} coordination, as well as indicating viable M^{2+} binding sites on these boro-tartrate ionophores.

CHAPTER 3

Experimental Methods and Data Analysis

3.1 pH Titration Methods

pK_a Determination

The accurate determination of the pK_a of both the boron acid and the ligand(s) is critical to the determination of the various stability constants associated with a particular boron acid / ligand system. The NaOH titration method is a simple and accurate technique by which the K_a values of each species can be determined under the same experimental conditions (temperature, ionic strength) as the stability constant determination experiment.

A solution of known initial concentration of the weak acid, $(HA)_o$, and inert electrolyte, $(KNO_3)_0$, adjusted to an ionic strength (μ) of 0.10M is titrated with standard 0.10M NaOH at the desired temperature. The K_a can then be calculated for each point on the titration curve, with the data in the buffered region (half equivalence point) giving the most accurate and precise results. The derivation of the K_a expression for a monoprotic weak acid follows:

The ionization of HA is given by

$$HA(aq) + H_2O \leftrightarrow H_3O^+(aq) + A^-(aq)$$

The K_a expression is

$$K_a = \frac{[H_3O^+]\,[A^-]}{[HA]} \qquad (3\text{-}1)$$

Mass balance gives

$$[HA] = (HA)_o - [A^-] \qquad (3\text{-}2)$$

Electroneutrality yields

$$[A^-] = [H_3O^+] + [Na^+] - [OH^-] \qquad (3\text{-}3)$$

where,

$$[Na^+] = [0.10M] \left(\frac{\upsilon}{V + \upsilon} \right) \qquad (3\text{-}4)$$

V = initial volume of the weak acid solution

υ = volume of 0.10M NaOH added

Substituting eqn. 3-2 and eqn. 3-3 into the K_a expression (eqn. 3-1) gives the final expression (eqn. 3-5).

$$K_a = \frac{[H^+] ([H^+] + [Na^+] - [OH^-])}{((HA)_o - ([H^+] + [Na^+] - [OH^-]))} \qquad (3\text{-}5)$$

Each titration experiment was carried out at a constant temperature (± 0.5°C) using a circulating water bath. The solution was purged with N_2 gas throughout the titration in order to remove any dissolved CO_2. The ionic strength was maintained at μ = 0.1M by the addition of KNO_3 as supporting electrolyte. The hydrogen ion activity coefficient was calculated using the Davies equation (eqn. 3-6) as appropriate for each temperature and ionic strength.

$$\log \gamma_{+,-} = -0.51 \left| Z_+ Z_- \right| \left\{ \frac{\sqrt{\mu}}{1 + \sqrt{\mu}} - 0.3\,\mu \right\} \qquad (3\text{-}6)$$

All pH measurements were obtained using a Fisher Accumet 620 pH meter or a Fisher Accumet 950 pH meter. A Fisher universal glass electrode {model # 13-639-3} and a Fisher Calomel electrode {model # 13-639-52} were used as the indicator and reference electrodes respectively. A multiple point standardization using Fisher certified buffer solutions was conducted for each temperature. The thermal characteristics of each certified buffer solution are recognized and accounted for by the Accumet 950 which was used in almost all of these experiments.

Thermodynamic parameters for the ionization of weak acids were determined by measuring the dependence of K_a on temperature (van't Hoff method) as described in Section 3.5. The K_a was determined at a minimum of five different temperatures over a range from 278K to 318K.

Although the predominant method of stability constant determination for borate complexation reactions used in this thesis is ^{11}B NMR, it is important to mention that pH titration and pH mixing experiments have been used with great success in this Laboratory [29 - 35]. An excellent derivation of the expressions required to determine stability constants using both pH methods is given by Tihal [36].

3.2 The ^{11}B NMR Experiment

^{11}B NMR spectra were obtained using a Bruker IBM 250 MHz FT NMR spectrometer equipped with a Bruker BVT -1000 variable - temperature unit. The Bruker BB VSP 250 broad - band probe was modified to contain only quartz glassware. Therefore, there was no background boron signal. The ^{11}B signal was observed at a spectrometer frequency of 80.254 MHz. The instrument was typically tuned for maximum sensitivity and resolution using a standard solution of 0.10M potassium borate in 20% (v/v) D_2O / H_2O at pH = 11. Probe tuning (tuning = 8922.5, matching = 884) significantly enhanced the spectral resolution and was most efficiently conducted by maximizing the FID lineshape of the standard sample. Quantitative ^{11}B NMR spectra were best recorded using the following acquisition and processing parameters:

Spectrometer frequency (SF) = 80.254 MHz
Observation frequency offset (01) = 4250
Spectral width (SW) = 20,000 Hz
Relaxation (prescan) delay (RD) = 0
Pulse width (PW) ~ 15 msec
Line broadening (LB) ≤ 2.44 Hz
Number of scans (NS) > 2000

The accuracy of the ^{11}B NMR integration was checked by preparing a solution containing known (gravimetric) concentrations of $CH_3B(OH)_2$, $B(OH)_3$ and $C_6H_5B(OH)_2$ and then comparing the NMR integrated areas with the gravimetric molar ratios. No measurable difference was observed. All samples

were prepared in 10mm quartz NMR sample tubes to avoid background interferences typically associated with borosilicate glass sample tubes.

^{11}B NMR Spectral Assignments

The chemical shifts (δ) of all ^{11}B NMR resonances are reported relative to external 0.15M $B(OH)_3$ in 20% D_2O / H_2O solution adjusted to pH = 2. The ^{11}B spectra were relatively easy to assign and results (Ch. 4, Ch. 5) are in very good agreement with the literature [44, 47, 51]. Since the chemical exchange between trigonal boron acids ($RB(OH)_2$) and their conjugate tetrahedral Lewis bases ($RB(OH)_3^-$) is fast on the NMR time scale, only one exchange broadened singlet which represents the sum of both forms of the boron acid is seen in the ^{11}B NMR spectra.

In contrast to the facile interconversion between $RB(OH)_2$ and $RB(OH)_3^-$, the exchange between borates and their mono - and diester complex ions is slow on the NMR time scale. This allows the determination of chemical shifts (δ), linewidths, and relative integration of the various boron species involved in the equilibria of interest. The relative integration of these signals, along with simple mass balance relationships, allows the straightforward calculation of the stability constants for these systems.

Stability Constant Determination

The stability constants for the various borate complexation reactions were determined by the direct integration of the resonances for the 1:1 and / or the 1:2 borate complexes with respect to the free boron acid / borate resonance at the appropriate pH and temperature. All solutions were prepared using 20%

D_2O in H_2O (v/v) as the solvent mixture. It is important to mention that a solvent composition study was conducted in which the % composition D_2O / H_2O (v/v) was varied from 0 to 100%. The stability constant (K_1) as measured by ^{11}B NMR for the borate / 1,2-propanediol system (Ch. 4) showed no dependence on % D_2O. The temperature dependencies of the stability constant also proved not be a function of % D_2O. These results are important because they allow us to compare stability constants and thermodynamic parameters as measured by three different experimental techniques: ^{11}B NMR (20% D_2O); ^1H NMR (100% D_2O) and pH titration (100% H_2O). Boron acid concentrations in various experiments ranged from 0.05M to 0.20M and ligand concentrations ranged from 0.10M to1.0 M. Divalent cation (Mg^{2+}, Ca^{2+} and Sr^{2+}) concentrations ranged from 5mM to 82mM in the metal ion binding studies reported in Chapter 6. Ionic strength was adjusted by the addition of the requisite amount of KNO_3 and it was maintained at 0.10M for the divalent cation binding studies (Ch. 6). Solution pH was adjusted by addition of NaOH(aq) or HNO_3(aq) prior to being brought to volume. The pH of the final sample was recorded before and after each experiment. These measurements were made directly in the 10mm quartz NMR tubes using a Fisher Ag / AgCl microprobe combination pH electrode.

Although the derivation of stability constant expressions for these experiments varies for different ligand types, the basic algorithm is similar. The derivation for borate (B^-) / diol (H_2D) systems is presented here as an example of this algorithm, with results for other representative systems being presented in Chapter 4 and Chapter 6.

At high pH (~ 11.5), borate (B^-) and fully protonated diol (H_2D) are the

only significant uncomplexed species in solution. The reaction scheme and corresponding stability constant expressions for this system are shown below:

$$B^- + H_2D \leftrightarrow BD^- + 2H_2O \qquad K_1$$

$$K_1 = \frac{[BD^-]}{[B^-]\,[H_2D]} \qquad (3\text{-}7)$$

$$BD^- + H_2D \leftrightarrow BD_2^- + 2H_2O \qquad K_2$$

$$K_2 = \frac{[BD_2^-]}{[BD^-]\,[H_2D]} \qquad (3\text{-}8)$$

The overall reaction (K_T) is expressed as

$$B^- + 2\,H_2D \leftrightarrow BD_2^- + 4\,H_2O \qquad K_T$$

$$K_T = \frac{[BD_2^-]}{[B^-]\,[H_2D]^2} \qquad (3\text{-}9)$$

where,

$$K_T = K_1 \cdot K_2 \qquad (3\text{-}10)$$

The initial concentrations $(B^-)_o$ and $(H_2D)_o$ are known. At low initial concentrations ($(B^-)_o \leq 0.1$, $(H_2D)_o \leq 0.1$) the 1:1 complex (BD^-) is the only observed borate complex in solution. Under these conditions, the spectrum can be integrated directly to give:

A_{B^-} and A_{BD^-} where A refers to the peak area.

The mass balance relationships give

$$(B^-)_o = [B^-] + [BD^-] \qquad \text{and}$$

$$(H_2D)_o = [H_2D] + [BD^-]$$

Since the sum of the concentrations of all the boron - containing species is equal to $(B^-)_o$, the following relationships are true.

$$A_T = A_{B^-} + A_{BD^-} ,$$

$$[B^-] = \left(\frac{A_{B^-}}{A_T} \right)(B^-)_o \qquad (3\text{-}11)$$

and

$$[BD^-] = \left(\frac{A_{BD^-}}{A_T} \right)(B^-)_o \qquad (3\text{-}12)$$

Mass balance for the ligand gives:

$$[H_2D] = (H_2D)_o - [BD^-] \qquad (3\text{-}13)$$

Substituting equations 3-11, 3-12 and 3-13 back into the stability constant expression for K_1 (eqn. 3-7) and rearranging gives:

$$K_1 = \left(\frac{A_{BD^-}}{A_{B^-}} \right) \left\{ (H_2D)_o - \left(\frac{A_{BD^-}}{A_T} \right)(B^-)_o \right\}^{-1} \qquad (3\text{-}14)$$

K_1 can then be calculated from the initial reactant concentrations and the integrated NMR peak areas.

The determination of the stability constant for 1:2 complex (BD_2^-) formation is simply a matter of decreasing the concentration of the borate ion ($(B^-)_o \sim 0.05M$) and increasing the diol concentration ($(H_2D)_o \sim 0.40M$). Under these conditions, ^{11}B NMR peaks can be easily integrated for A_{B^-}, A_{BD^-} and A_{BD2^-}. K_2 can be calculated by three independent methods, one which is independent of the previously determined value of K_1 and two which are not.

Method 1

In the first method K_2 (eqn. 3-8) can be determined independent of K_1 as follows:

The mass balance relationship give

$$(B^-)_o = [B^-] + [BD^-] + [BD_2^-] \qquad \text{and,}$$

$$(H_2D)_o = [H_2D] + [BD^-] + 2[BD_2^-]$$

Since the sum of the concentrations of all boron - containing species is equal to $(B^-)_o$, the following relationships are true.

$$A_T = A_{B^-} + A_{BD^-} + A_{BD2^-} ,$$

$$[B^-] = \left(\frac{A_{B^-}}{A_T}\right)(B^-)_o \qquad (3\text{-}15)$$

$$[BD^-] = \left(\frac{A_{BD^-}}{A_T}\right)(B^-)_o \qquad (3\text{-}16)$$

and

$$[BD_2^-] = \left(\frac{A_{BD2-}}{A_T}\right)(B^-)_o \qquad (3\text{-}17)$$

Mass balance for the ligand gives:

$$[H_2D] = (H_2D)_o - [BD^-] - 2[BD_2^-] \qquad (3\text{-}18)$$

Substituting 3-16, 3-17 and 3-18 back into the stability constant expression for K_2 (eqn. 3-8) and rearranging gives:

$$K_2 = \left(\frac{A_{BD2-}}{A_{BD-}}\right)\left\{(H_2D)_o - \left(\left(\frac{A_{BD-}}{A_T}\right) + \left(\frac{2\,A_{BD2-}}{A_T}\right)\right)(B^-)_o\right\}^{-1} \qquad (3\text{-}19)$$

Method 2

The ratio of stability constants K_2 / K_1 obtained by dividing eqn. 3-8 by eqn. 3-7 is given by eqn. 3-20.

$$\frac{K_2}{K_1} = \frac{[BD_2^-][B^-]}{[BD^-]^2} \qquad (3\text{-}20)$$

This dimensionless ratio is independent of ligand concentration. Experimentally, this ratio can be determined from the relative integration of the ^{11}B NMR spectra alone, since the dependence of each of the concentration terms (3-15), (3-16) and (3-17) on $(B^-)_o$ cancels out in eqn. 3-21.

$$\frac{K_2}{K_1} = \frac{A_{BD2-}\, A_{B-}}{(A_{BD-})^2} \qquad (3\text{-}21)$$

Solving equation 3-21 for K_2 gives eqn. 3-22

$$K_2 = K_1\left(\frac{A_{BD2-}\, A_{B-}}{(A_{BD-})^2}\right) \qquad (3\text{-}22)$$

which gives K_2 in terms of the previously determined value of K_1 and the ^{11}B NMR integration.

Method 3

In the third method, the overall stability constant (K_T) given in eqn. 3-9 is initially determined using the relative ^{11}B NMR integration and mass balance. The result of this derivation, which is similar to the derivation of eqn. 3-19, is given by eqn. 3-23.

$$K_T = \left(\frac{A_{BD2-}}{A_{B-}}\right)\left\{(H_2D)_o - \left(\left(\frac{A_{BD-}}{A_T}\right) + \left(\frac{2\, A_{BD2-}}{A_T}\right)\right)(B^-)_o\right\}^{-2} \qquad (3\text{-}23)$$

$$K_T = K_1 \cdot K_2 \qquad (3\text{-}10)$$

$$K_2 = K_T / K_1 \qquad (3\text{-}24)$$

Therefore, in the third method, K_2 can be determined from the ^{11}B NMR

integration, mass balance and the previously determined value of K_1.

Excellent agreement (± 10%) among the three methods of K_2 calculation was observed for all of the systems studied. This agreement is not only a critical validation of the accuracy of the K_1 and K_2 values for each system, but is also crucial to our calculation of stability constants for metal ion binding by bis borotartrate complex ions (Ch. 6) because free bis borotartrate (BT_2^{5-}) can only be determined in these experiments using the following equation.

$$[BT_2^{5-}] = \left(\frac{K_2}{K_1}\right)\frac{[BT^{3-}]^2}{[B^-]}$$

The thermodynamic parameters for the complexation reactions of borate with various ligands were determined by measuring the temperature dependence of the stability constants (van't Hoff method) as described in Sections 3.4 and 3.5.

3.3 The ^1H NMR Experiment

^1H NMR spectra were obtained using a Bruker IBM 250 MHz FT NMR spectrometer equipped with a Bruker BVT - 1000 variable temperature unit. Quantitative ^1H NMR spectra were easily recorded using typical (default) acquisition and processing parameters. Usually no special tuning procedures were required prior to acquisition. All spectra were recorded using at least 64 scans to insure a significant enhancement of the signal to noise such that accurate integration could take place.

All samples were prepared in 100% D_2O as the solvent. Chemical shifts (δ) of all resonances were measured relative to external 3-(trimethysilyl) propionic acid - sodium salt in D_2O.

^1H NMR Spectral Assignments

In all but one of the systems studied ($B(OH)_4^-$ / 1,2-propanediol), the ^1H NMR gives an easy to interpret spectrum. In these simple cases, at least one set of equivalent protons either on the boron acid or on the ligand is shifted due to complexation to give a new resolved signal. In those cases, direct integration of the free (A_F) vs complexed (A_C) form, along with mass balance, allows the calculation of the stability constant for 1:1 complex formation.

These simple systems fall into two categories: (1) those involving $CH_3B(OH)_2$ as the boron acid, and (2) those involving 1,2-ethanediol as the ligand. In basic solution, the methyl singlet on $CH_3B(OH)_3^-$ is shifted significantly upfield to give a well separated methyl singlet for the 1:1 complex. In the case of systems involving the ligand 1,2-ethanediol, the four aliphatic

hydrogens are equivalent in the free ligand, thus giving rise to a sharp singlet. Upon complexation with tetrahedral borate ($B(OH)_4^-$) the four protons remain equivalent to each other but the signal is shifted substantially downfield, giving a simple two singlet pattern in the aliphatic region. The spectrum is slightly complicated in cases where 1,2-ethanediol complexes with less symmetrical, substituted borates such as ϕ-$B(OH)_3^-$ or CH_3-$B(OH)_3^-$. The aliphatic protons on the ligand lose their equivalency upon complexation because the protons are forced to be either syn or anti to the R group in the rigid heterocyclic complex (shown below).

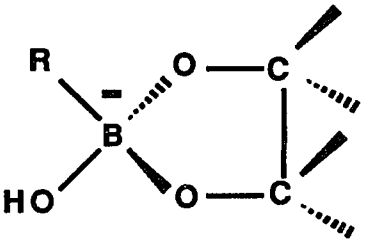

Fortunately, the multiplet caused by this homonuclear coupling can be integrated as a whole relative to the free ligand (H_2E) singlet.

The more complicated system alluded to at the beginning of this section is the $B(OH)_4^-$ / 1,2-propanediol (H_2P) system. The ^1H NMR spectrum of this system is shown in Figure 3-1. The spectrum of free 1,2-propanediol is presented in Fig. 3-1a. The multiplet at 3.3 ppm is assigned to the two protons on C(1) and the multiplet at 3.7 ppm is due to the one proton on C(2). The spectrum with added $B(OH)_4^-$ is presented in Fig. 3-1b. The methyl protons (δ =1 ppm) are unaffected by complexation. The three non-methyl protons in the complex are non-equivalent and they give rise to three new multiplets in the spectrum. The protons on C(1) are no longer magnetically equivalent in the

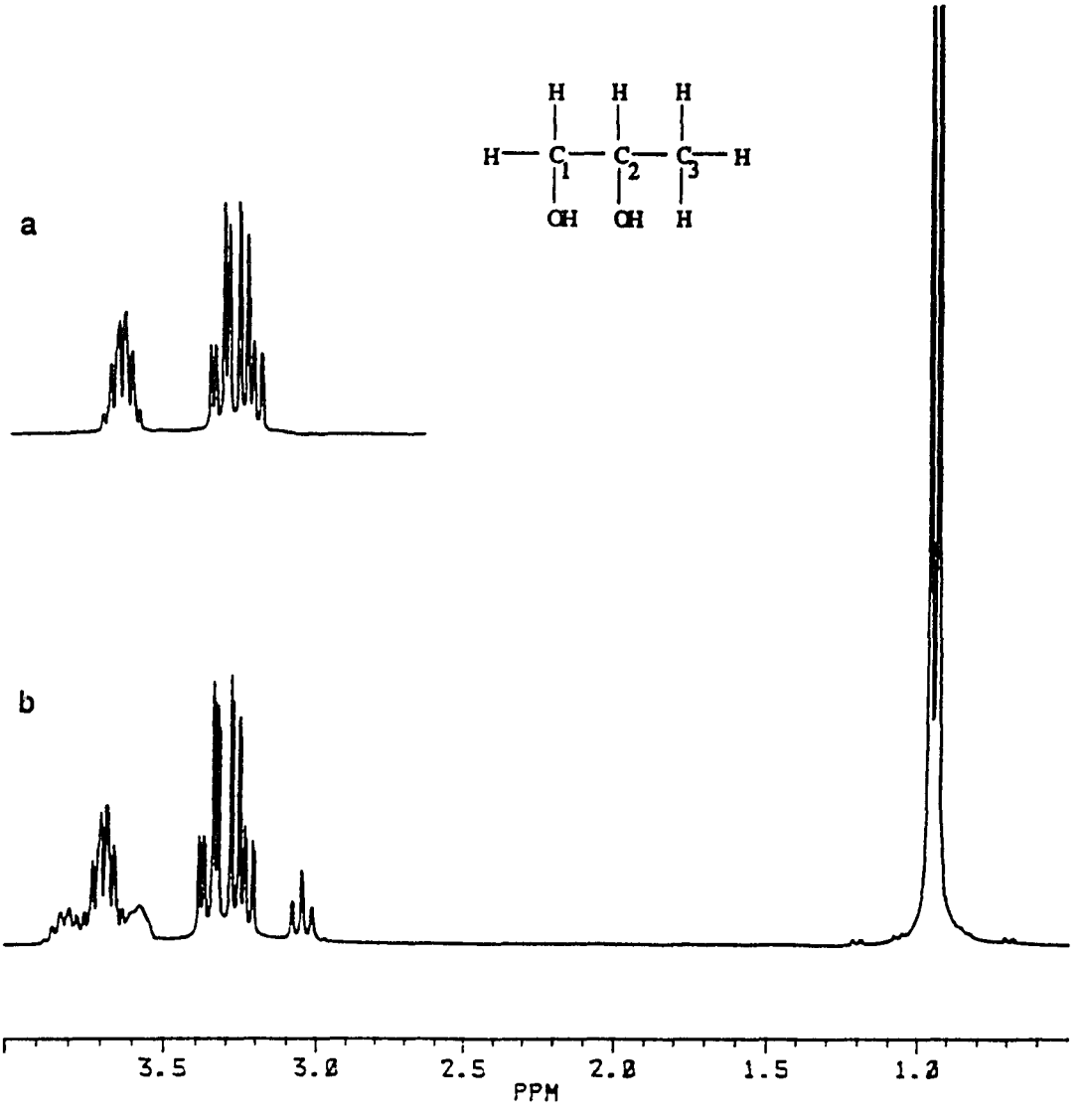

Figure 3.1: ^1H NMR spectra: (a) The methylene / methyne [C(1) / C (2)] region of 0.13 M H_2P in D_2O; pD = 11.5; T = 25.0° C. (b) $(B(OH)_4^-)_o$=0.10 M; $(H_2P)_o$ = 0.13 M in D_2O; pD = 11.5; T = 25.0° C. The solvent H_2O / D_2O peak is not shown. All ^1H NMR chemical shifts are relative to external 3-(trimethylsilyl) propionic acid in D_2O; pD = 11.5; T = 25.0° C.

complex. One proton is shifted upfield to 3.1 ppm and the other is shifted to 3.6 ppm. This loss of equivalency is due to the structural requirements of the five membered chelate ring in the 1:1 complex (shown below). In this structure one of the methylene protons is forced into a cis orientation with respect to the methyl group C(3) while the other methylene proton is forced into a trans orientation with respect to the methyl group.

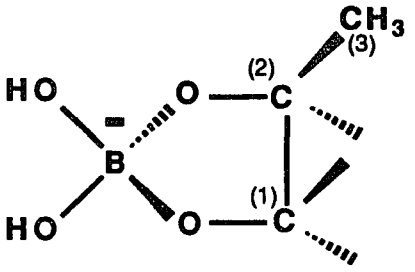

The new multiplet at 3.8 ppm is almost certainly due to the methyne C(2) proton in the 1:1 complex. Regardless of the exact assignment of peaks for the complex, the new triplet at 3.1 ppm (one position) is well separated from the free ligand multiplet (two positions) at 3.3 ppm. The relative integration of these two peaks can then be used to calculate the stability constant for 1:1 complex formation as long as a statistical factor of two is included for the complex triplet at 3.1 ppm.

Stability Constant Determination

The stability constants for the following 1:1 complexation reactions were determined by ^1H NMR: borate (B^-) / 1,2-ethanediol (H_2E), borate (B^-) / 1,2-propanediol (H_2P) and phenylboronate (ϕB^-) / 1,2 ethanediol (H_2E). Boron acid concentrations in various experiments ranged from 0.05M to 0.20M while ligand concentrations ranged from 0.10M to 1.0M. Solution pH was adjusted

by the addition of NaOD / D_2O or DCl / D_2O prior to bringing the solution to volume. The pH of the final sample was recorded before and after each experiment using a Fisher Ag / AgCl microprobe combination pH electrode. Although the ionic strength was typically maintained at 0.10M by addition of the requisite amount of KNO_3, in a few experiments reactant concentrations alone provided an ionic strength in excess of 0.10M. Therefore, the effect of ionic strength was evaluated. Ionic strength was increased up to 0.60M by addition of KNO_3 and no measurable effect on either stability constants or thermodynamic parameters was observed for the borate / 1,2-propanediol system.

The derivation of the stability constant expression (K_1) for the 1:1 complexation between a boronate ion (RB^-) and a diol (H_2D) at high pH using ^1H NMR is analogous to the derivation of eqn. 3-14 used in ^{11}B NMR experiments (Sect. 3.2) and, therefore, is not included.

The thermodynamic parameters for these systems were determined by measuring the temperature dependence of the stability constant, K_1, using the van't Hoff method as described in Sections 3.4 and 3.5.

3.4 Variable Temperature FTNMR

All ^{1}H and ^{11}B NMR spectra were recorded using a Bruker - IBM 250MHz FTNMR Spectrometer. The spectrometer was equipped with a Bruker BVT - 1000 variable temperature unit [111] capable of operation over a wide temperature range (200K to 350K). The temperature at the probe head given by the variable temperature unit was calibrated by a standard method described in the literature [112]. The accuracy of the variable temperature unit, over the required range (276K to 325K), was determined by this technique to be $\sim \pm 1K$. The stability constants for 1:1 (^{1}H and ^{11}B NMR) and 1:2 complex formation (^{11}B NMR) were measured as a function of temperature as described in Sections 3.2 and 3.3. For each system at least five different temperatures were studied over a temperature range from 276K to 325K. This temperature range is limited by the freezing point of the solution (~273K) at low temperatures and negligible complexation at high temperatures (~330K). For each stability constant determination the sample was allowed to reach thermal equilibrium in the spectrometer (~15 min.) before data acquisition. The solution pH of each NMR sample was also determined at each temperature. In this way small changes in pH with temperature could be accounted for. This is especially important in those cases where $[H_3O^+]$ is explicitly included in the stability constant expression.

3.5 van't Hoff Determination of Reaction Thermodynamics

The thermodynamic parameters ($\Delta G°$, $\Delta H°$, $\Delta S°$) for borate complexation reactions and related ionization equilibria were determined by measuring the temperature dependence of the various equilibrium constants. Regardless of the experimental technique (^{11}B NMR, ^{1}H NMR or pH titration), the theoretical treatment of these measurements is given by the derivation below.

According to van't Hoff equation:

$$\left(\frac{\partial \ln K}{\partial T}\right)_P = \frac{\Delta H°}{RT^2} \qquad (3\text{-}25)$$

Assuming that $\Delta H°$ is approximately constant over a small temperature range (~50K) eqn. 3-25 can be rearranged to give:

$$d \ln K = \left(\frac{\Delta H°}{R}\right)(T^{-2})\, dT \qquad (3\text{-}26)$$

Since $d(1/T) = -(T^{-2})\, dT$, eqn. 3-26 may be rewritten as:

$$\frac{d \ln K}{d(1/T)} = -\left(\frac{\Delta H°}{R}\right) \qquad (3\text{-}27)$$

If the enthalpy change is constant over the temperature range of the experiment, as assumed, then:

$$\frac{d\ \ln K}{d\ (1/T)} = \frac{\Delta\ \ln K}{\Delta\ (1/T)}$$

and,

$$\frac{\Delta\ \ln K}{\Delta\ (1/T)} = -\left(\frac{\Delta H^\circ}{R}\right) \qquad \textbf{(3-28)}$$

A plot of ln K vs 1 / T (van't Hoff plot) should give a straight line with a slope of $-\Delta H^\circ / R$.

therefore $\Delta H^\circ = -R\ (\text{slope})$ **(3-29)**

Since ΔG° at 298K can be determined directly from the equilibrium constant,

$$\Delta G^\circ = -RT\ (\ln K) \qquad \textbf{(3-30)}$$

ΔS° can be determined at 298K using the Gibbs - Helmholtz equation.

$$\Delta S^\circ = (\Delta H^\circ - \Delta G^\circ) / T \qquad \textbf{(3-31)}$$

The van't Hoff plots for all the systems studied (Ch. 4) were linear. This result validates the approximation to neglect the temperature dependence of ΔH° under the experimental conditions.

An alternative method for determining ΔS° can be derived by equating eqns. 3-30 and 3-31 and solving the resulting equation for ln K.

$$\ln K = \left(-\frac{\Delta H^\circ}{R}\right)\frac{1}{T} + \left(\frac{\Delta S^\circ}{R}\right) \qquad (3\text{-}32)$$

Eqn. 3-32 is an equation for a straight line in which a plot of ln K vs 1/ T will have a slope $-\Delta H^\circ / R$ and an intercept of $\Delta S^\circ / R$. Therefore, both ΔH° and ΔS° can be determined directly from the slope and the intercept of the van't Hoff plot.

$$\Delta H^\circ = -R \text{ (slope)} \qquad (3\text{-}29)$$

$$\Delta S^\circ = R \text{ (intercept)} \qquad (3\text{-}33)$$

ΔG° can then be determined at 298K using the Gibbs - Helmholtz equation, eqn. 3-31, in its more familiar form.

$$\Delta G^\circ = \Delta H^\circ - T\,\Delta S^\circ \qquad (3\text{-}34)$$

ΔS° values determined by both methods showed excellent agreement (±10%) for all systems studied. This agreement also helps to validate the assumptions made and to support the use of the van't Hoff method for the determination of reaction thermodynamics in these studies.

3.6 The Distribution of Equilibrium Species as a Function of pH

An understanding of the distribution of equilibrium species as a function of initial concentration and pH is of fundamental importance to both the thermodynamic [39-40] and kinetic studies [29-35] conducted in this laboratory. Furthermore, the application of borate complexation reactions to industrial, environmental and biochemical problems requires a knowledge of the pH, concentration and temperature dependence of each system. Once the various ionization and stability constants for the boron acid (HB) / ligand (H_2X) system have been determined at a particular temperature, the distribution of equilibrium species at any pH can be calculated. The most general system is that for boric acid reacting with a diprotic ligand (H_2X) to form both 1:1 (BX^-) and 1:2 (BX_2^-) complexes. The derivation for this system is given below:

The protolylic equilibria are:

$$HB + 2H_2O \leftrightarrow B^- + H_3O^+ ; \qquad K_{HB} = [B^-]\,[H_3O^+] / [HB] \qquad (3\text{-}35)$$

$$H_2X + 2H_2O \leftrightarrow HX^- + H_3O^+ ; \qquad K_{H2X} = [HX^-]\,[H_3O^+] / [H_2X] \qquad (3\text{-}36)$$

$$HX^- + 2H_2O \leftrightarrow X^{2-} + H_3O^+ ; \qquad K_{HX^-} = [X^{2-}]\,[H_3O^+] / [HX^-] \qquad (3\text{-}37)$$

The complexation reactions are:

$$HB + H_2X \leftrightarrow BX^- + H_3O^+ ; \qquad K'_1 = [BX^-]\,[H_3O^+] / [HB]\,[H_2X] \qquad (3\text{-}38)$$

$$BX^- + H_2X \leftrightarrow BX_2^- + 2H_2O ; \qquad K_2 = [BX_2^-] / [BX^-]\,[H_2X] \qquad (3\text{-}39)$$

K'_1, the stability constant for 1:1 complex formation written in terms of the reaction of boric acid and fully protonated ligand, is related to the more familiar K_1 as follows:

$$K'_1 = K_1 K_{HB} \qquad (3\text{-}40)$$

where,

$$B^- + H_2X \leftrightarrow BX^- + 2H_2O \; ; \quad K_1 = [BX^-] \; / [B^-] \; [H_2X] \qquad (3\text{-}41)$$

Conservation of mass gives

$$(H_2X)_o = [H_2X] + [HX^-] + [X^{2-}] + [BX^-] + 2\,[BX_2^-] \qquad (3\text{-}42)$$

$$(HB)_o = [HB] + [B^-] + [BX^-] + [BX_2^-] \qquad (3\text{-}43)$$

Substituting eqns. 3-36 and 3-37 into eqn 3-42 and rearranging gives 3-44.

$$(H_2X)_o = \alpha\,[H_2X] + [BX^-] + 2\,[BX_2^-] \qquad (3\text{-}44)$$

where,

$$\alpha = \left(1 + \frac{K_{H2X}}{[H_3O^+]} + \frac{K_{H2X}\,K_{HX^-}}{[H_3O^+]^2}\right) \qquad (3\text{-}45)$$

Substituting eqns. 3-38 and 3-39 into eqn. 3-44 and rearranging gives eqn. 3-46.

$$(H_2X)_o = \alpha\,[H_2X] + \beta\,[HB]\,[H_2X] + 2\gamma\,[HB]\,[H_2X]^2 \qquad (3\text{-}46)$$

where,

$$\beta = \frac{K'_1}{[H_3O^+]} \qquad (3\text{-}47)$$

and

$$\gamma = \frac{K'_1 K_2}{[H_3O^+]} \qquad (3\text{-}48)$$

Solving eqn. 3-46 for [HB] gives eqn. 3-49.

$$[HB] = \frac{((H_2X)_o - \alpha\ [H_2X])}{(\beta\ [H_2X] + 2\ \gamma\ [H_2X]^2)} \qquad (3\text{-}49)$$

Similarly, substituting eqns. 3-35, 3-38 and 3-39 into eqn. 3-43 and rearranging gives eqn. 3-50.

$$(HB)_o = \delta\ [HB] + \beta\ [HB]\ [H_2X] + \gamma\ [HB]\ [H_2X]^2 \qquad (3\text{-}50)$$

where,

$$\delta = 1 + \frac{K_{HB}}{[H_3O^+]} \qquad (3\text{-}51)$$

Substituting eqn. 3-49 into 3-50 and simplifying gives eqn. 3-52 which is a cubic equation in $[H_2X]$ with all the other variables defined.

$$\alpha\gamma[H_2X]^3 + (2\gamma(HB)_o + \alpha\beta - \gamma(H_2X)_o)[H_2X]^2 + \quad (3\text{-}52)$$

$$(\beta(HB)_o + \alpha\delta - \beta(H_2X)_o)[H_2X] + (-\delta(H_2X)_o) = 0$$

This cubic equation can then be evaluated numerically using a BASIC algorithm derived from the Newton-Raphson method [113] for the iterative determination of the roots of polynomial equations. Once $[H_2X]$ is determined numerically, the remaining equilibrium concentrations can be easily evaluated as shown below.

$$[HX^-] = K_{H2X}[H_2X] / [H_3O^+] \quad (3\text{-}53)$$

$$[X^{2-}] = K_{H2X} K_{HX^-}[H_2X] / [H_3O^+]^2 \quad (3\text{-}54)$$

$$[HB] = ((H_2X)_o - \alpha[H_2X]) / (\beta[H_2X] + 2\gamma[H_2X]^2) \quad (3\text{-}55)$$

$$[B^-] = K_{HB}[HB] / [H_3O^+] \quad (3\text{-}56)$$

$$[BX^-] = K'_1[HB][H_2X] / [H_3O^+] \quad (3\text{-}57)$$

$$[BX_2^-] = K'_1K_2[HB][H_2X]^2 / [H_3O^+] \quad (3\text{-}58)$$

The total concentrations of ligand (T_X) and boric acid (T_B) can be determined from the calculated equilibrium concentrations using the conservation relationships given in eqns. 3-39 and 3-40. T_X and T_B must therefore be equal to $(H_2X)_o$ and $(HB)_o$, respectively. This is a necessary check of the accuracy of

the calculation. Simpler systems can also be calculated using this derivation just by setting those equilibrium constants which do not apply to the system equal to zero. For example, in the boric acid / 1,2-ethanediol case, the ligand is essentially non acidic, making K_{H_2X} and $K_{HX^-} \sim 0$. Therefore, by eqn. 3-45, α becomes equal to 1 and eqn. 3-52 simplifies considerably.

Distribution diagrams for all of the systems studied are presented throughout Chapter 4. These diagrams are easily obtained using a "BASIC" program which applies the derivation presented here as the basis of its algorithm.

3.7 The Spectrophotometric Competitive Binding Experiment

Although stability constants for Mg^{2+}, Ca^{2+} and Sr^{2+} binding to both *l* - tartrate and *meso* - tartrate have been published [114], no measurements consistent with the experimental conditions used in ^{11}B NMR studies of metal ion binding by borotartrate complexes (Ch. 6) have been reported. To determine these stability constants, a spectrophotometric technique which has been previously used in this laboratory in studies of lanthanide [86] and alkaline earth [87, 89] cryptate formation was chosen. This technique was used rather than a potentiometric technique in order to circumvent typical interferences associated with potentiometric techniques at high ionic strength (μ = 1.5M). Calmagite (shown below) was used as the metal ion indicator [114, 115] because reasonable conditions for competitive binding could be established under our experimental conditions for Ca^{2+} and Sr^{2+} with both tartrate diastereomers.

Calmagite (H_3In)

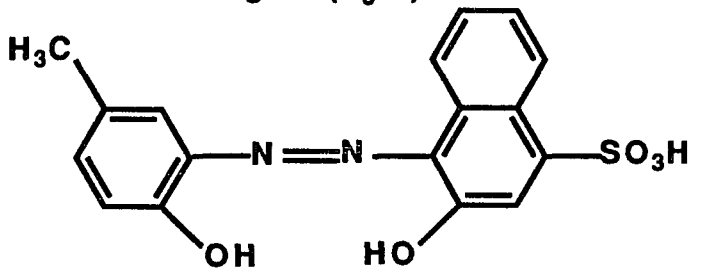

These spectrophotometric experiments were conducted under similar experimental conditions of pH, ionic strength and temperature as those used in ^{11}B NMR studies described in Section 3.2. The only exception is that tetramethylammonium compounds were used instead of potassium

compounds to avoid possible problems associated with the complexation of potassium ion with calmagite. In each experiment the analytical concentration of the chromophore ($(calmagite)_o = 6.64 \times 10^{-5}$ M) was held constant while the concentration of the divalent metal cation $(M^{2+})_o$ was varied from zero (λ max = 602nm) to an excess $(M^{2+})_o$ value at which all the calgamite is in a bound state (λ max = 525nm). All spectra were recorded with a Perkin - Elmer Lambda 3B UV / VIS spectrophotometer using a matched set of quartz cells.

Ca^{2+} / Calmagite: $(Ca^{2+})_o$ was varied over a range from 5.0×10^{-5} M to 4.0×10^{-4} M with the excess Ca^{2+} experiment being conducted at $(Ca^{2+})_o = 8.0 \times 10^{-3}$ M. **Sr^{2+} / Calmagite:** $(Sr^{2+})_o$ was varied over a range from 4.5×10^{-3} M to 5.0×10^{-2} M with the excess Sr^{2+} experiment being conducted at $(Sr^{2+})_o$ =0.20 M. **Ca^{2+} / Calmagite / *l*- or *meso* - tartrate:** $(Ca^{2+})_o$ was varied over a range from 5.0×10^{-5} M to 4.0×10^{-4} M and either *l* - or *meso* - tartrate was varied over a range from 1.2×10^{-2} M to 0.10 M. **Sr^{2+}/ Calmagite / *l* - tartrate:** $(Sr^{2+})_o$ was varied over a range from 4.5×10^{-3} M to 5.0×10^{-2} M while *l* - tartrate was varied over a range from 0.10 M to 0.32 M.

The conditional indicator constant ($K_{In'}$) which depends on the pH of the solution is defined in the literature [116] for the M^{2+} / calmagite system as

$$In' + M^{2+} \leftrightarrow MIn^- \qquad K_{In'} = \frac{[MIn^-]}{[In'][M^{2+}]} \qquad (3\text{-}59)$$

where [In'] is the total concentration of indicator not complexed with M^{2+}.

$$[In'] = [H_3In] + [H_2In^-] + [HIn^{2-}] + [In^{3-}] \qquad (3\text{-}60)$$

The conditional indicator constant for each M^{2+} / calmagite system can be determined at the pH of interest (pH = 11.5) by visible spectrophotometry. The derivation of the $K_{In'}$ expression follows.

At a fixed λ, if In′ and MIn⁻ are the only absorbing species, then

$$A = A_{In'} + A_{MIn^-} \qquad (3\text{-}61)$$

where A is the total absorbance of the sample at equilibrium, $A_{In'}$ is the absorbance due to uncomplexed calmagite and A_{MIn^-} is the absorbance of complexed calmagite (MIn^-). $A_{In'}$ is determined in the absence of M^{2+} while A_{MIn^-} is determined in the presence of excess M^{2+} under the same experimental conditions as the equilibrium experiment.

Then, at a fixed λ, the fraction of calmagite bound must be equal to α where,

$$\alpha = \left(\frac{A - A_{In'}}{A_{MIn^-} - A_{In'}} \right) \qquad (3\text{-}62)$$

The conservation relationships then give:

$$[MIn^-] = \alpha (In')_o \qquad (3\text{-}63)$$

$$[In'] = (1 - \alpha) (In')_o \qquad (3\text{-}64)$$

$$[M^{2+}] = ((M^{2+})_o - \alpha) (In')_o \qquad (3\text{-}65)$$

Substituting eqns. 3-63 to 3-65 back into the conditional indicator constant ($K_{In'}$) expression eqn. 3-59 gives eqn. 3-66.

$$K_{In'} = \frac{\alpha}{(1 - \alpha)\,((M^{2+})_o - \alpha)\,(In')_o} \qquad (3\text{-}66)$$

$K_{In'}$ was calculated for each equilibrium experiment at two independent wavelengths (525nm and 615nm). Identical results were obtained at each wavelength. The results for the binding of Mg^{2+}, Ca^{2+} and Sr^{2+} to calmagite at pH = 11.5 along with representative spectra are presented in Chapter 6.

Once the $K_{In'}$ values for each M^{2+} cation are known, the stability constants for M^{2+} / tartrate (T^{2-}) complexation (K_{MT}) can be determined simply by repeating each experimental set in the presence of varying amounts of either *l* - or *meso* - tartrate while holding $(In')_o$, pH, μ and temperature constant.

The derivation for K_{MT} using this competitive binding method is given below.

The complexation equilibria are

$$M^{2+} + In' \leftrightarrow MIn^- \qquad K_{In'} = \frac{[MIn^-]}{[M^{2+}]\,[In']} \qquad (3\text{-}59)$$

$$M^{2+} + T^{2-} \leftrightarrow MT^{2-} \qquad K_{MT} = \frac{[MT]}{[M^{2+}]\,[T^{2-}]} \qquad (3\text{-}67)$$

Conservation of mass gives

$$(In')_o = [In'] + [MIn^-] \qquad (3\text{-}68)$$

$$(M^{2+})_o = [M^{2+}] + [MIn^-] + [MT] \qquad (3\text{-}69)$$

$$(T^{2-})_o = [T^{2-}] + [MT] \qquad (3\text{-}70)$$

At a fixed λ, if In' and MIn^- are still the only absorbing species in solution, eqns. 3-62, 3-63 and 3-64 still hold.

Solving eqn. 3-59 for $[M^{2+}]$ gives

$$[M^{2+}] = \frac{[MIn^-]}{K_{In'}\,[In']} \qquad (3\text{-}71)$$

Substituting eqns. 3-63 and 3-64 into eqn. 3-71 and simplifying gives eqn. 3-72.

$$[M^{2+}] = \left(\frac{\alpha}{1-\alpha}\right)\frac{1}{K_{In'}} \qquad (3\text{-}72)$$

Let

$$\zeta = \left(\frac{\alpha}{1-\alpha}\right) \qquad (3\text{-}73)$$

then

$$[M^{2+}] = \frac{\zeta}{K_{In'}} \qquad (3\text{-}74)$$

Substituting eqns. 3-63 and 3-74 back into eqn. 3-69 and rearranging gives eqn. 3-75.

$$[MT] = (M^{2+})_o - \alpha\,(In')_o - (\zeta / K_{In'}) \qquad (3\text{-}75)$$

Similarly, substituting eqn. 3-75 back into eqn. 3-70 and rearranging gives eqn. 3-76.

$$[T^{2-}] = (T^{2-})_o - (M^{2+})_o + \alpha\,(In')_o + (\zeta / K_{In'}) \qquad (3\text{-}76)$$

Finally, substituting eqns. 3-74, 3-75 and 3-76 into the association constant expression, K_{MT} (eqn 3-67), gives eqn. 3-77.

$$K_{MT} = \frac{(M^{2+})_o - \alpha\,(In')_o - (\zeta / K_{In'})}{(\zeta / K_{In'})\left\{(T^{2-})_o - (M^{2+})_o + \alpha\,(In')_o + (\zeta / K_{In'})\right\}} \qquad (3\text{-}77)$$

K_{MT} was calculated, using eqn. 3-77, for each equilibrium experiment at two independent wavelengths (525nm and 615nm). Results well within experimental error (± 10%) were obtained at each wavelength. The results for Ca^{2+} and Sr^{2+} binding to the tartrate diastereomers along with representative spectra are presented in Chapter 6. All spectra for either binary systems (M^{2+} / calmagite) or ternary systems (M^{2+} / calmagite / tartrate) have a common isosbestic point at 555nm. Competitive binding conditions could not be established for the Mg^{2+} / calmagite / tartrate system at high pH due to the very large conditional indicator constant ($K_{In'}$) compared with Mg^{2+} binding by tartrate.

3.8 Stability Constants for Divalent Metal Ion Binding by Borate Complexes

The Ca^{2+} / borate / *l* - tartrate, Sr^{2+} / borate / *l* - tartrate and Ca^{2+} / borate / *meso* - tartrate systems have been quantitatively evaluated at pH = 11.5 by considering the following set of coupled equilibria:

$$B^- + T^{2-} \leftrightarrow BT^{3-} + 2\,H_2O \qquad K_1 \qquad (3\text{-}78)$$

$$BT^{3-} + T^{2-} \leftrightarrow BT_2^{5-} + 2\,H_2O \qquad K_2 \qquad (3\text{-}79)$$

$$M^{2+} + T^{2-} \leftrightarrow MT \qquad K_{MT} \qquad (3\text{-}80)$$

$$M^{2+} + B^- \leftrightarrow MB^+ \qquad K_{MB} \qquad (3\text{-}81)$$

$$M^{2+} + BT^{3-} \leftrightarrow MBT^- \qquad K_{MBT} \qquad (3\text{-}82)$$

$$M^{2+} + BT_2^{5-} \leftrightarrow MBT_2^{3-} \qquad K_{MBT2} \qquad (3\text{-}83)$$

$$MT + BT_2^{5-} \leftrightarrow MBT_2^{3-} + T^{2-} \qquad K_{ex} \qquad (3\text{-}84)$$

where

$$K_{ex} = K_{MBT2} / K_{MT}$$

K_1, K_2 and K_{MT} (eqns. 3-78 through 3-80) are determined as described in previous sections. Eqn. 3-81, which represents M^{2+} coordination to borate (B^-), can be ignored under our experimental conditions because of the low stability constants for CaB^+ and SrB^+ complex formation [117]. The fact that added Ca^{2+} or Sr^{2+} has no effect (Fig. 6.3) on the chemical shift or linewidth of the B^-

peak also supports this point. In the mathematical analysis which follows, K_{MBT} (eqn. 3-82) is set equal to K_{MT} (eqn. 3-80) in each system. This assumes that M^{2+} coordination by BT^{3-} is essentially the same as M^{2+} coordination by T^{2-} (eqn. 3-80). Experimentally this approximation is supported by the following observations: 1) almost no change in the relative integration, chemical shift, or linewidth is observed for the BT^{3-} peak in the ^{11}B NMR spectrum with added Ca^{2+} or Sr^{2+}, 2) ^{11}B NMR spectra of the phenylborate / *l* - tartrate system (which can form only the 1:1 borate complex, ϕBT^{3-}) are virtually identical in the absence and presence of Ca^{2+}, and 3) calcium ion specific electrode experiments [97] conducted in this laboratory [118] for the Ca^{2+} / phenylborate / *l* - tartrate system are identical with those conducted for the Ca^{2+} / *l* - tartrate system showing that formation of ϕBT^{3-} does not significantly increase or decrease the concentration of free Ca^{2+} in the solution. The approximation that K_{MBT} is about equal to K_{MT} has also been made by Peters and co-workers [69].

Stability constants for eqns. 3-78 through 3-82, along with ^{11}B NMR integration and mass balance, allow the calculation of the stability constants for eqn. 3-83 (K_{MBT2}) and eqn. 3-84 (K_{ex}) in each system as shown below.

The rearranged stability constant expressions are:

$$K_1 [B^-] [T^{2-}] = [BT^{3-}] \qquad (3\text{-}85)$$

$$K_2 [BT^{3-}] [T^{2-}] = [BT_2^{5-}] \qquad (3\text{-}86)$$

$$K_{MT} [M^{2+}] [T^{2-}] = [MT] \qquad (3\text{-}87)$$

$$K_{MBT} [M^{2+}] [BT^{3-}] = [MBT^-] \qquad (3\text{-}88)$$

The mass balance equations are:

$$(T^{2-})_o = [T^{2-}] + [MT] + [BT^{3-}] + [MBT^{-}] + 2[BT_2^{5-}] + 2[MBT_2^{3-}] \quad (3\text{-}89)$$

$$(M^{2+})_o = [M^{2+}] + [MT] + [MBT^{-}] + [MBT_2^{3-}] \quad (3\text{-}90)$$

$$(B^{-})_o = [B^{-}] + [BT^{3-}] + [MBT^{-}] + [BT_2^{5-}] + [MBT_2^{3-}] \quad (3\text{-}91)$$

From the ^{11}B NMR integration and eqn. 3-91, $[B^-]$, $[BT^{3-}]$, $[BT_2^{5-}]$ and $[MBT_2^{3-}]$ can be determined for any experiment as follows:

$$A_T = A_{B^-} + A_{1:1} + A_{1:2}$$

where A_i is the peak area of a particular resonance and A_T is the sum total of all the peak areas ($A_T = \Sigma_i A_i$)

$$[B^-] = \left(\frac{A_{B^-}}{A_T}\right)(B^-)_o \;;\; [1:1] = \left(\frac{A_{1:1}}{A_T}\right)(B^-)_o \;;\; [1:2] = \left(\frac{A_{1:2}}{A_T}\right)(B^-)_o$$

where $[1:1] = [BT^{3-}] + [MBT^{-}]$

But, $[BT^{3-}] >> [MBT^{-}]$ (3-92)

Therefore, $[1:1] = [BT^{3-}]$

Similarly, $[1:2] = [BT_2^{5-}] + [MBT_2^{3-}]$ (3-93)

Rearranging eqn. 3-93 gives eqn. 3-94

$$[MBT_2^{3-}] = [1:2] - [BT_2^{5-}] \qquad (3\text{-}94)$$

where $[BT_2^{5-}]$ can be calculated using the 1:1 peak and the B^- peak together with the ratio of the stability constants, K_2 / K_1 (eqn. 3-95).

$$[BT_2^{5-}] = \left(\frac{K_2}{K_1}\right)\frac{[BT^{3-}]^2}{[B^-]} \qquad (3\text{-}95)$$

Substituting eqn. 3-95 back into eqn. 3-94 gives eqn. 3-96

$$[MBT_2^{3-}] = [1:2] - \left\{\left(\frac{K_2}{K_1}\right)\frac{[BT^{3-}]^2}{[B^-]}\right\} \qquad (3\text{-}96)$$

At this point, $[BT_2^{5-}]$, $[BT^{3-}]$, $[B^-]$ and $[MBT_2^{3-}]$ have been evaluated. $[T^{2-}]$, $[M^{2+}]$, $[MT]$ and $[MBT^-]$ can be determined in the following manner.

Subtracting eqn. 3-91 from eqn. 3-89 gives eqn. 3-97.

$$[T^{2-}] = [M^{2+}] + \alpha \qquad (3\text{-}97)$$

where

$$\alpha = \left\{(T^{2-})_o - (M^{2+})_o - [BT^{3-}] - [MBT_2^{3-}] - 2[BT_2^{5-}]\right\}$$

Solving eqn. 3-87 for [MT] and eqn. 3-88 for [MBT^-], substituting them into eqn. 3-90 and rearranging gives eqn. 3-98.

$$[M^{2+}] = \frac{\beta}{(K_{MT}[T^{2-}] + \xi)} \qquad (3\text{-}98)$$

where

$$\beta = \left\{(M^{2+})_o - [MBT_2^{3-}]\right\}$$

and

$$\xi = 1 + K_{MBT}[BT^{3-}]$$

Substituting eqn. 3-98 into eqn. 3-97 and rearranging gives eqn. 3-99

$$K_{MT}[T^{2-}]^2 + (\xi - \alpha K_{MT})[T^{2-}] - (\beta + \alpha\xi) = 0 \qquad (3\text{-}99)$$

which is a quadratic equation in [T^{2-}]. The positive root of the quadratic equation gives [T^{2-}], from which the remainder of the equilibrium terms can be evaluated as follows:

$$[M^{2+}] = [T^{2-}] - \alpha$$

$$[MBT^-] = K_{MBT}[M^{2+}][BT^{3-}]$$

and

$$[MT] = (M^{2+})_o - [M^{2+}] - [MBT^-] - [MBT_2^{3-}]$$

K_{MBT2} and K_{ex} can then be calculated directly from these results by making the appropriate substitutions into eqns. 3-83 and 3-84.

$$M^{2+} + BT_2^{5-} \leftrightarrow MBT_2^{3-} \qquad K_{MBT2} = \frac{[MBT_2^{3-}]}{[M^{2+}]\,[BT_2^{5-}]} \qquad (3\text{-}83)$$

$$MT + BT_2^{5-} \leftrightarrow MBT_2^{3-} + T^{2-} \qquad K_{ex} = \frac{[MBT_2^{3-}]\,[T^{2-}]}{[MT]\,[BT_2^{5-}]} \qquad (3\text{-}84)$$

The only approximation used in this derivation is that $[BT^{3-}] >> [MBT^-]$. This approximation allows the integration of the 1:1 peak to determine $[BT^{3-}]$ directly and is validated by the final results of the calculation which show $[MBT^-]$ to be < 1% of $[BT^{3-}]$ in all cases. This result is consistent with the observed independence of the 1:1 peak as a function of $(M^{2+})_o$.

The results for all the systems which were modeled using this derivation are presented in Chapter 6.

CHAPTER 4

Thermodynamics of 1:1 and 1:2 Complexation Reactions of Borate Ion with Bidentate Ligands

4.1 Introduction

Borate ion, $B(OH)_4^-$, can react with bidentate chelating ligands to form anionic complexes of both 1:1 and 1:2 stoichiometries. The overall reactions are:

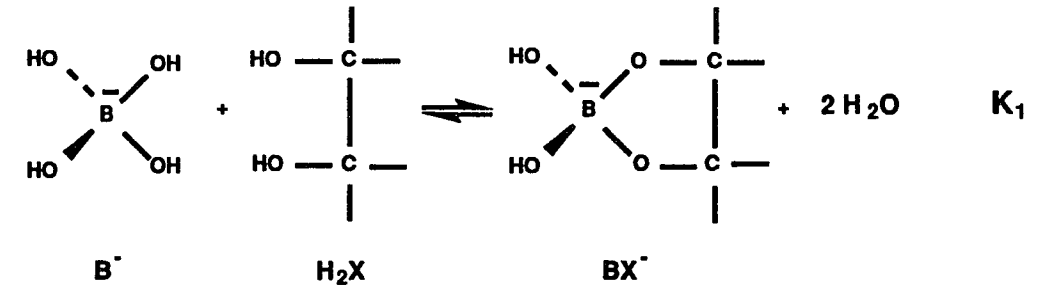

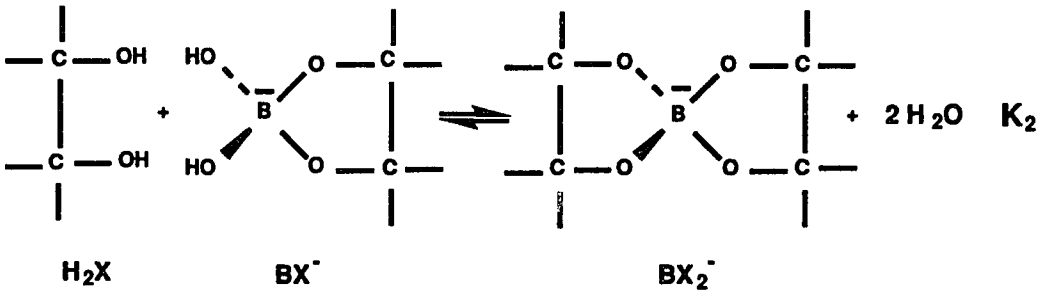

Some ligands which undergo this type of reaction are, in order of increasing acidity, polyols, 1,2-dihydroxybenzenes, α-hydroxy carboxylic acids and dicarboxylic acids. Stability constants for BX^- complex formation (K_1) increase as the acidity of the ligand increases [32,38,119-121]. The ratio of successive

stability constants (K_1 / K_2) also increases with increasing ligand acidity. For polyols the ratio is close to a purely statistical ratio[121,122], but the more acidic ligands have ratios which exceed the statistical ratio by factors which are $\geq 10^3$. Although these results have been in the literature for some time, no complete thermodynamic study has ever been carried out to provide an explanation for the remarkably different behavior of the various ligands. With these ideas in mind, variable temperature ^{11}B and ^1H NMR was used to determine the stability constants (K_1 and K_2) and thermodynamic parameters ($\Delta H°$ and $\Delta S°$) for a series of borate / ligand systems. In order to study the effect of the first ligand coordination on the thermodynamics of subsequent bis complex formation, ligands from over the entire acidity range were chosen. Selected mixed ligand systems were also studied to help elucidate these points.

All of the results presented for these systems are expressed in terms of the reaction of borate ion (B^-) with fully protonated ligand (H_2X). In this way, direct comparison of thermodynamic parameters can be made between any of the systems studied. Experimentally, however, the pH best suited for these determinations varies from system to system, and may be one in which either B^- or H_2X is not the predominant state of protonation for HB and / or H_2X. In these cases the experimentally determined parameters can be easily converted to the form: $H_2X + B^- \leftrightarrow BX^- + 2\ H_2O$ using the thermodynamic parameters for the appropriate ionization reactions (Table 4.1) in a Hess's law calculation.

Results and Treatment of Data

4.2 Thermodynamics of Weak Acid Ionization.

pK_a, enthalpies and entropies of ionization for phenylboronic acid ($\phi B(OH)_3$), glycolic acid (H_2G) and lactic acid (H_2L) were determined (μ = 0.1M (KNO_3)) by measuring K_a as a function of temperature as described in the experimental section (Sect. 3.1). The results of these determinations are presented in Table 4.1.

Reliable ionization parameters (pK_a , $\Delta H°$ and $\Delta S°$) for boric acid [22,123], phenylboronic acid [23], methylboronic acid [124] and oxalic acid [125-127] were found in the literature. These literature determinations were conducted using experimental conditions which were consistent with our own and are included in Table 4.1. Our results for phenylboronic acid agree very well with the study conducted by Edwards [23] and, as such, add to the validity of this technique. The van't Hoff plot for the ionization of phenylboronic acid (shown below) is given in Figure 4.1.

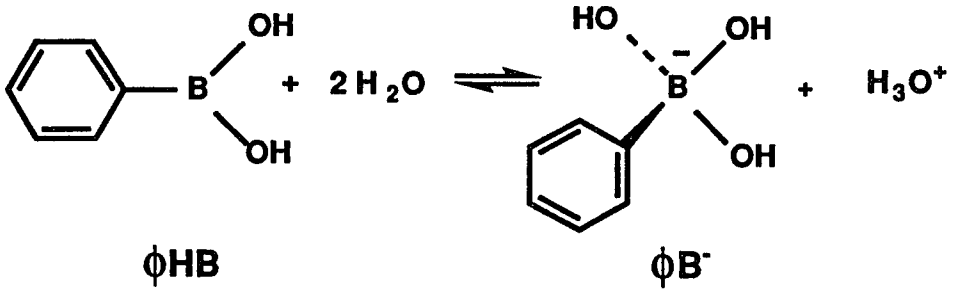

Table 4.1 pK_a values and thermodynamics of ionization for the acidic species important to this study.[a]

Acid	pK_a (298K)	$\Delta H°$ (kJ / mol)	$\Delta S°$ (J / mol K)
$B(OH)_3$	8.98[b]	12.8[c]	-129[c]
$\phi B(OH)_2$	8.72[d]	7.7 (±1) [d]	-141(±5) [d]
	8.76[e]	6.6 [e]	-144 [e]
$CH_3B(OH)_2$[f]	10.40	28 (±2)	-105 (±8)
H_2G[d]	3.65	1.5 (±1)	-65(±4)
H_2L[d]	3.64	-2.9 (±0.2)	-79(±1)
H_2Ox	1.13[g]	-2.9 [h]	-31 [h]
HOx^- [i]	3.38	-5.4	-96

a Errors associated with K_a determinations conducted in this lab are typically ± 10%. Numbers in parentheses denote the standard deviation (±s).

b Reference 123 { μ = 0.1M $NaClO_4$)}.

c Reference 22 { μ ~ 0.1M NaCl)}.

d This study.

e Reference 23 { μ ~ 0.1M ($NaNO_3$)}.

f Reference 124 { μ = 0.1M (KNO_3)}.

g Reference 125 { μ ~ 0.1M ($NaClO_4$)}.

h Reference 126 { μ = 0.15M ($NaNO_3$)}.

i Reference 127 { μ = 0.1M ($NaClO_4$)}.

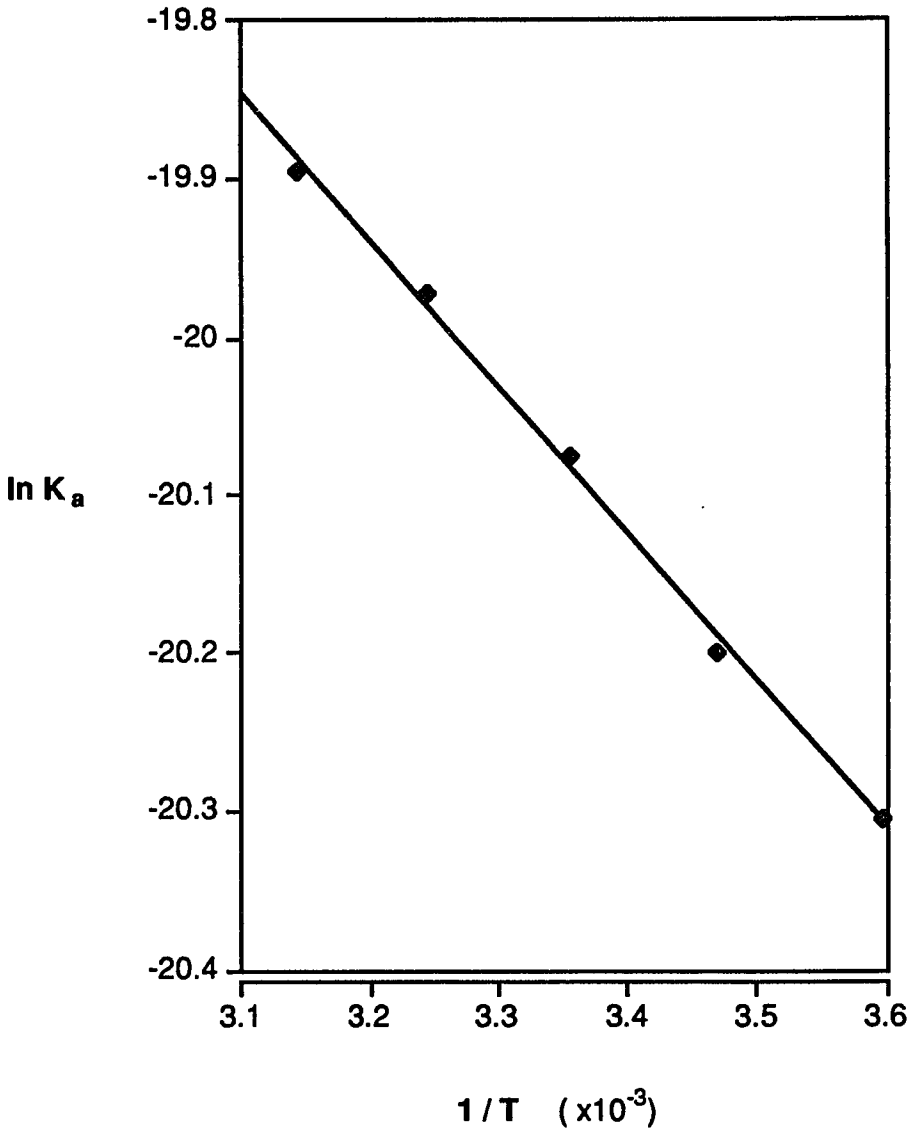

Figure 4.1: van't Hoff plot for the ionization of phenylboronic acid.

4.3 Thermodynamics of Borate Complex Formation. ^{11}B and ^{1}H NMR Studies.

Diols. Stability constants and thermodynamic parameters for both 1:1 and 1:2 complexation reactions of borate ion (B^-) with 1,2-ethanediol (H_2E) and 1,2 - propanediol (H_2P) were determined by ^{11}B NMR spectroscopy. Additionally, stability constants and thermodynamic parameters for 1:1 complexation reactions were also conducted by ^{1}H NMR for the following systems: B^- / H_2E, B^- / H_2P and phenylboronate (ϕB^-) / H_2P. Both the ^{11}B NMR and ^{1}H NMR experiments were conducted exclusively at pH = 11.5 so that the reaction of borate or phenylboronate with fully protonated diol could be studied directly, as described in the experimental section (Sections 3.2 and 3.3). Since the diol is not acidic, reactant concentrations can be quite high and the ionic strength can still be maintained at 0.10M.

Since ^{11}B NMR signals of substituted boronate ions ($RB(OH)_3^-$), such as phenylboronate ion (ϕB^-), are relatively broad and often overlap with the resonances of the borate complex ions, ^{1}H NMR spectroscopy is frequently the method of choice for these systems. ^{11}B NMR spectroscopy is particularly useful for $B(OH)_4^-$ systems because the borate resonance is quite sharp and adequate separation of the resonances makes integration much more accurate. Both techniques were used to study 1:1 complex formation in the B^- / H_2E and B^- / H_2P systems and excellent agreement was found for K_1, $\Delta H°$ and $\Delta S°$ for each system.

Stability constants (K_1) for 1:1 borate complex formation reactions were calculated using eqn. 3-14 for both ^{11}B NMR and ^1H NMR experiments. Stability constants (K_2) for 1:2 borate complex formation were calculated using the three methods described in Section 3.2 (eqns. 3-19, 3-22 and 3-23). Excellent agreement (± 10%) was found among the three independent methods. The thermodynamic parameters ($\Delta H°$ and $\Delta S°$) for 1:1 and 1:2 complexation reactions were determined by measuring the temperature dependence of the appropriate stability constants as described in Chapter 3 (Sections 3.4 and 3.5).

Stability constants and thermodynamic parameters for the various borate complexation reactions with diols are presented in Table 4.2 (p. 102). The error associated with stability constants is ± 10%. Errors associated with the thermodynamic parameters ($\Delta H°$ and $\Delta S°$) were determined from the variances [128] of the slope and intercept of the appropriate van't Hoff plots and are specifically included in Table 4.2.

Since ^{11}B NMR and ^1H spectra, van't Hoff plots and distribution diagrams are all very similar for these systems, it is not necessary to include every spectrum and diagram associated with each system. The borate (B^-) / 1,2-propanediol (H_2P) system is presented as representative for borate / diol interactions at high pH.

The ^1H NMR spectrum for this system under conditions {$(B^-)_0$ = 0.10 M, $(H_2P)_0$ = 0.13 M)} in which only 1:1 complexation is important was given in Fig. 3.1. The spectral assignment and method of stability constant determination from ^1H NMR spectra are described in detail in Section 3.3.

The ^{11}B NMR spectrum for this system under similar conditions is given in Fig. 4.2. At these concentrations, only two resonances are observed. The peak

at -18 ppm is due to $B(OH)_4^-$ and the downfield peak (-14 ppm) is assigned to the 1:1 complex (BP^-). Direct integration of these peaks allows the calculation of the stability constant for 1:1 complex (BP^-) formation using eqn. 3.14. A trace amount (<1% by integration) of the 1:2 complex (BP_2^-) can be seen at ~-11 ppm by careful inspection of Fig. 4.2. By simply decreasing the concentration of B^- (~0.05 M) and increasing the H_2P concentration (~0.50 M), the ^{11}B NMR spectrum shown in Fig. 4.3 can be easily integrated for B^-, BP^- and BP^-_2. The chemical shifts of B^- and BP^- remain unchanged with the BP_2^- resonance growing in at -11 ppm. The stability constant (K_2) for 1:2 complex formation can be determined directly from the relative integration of the three peaks (B^-, BP^- and BP_2^-) using the three independent calculation methods described in Section 3.2 (eqns. 3-19, 3-22 and 3-23). Excellent agreement (± 10%) among these independent calculations was found for all of the borate / diol systems studied by ^{11}B NMR. This agreement is a critical validation of the accuracy of the K_1 and K_2 values for each system.

Fig. 4.4 shows the distribution diagram (Section 3.6) for the borate (B^-) / 1,2 propanediol (H_2P) system calculated for the experimental conditions used in the ^{11}B NMR experiments just described. Fig. 4.4(a) shows the distribution of equilibrium species calculated with 0.10M concentrations for each reactant. Notice that while the concentration of BP_2^- is very small, it is non-zero. This accounts for the trace amount of BP_2^- seen in Fig. 4.2. Fig. 4.4(b) shows the distribution of equilibrium species calculated for a much higher $(H_2P)_o$ / $(B^-)_o$

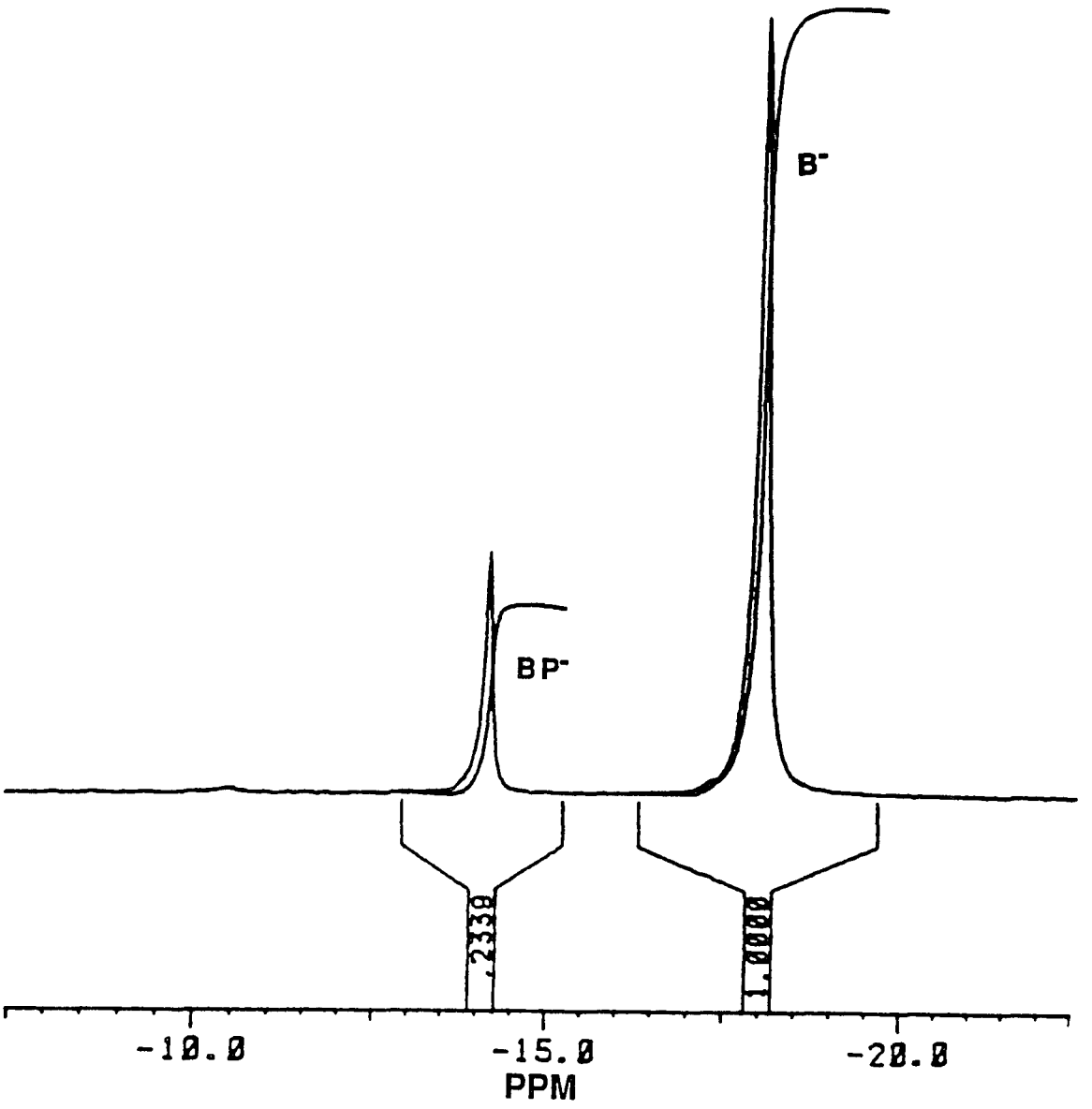

Figure 4.2 ^{11}B NMR spectrum for the borate ($(B(OH)_4^-)_o$= 0.10M) / 1,2-propanediol ($(H_2P)_o$ = 0.10M) system at pH(D) = 11.5. All solutions were prepared in 20% D_2O / H_2O (v/v). T = 298K. Chemical shifts are relative to external 0.15M boric acid in 20% D_2O / H_2O (v/v) at pH(D) = 2.0. The bracketed numbers are the relative integrations.

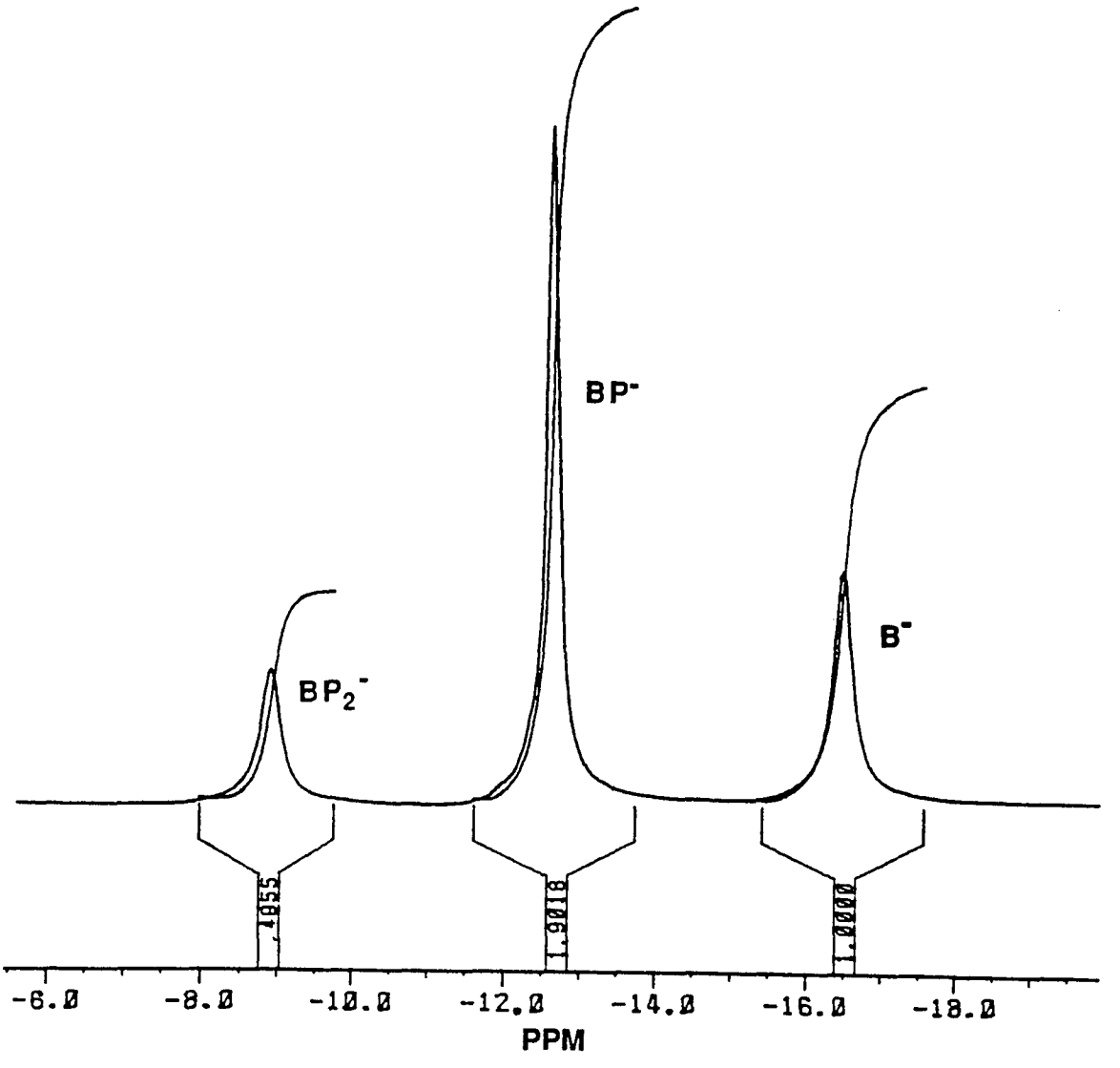

Figure 4.3 ^{11}B NMR spectrum for the borate ($(B(OH)_4^-)_o$= 0.046M) / 1,2-propanediol ($(H_2P)_o$ = 0.52M) system at pH(D) = 11.5. All solutions were prepared in 20% D_2O / H_2O (v/v). T = 298K. Chemical shifts are relative to external 0.15M boric acid in 20% D_2O / H_2O (v/v) at pH(D) = 2.0. The bracketed numbers are the relative integrations.

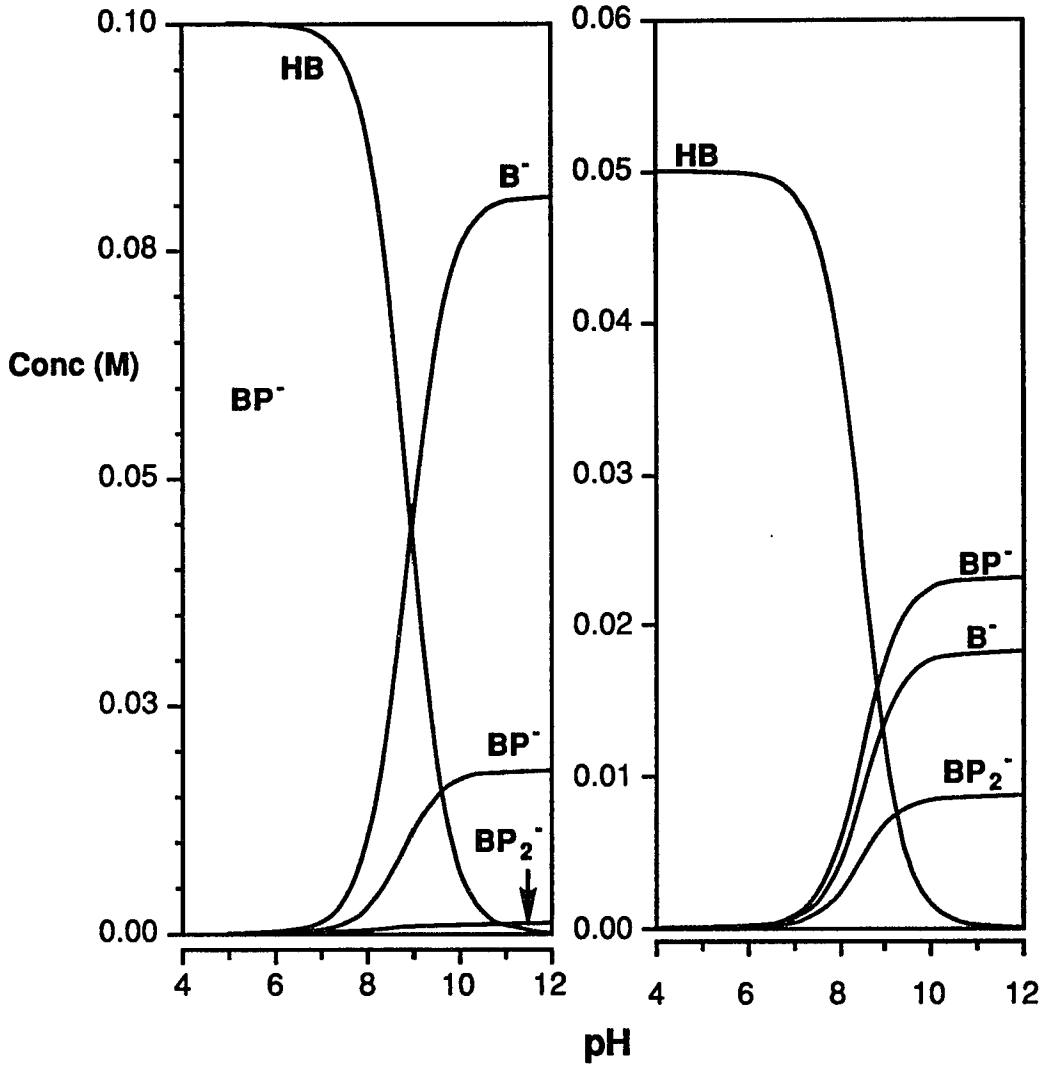

Figure 4.4: Distribution diagram for the borate / 1,2-propanediol system: **a)** *left)* $(B(OH)_4^-)_o$= 0.10M, $(H_2P)_o$ = 0.10M. **b)** *right)* $(B(OH)_4^-)_o$= 0.05M, $(H_2P)_o$ = 0.50M. Calculated using the K_1 and K_2 values given in Table 4.2.

ratio. Both distribution diagrams show that no complexation (1:1 or 1:2) occurs in acidic solution for diol systems and that above pH ~ 11 both [BP^-] and [BP_2^-] level off. Lastly, Fig. 4.4(b) shows that the ratio of [BP_2^-] / [BP^-] is not a function of pH for non acidic ligands such as diols. This can be easily explained by solving the K_2 expression for the ratio [BP_2^-] / [BP^-].

$$H_2P + BP^- \leftrightarrow BP_2^- + 2\,H_2O \;; \quad K_2$$

$$\frac{[BP_2^-]}{[BP^-]} = K_2\,[H_2P] \qquad (4\text{-}1)$$

Since diols, such as H_2P, are not acidic, neither K_2 nor [H_2P] is explicitly a function of pH and, therefore, the ratio of [BP_2^-] to [BP^-] is also independent of pH.

The van't Hoff plot used to determine $\Delta H°$ and $\Delta S°$ for the reaction $B^- + H_2P \leftrightarrow BP^- + 2\,H_2O$ is given in Fig. 4.5. Experimental data points from both ^1H NMR and ^{11}B NMR are included.

There have been several other ^{11}B NMR spectroscopic studies [45-48, 51] of equilibrium constants for reactions of diols with $B(OH)_4^-$ at room temperature. Although we are in generally good agreement with van Duin and co-workers [47, 51], other studies [46, 48] give values for the $B(OH)_4^-$ / H_2P reaction which

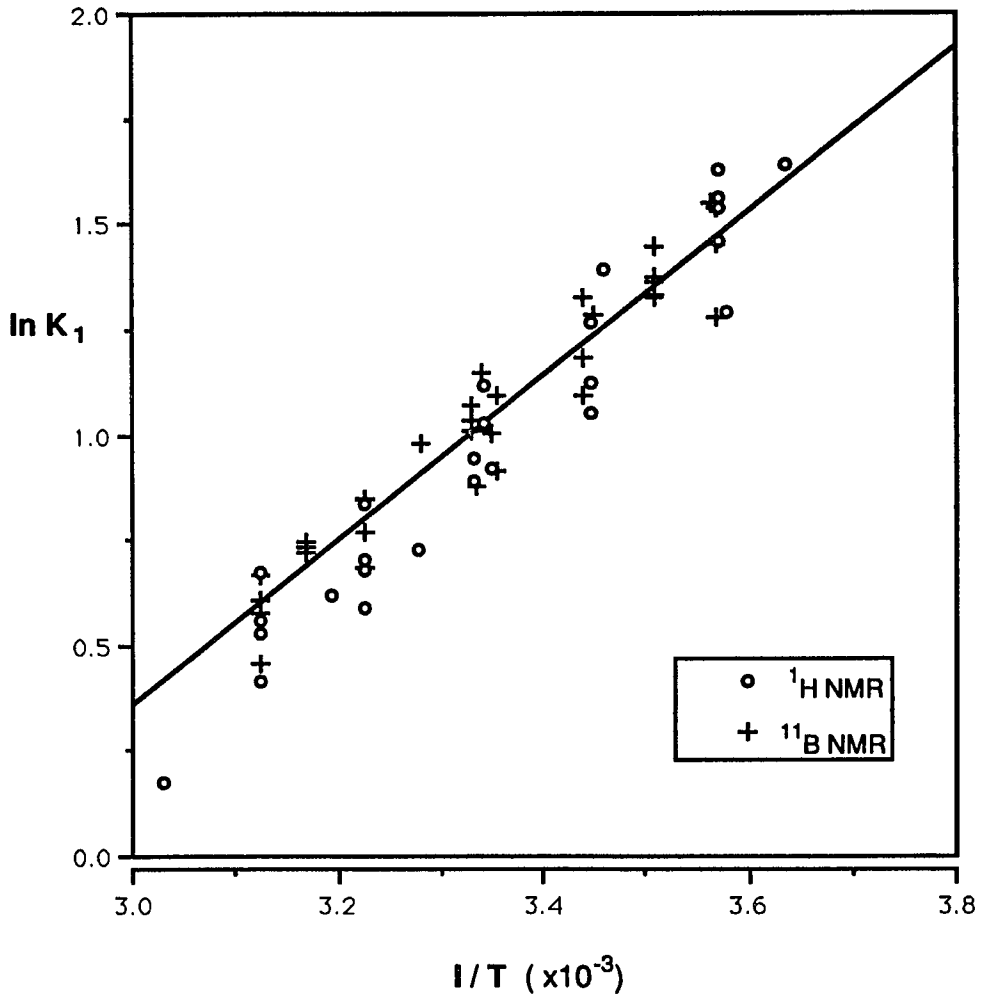

Figure 4.5: van't Hoff plot for the $B(OH)_4^-$ / 1,2-propanediol system.

differ. Experimental conditions in these studies were quite different from ours, with ionic strength being as high as 3M [45, 47, 51] and borate concentration being as high as 0.6 M [45].

Table 4.2 : Stability constants and thermodynamic parameters for 1:1 and 1:2 complexation reactions of boronate ions (B^- and ϕB^-) with 1,2-diols (H_2X).

$$H_2X + B^- \leftrightarrow BX^- + 2\,H_2O \qquad K_1$$

$$H_2X + BX^- \leftrightarrow BX_2^- + 2\,H_2O \qquad K_2$$

$$H_2X + \phi B^- \leftrightarrow \phi BX^- + 2\,H_2O \qquad K_1$$

Reaction	K (298K)	$\Delta H°$ (kJ / mol)	$\Delta S°$ (J / mol K)	NMR method
$H_2E + B^-$	1.4	-18 (±2)	-58 (±8)	^1H, ^{11}B
$H_2E + BE^-$	0.18	-3 (±3)	-24 (±10)	^{11}B
$H_2P + B^-$	2.8	-17 (±1)	-50 (±2)	^1H, ^{11}B
$H_2P + BP^-$	0.82	-15 (±3)	-49 (±7)	^{11}B
$H_2E + \phi B^-$	2.4	-20 (±3)	-60 (±9)	^1H

where $B^- = B(OH)_4^-$, $\phi B^- = \phi B(OH)_3^-$, H_2E = 1,2-ethanediol and H_2P = 1,2-propanediol. The error associated with the stability constants K_1 and K_2 is ± 10%. Numbers in parentheses denote the standard deviation (±s).

α-Hydroxy Carboxylic Acids. Stability constants (K_1 and K_2) and thermodynamic parameters were determined for the reaction of $B(OH)_4^-$ with both glycolic acid (H_2G) and lactic acid (H_2L).

Near neutral pH, only 1:1 borate / α-hydroxy carboxylic acid complexes are observed. At pH ~7, essentially all uncomplexed boron is present as $B(OH)_3$ (HB), not as B^-. Similarly, since the pK_a values of α-hydroxy carboxylic acids are much less than 7, all uncomplexed H_2X is present as HX^-. The reaction of HB with HX^- to form the 1:1 complex (BX^-) is shown below:

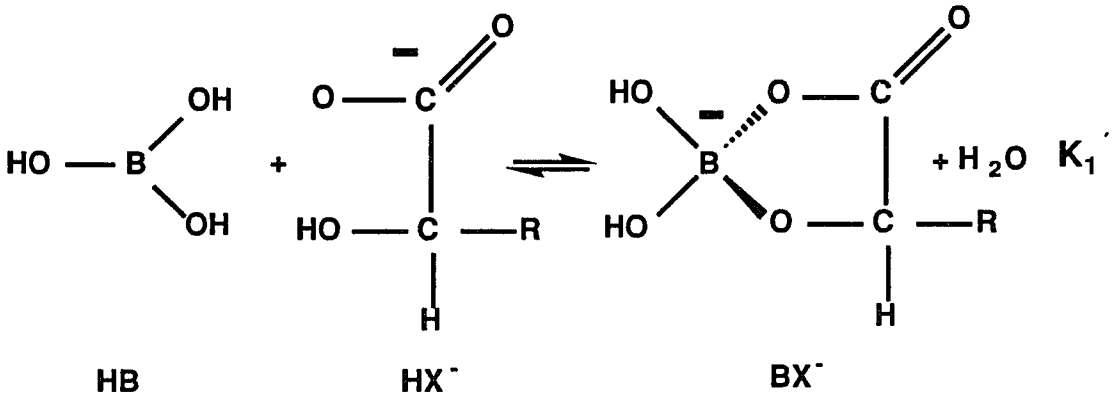

where R = H (glycolic acid) or CH_3 (lactic acid). At low reactant concentrations (≤ 0.10 M) and pH ~ 7, the ^{11}B NMR spectrum (Fig. 4.6c, p109) contains only two resonances, one for free HB (δ = 0) and one for the 1:1 complex, BX^- (δ = - 12 ppm). Direct integration of the ^{11}B NMR spectrum under these conditions affords the calculation of the equilibrium constant (K_1') for the reaction $B(OH)_3 + HX^- \leftrightarrow BX^- + H_2O$. The measurement of K_1' as a function of

temperature (van't Hoff method) gives $\Delta H°$ and $\Delta S°$ for this reaction. Since we have chosen to express all equilibria and thermodynamic parameters in terms of the reaction of $B(OH)_4^-$ with H_2X, the experimentally determined values of K_1', $\Delta H°$ and $\Delta S°$ are easily converted to K_1, $\Delta H_1°$ and $\Delta S_1°$ using Hess's Law as follows:

$B(OH)_3 + HX^- \leftrightarrow BX^- + H_2O$	K_1',	$\Delta H°$,	$\Delta S°$
$B(OH)_4^- + H_3O^+ \leftrightarrow B(OH)_3 + 2\,H_2O$	$1 / K_{HB}$,	$-\Delta H_{HB}°$,	$-\Delta S_{HB}°$
$H_2X + H_2O \leftrightarrow HX^- + H_3O^+$	K_{H2X},	$\Delta H_{H2X}°$,	$\Delta S_{H2X}°$
$B(OH)_4^- + H_2X \leftrightarrow BX^- + 2\,H_2O$	K_1,	$\Delta H_1°$,	$\Delta S_1°$

Therefore,

$$K_1 = (K_1' K_{H2X}) / K_{HB},$$

$$\Delta H_1° = \Delta H° + \Delta H_{H2X}° - \Delta H_{HB}°$$

$$\Delta S_1° = \Delta S° + \Delta S_{H2X}° - \Delta S_{HB}°$$

The ionization constants and thermodynamic parameters needed in these calculations were discussed previously (Sect. 4.1) and are contained in Table 4.1. The results for the $B(OH)_4^- / H_2G$ and $B(OH)_4^- / H_2L$ systems expressed in terms of the reaction $B(OH)_4^- + H_2X \leftrightarrow BX^- + 2\,H_2O$ are presented in Table 4.3.

Table 4.3 : Stability constants and thermodynamic parameters for 1:1 and 1:2 complexation reactions between borate ion (B^-) and α-hydroxy carboxylic acids (H_2X).

$$H_2X + B^- \leftrightarrow BX^- + 2\,H_2O \qquad K_1$$

$$H_2X + BX^- \leftrightarrow BX_2^- + 2\,H_2O \qquad K_2$$

Reaction	K (298K)	ΔH° (kJ / mol)	ΔS° (J / mol K)
$H_2G + B^-$	1.3×10^5	-43 (±2)	-46 (±6)
$H_2G + BG^-$	10	8 (±3)	45 (±10)
$H_2L + B^-$	7.2×10^5	-51 (±2)	-60 (±5)
$H_2L + BL^-$	61	11 (±4)	74 (±10)

where, $B^- = B(OH)_4^-$, H_2G = glycolic acid and H_2L = lactic acid. The error associated with the stability constants K_1 and K_2 is ± 10%. Numbers in parentheses denote the standard deviation (±s).

Stability constants (K_2) and thermodynamic parameters for the reaction of the 1:1 complex (BX^-) with a second molecule of H_2X, shown below, were determined for the $B(OH)_4^-$ / H_2G and $B(OH)_4^-$ / H_2L systems.

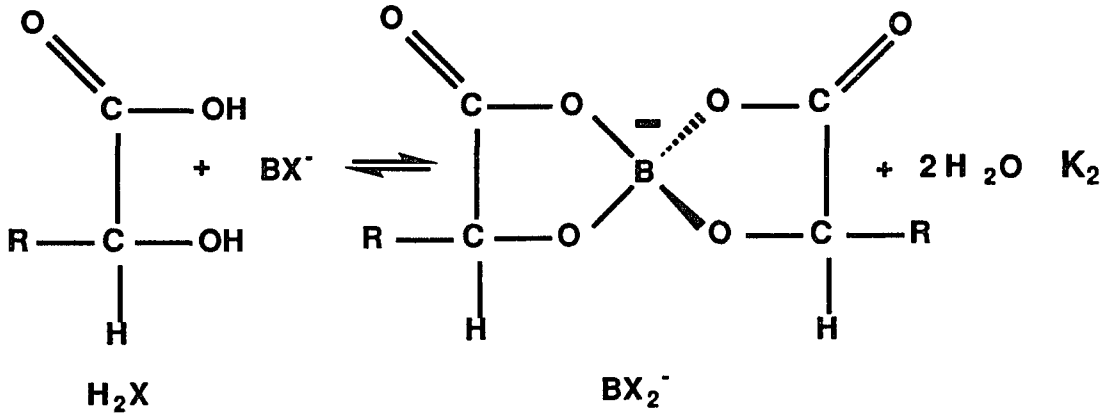

The determination of K_2 is facilitated by the fact that formation of BX_2^- is strongly favored in acidic media [34,121]. At low pH (~2.0) and approximately equimolar reactant concentrations ($\leq$ 0.10M) , BX_2^- is the only complex species present (Fig. 4.6a, p109). Under these conditions, the overall reaction is $B(OH)_3 + 2H_2X \leftrightarrow BX_2^- + H_3O^+ + 2H_2O$. The overall equilibrium constant, K_T (= K_1 K_2), for this reaction can be determined by ^{11}B NMR at any temperature from the relative integration of the BX_2^- peak (δ = -9 ppm) to the free $B(OH)_3$ peak (δ = 0 ppm), as long as the pH has been precisely determined. The temperature dependence of K_T gives $\Delta H_T°$ and $\Delta S_T°$. K_2 , $\Delta H_1°$ and $\Delta S_1°$ can be easily calculated as follows:

$B(OH)_3 + 2H_2X \leftrightarrow BX_2^- + H_3O^+ + 2H_2O$	$K_T,\ \Delta H_T^\circ,\ \Delta S_T^\circ$
$B(OH)_4^- + H_3O^+ \leftrightarrow B(OH)_3 + 2H_2O$	$1/K_{HB},\ -\Delta H_{HB}^\circ,\ -\Delta S_{HB}^\circ$
$BX^- + 2H_2O \leftrightarrow B(OH)_4^- + H_2X$	$1/K_1,\ -\Delta H_1^\circ,\ -\Delta S_1^\circ$
$BX^- + H_2X \leftrightarrow BX_2^- + 2H_2O$	$K_2,\ \Delta H_2^\circ,\ \Delta S_2^\circ$

Therefore, $K_2 = K_T / (K_1 K_{HB})$,

$$\Delta H_2^\circ = \Delta H_T^\circ - \Delta H_{HB}^\circ - \Delta H_1^\circ$$

$$\Delta S_2^\circ = \Delta S_T^\circ - \Delta S_{HB}^\circ - \Delta S_1^\circ$$

The results (K_2, ΔH_2° and ΔS_2°) for the $B(OH)_4^-$ / H_2G and $B(OH)_4^-$ / H_2L systems were previously presented in Table 4.3.

Since there is a small concentration of HX^- at low pH, this must be explicitly taken into account in the mass balance equations which are used in calculating the equilibrium constants. In these particular experiments, the correction for HX^- is quite small ($\leq$ 2% of total free ligand concentration). We have also shown [39] for polyols that equilibrium constants and thermodynamic parameters are independent of solvent composition (D_2O/H_2O) within experimental error. Therefore, in calculations of equilibrium constants and in Hess's Law determinations of thermodynamic parameters, we have used the aqueous values [129] of pK_a , ΔH° and ΔS° given in Table 4.1.

The errors specifically given in Table 4.3 for ΔH° and ΔS° are the sums of the errors associated with each reaction used in the Hess's Law determination of

that parameter. Errors associated with thermodynamic parameters derived from variable temperature ^{11}B NMR experiments were determined from the variances [128] of the slope and intercept of the appropriate van't Hoff plot.

Fig. 4.6 shows the ^{11}B NMR spectra for the boric acid ($(HB)_o$= 0.10M) / lactic acid ($(H_2L)_o$= 0.11M) system at various pH values. As previously mentioned, the HB / B^- interconversion is rapid on the NMR time scale and, as a consequence, only one pH dependent peak is observed for uncomplexed boron [44]. Fig. 4.7 shows the distribution diagram for the boric acid (HB) / lactic acid (H_2L) system calculated with 0.10 M concentration for each reactant. The agreement between the ^{11}B NMR spectra (experimental) and the distribution diagram (calculated) shows the accuracy of the stability constants used in the calculation.

The dramatic pH dependence found in the distribution diagrams of borate / α - hydroxy carboxylic acid systems is illustrated using the B^- / H_2L system in Fig. 4.7. The fact that no complex formation (1:1 or 1:2) occurs above pH ~ 7 is due to the acidic nature of complexes formed from α - hydroxy carboxylate ligands as follows.

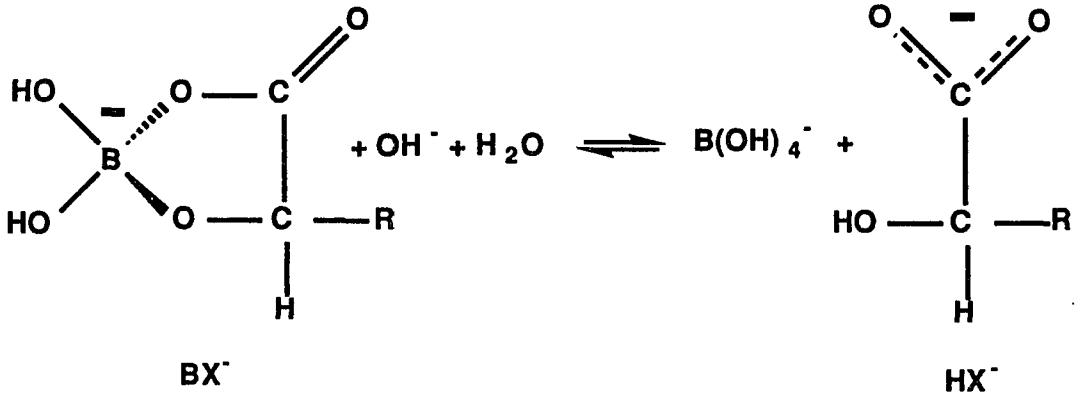

BX^- HX^-

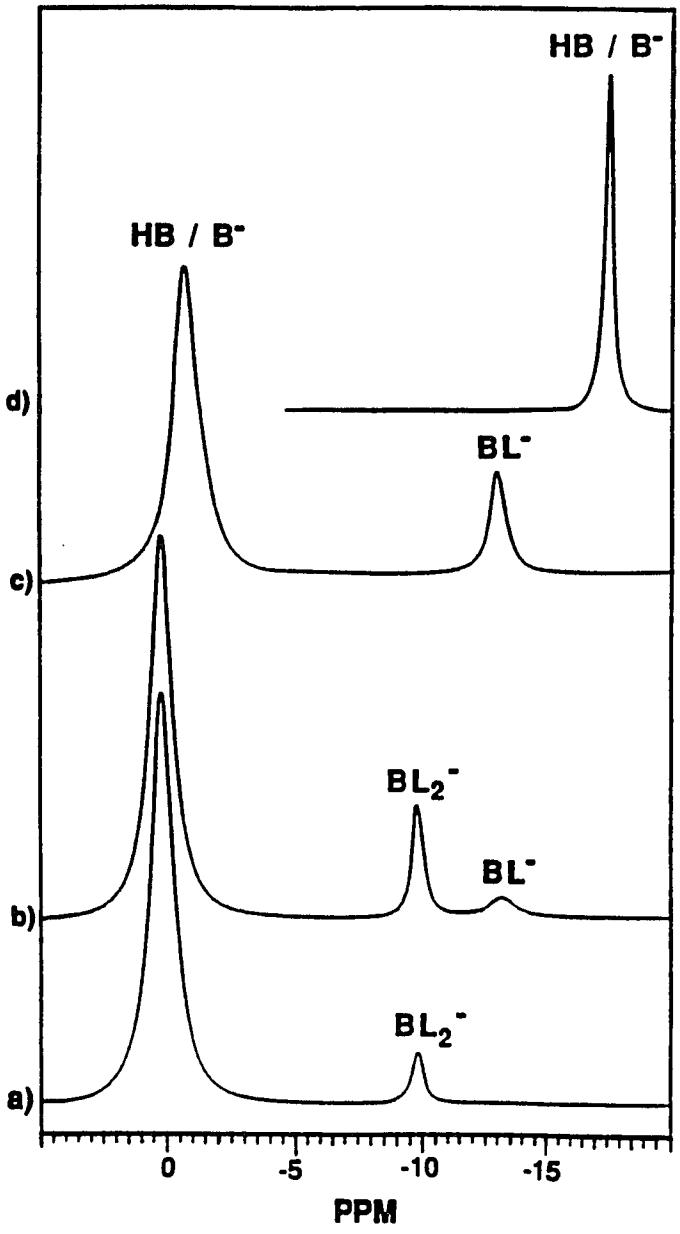

Figure 4.6 ^{11}B NMR spectra for the boric acid ($(HB)_o$= 0.10M) / lactic acid ($(H_2L)_o$ = 0.11M) system at various pH values: (**a**) pH(D) = 2.0 , (**b**) pH(D) = 3.3, (**c**) pH(D) = 7.8, (**d**) pH(D) = 11.0, All solutions were prepared in 20% D_2O / H_2O (v/v). T = 298K. Chemical shifts are relative to external 0.15M boric acid in 20% D_2O / H_2O (v/v) at pH(D) = 2.0 .

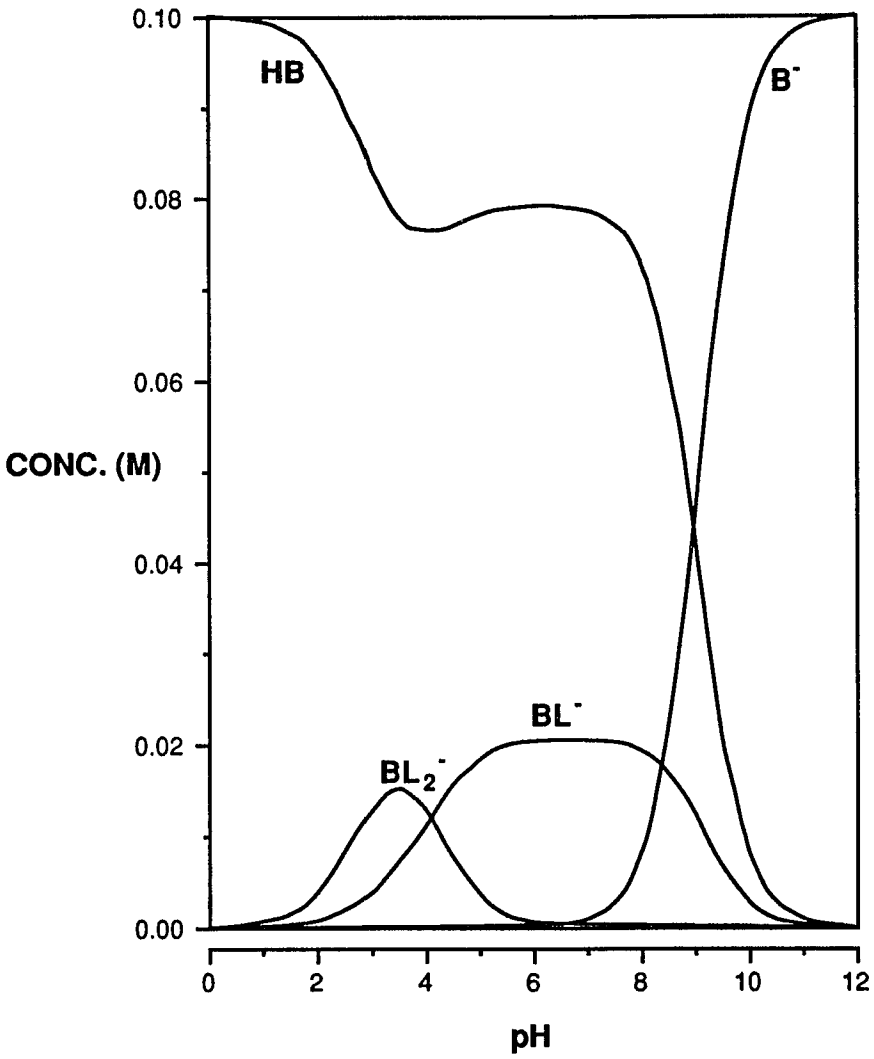

Figure 4.7: Distribution diagram for the boric acid (HB) / lactic acid (H_2L) system, calculated with 0.10M concentration for each reactant (using the K_1 and K_2 values given in Table 4.3).

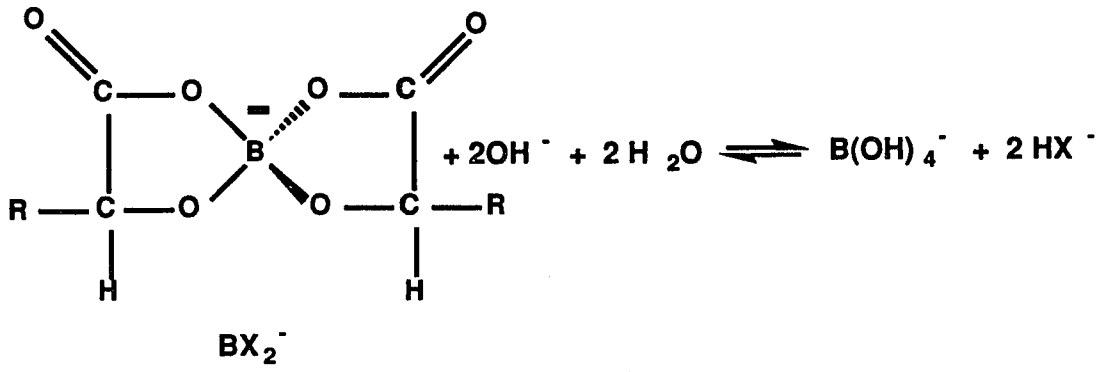

BX_2^-

The dissociation of BL^- and BL_2^- at high pH can be explained thermodynamically in terms of these base hydrolysis reactions. Fig. 4.7 also shows that, unlike diols, the ratio of the 1:2 to 1:1 complex is a function of pH, with the 1:2 complex (BL_2^-) predominating at low pH (~ 2) and the 1:1 complex (BL^-) at pH ~ 7. This pH dependence can be explained by solving the K_2 expression for the ratio $[BL_2^-] / [BL^-]$.

$$\frac{[BL_2^-]}{[BL^-]} = K_2 [H_2L] \qquad (4\text{-}2)$$

Eqn. 4-2 is very similar to eqn. 4-1, which was previously used to explain the lack of pH dependence of $[BP_2^-] / [BP^-]$ for diol systems. For borate / α - hydroxy carboxylic acid systems such as B^- / H_2L, however, the ligand itself is acidic.

$$H_2L + 2H_2O \leftrightarrow HL^- + H_3O^+ \qquad K_{H2L}$$

Solving the K_{H2L} expression for $[H_2L]$ gives eqn. 4-3,

$$[H_2L] = \frac{[H_3O^+][HL^-]}{K_{H2L}} \qquad (4\text{-}3)$$

and substituting eqn. 4-3 back into eqn. 4.2 gives eqn. 4-4.

$$\frac{[BL_2^-]}{[BL^-]} = (K_2 / K_{H2L})\,[H^+]\,[HL^-] \qquad (4\text{-}4)$$

Eqn. 4-4 shows: 1) that the ratio of $[BL_2^-] / [BL^-]$ is proportional to $[H_3O^+]$ and, therefore, is exponentally related to pH; 2) the ratio of $[BL_2^-] / [BL^-]$ is independent of $(HB)_o$; and, 3) the ratio $[BL_2^-] / [BL^-]$ is inversely proportional to the K_a of the ligand, lactic acid (K_{H2L}).

Pizer and Selzer previously determined K_1 and K_2 for H_2L by pH titration methods [34]. While agreement between our two determinations of K_2 is within reported experimental errors, the present study shows that the former value of K_1 was too low. The K_1 and K_2 values reported in this study (Table 4.3) for the $B(OH)_4^- / H_2G$ are in excellent agreement with the literature [51].

Oxalic Acid. The one dicarboxylic acid included in this study is oxalic acid (H_2Ox). The reaction of borate ion with fully protonated oxalic acid is shown below.

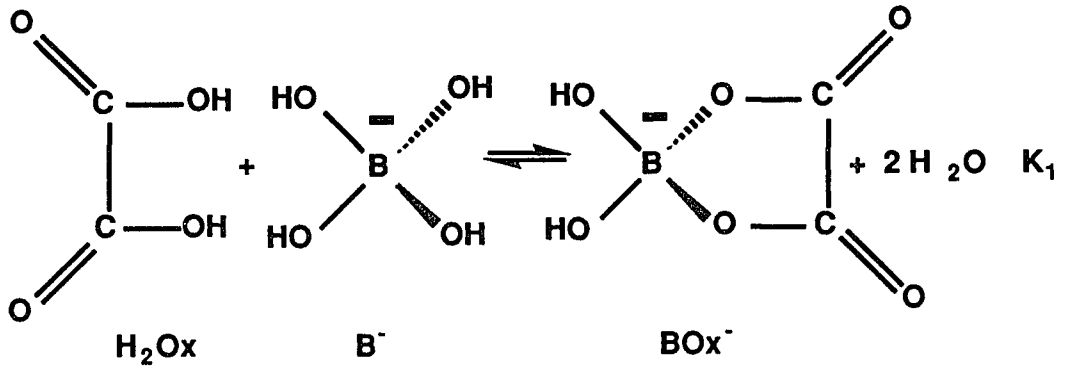

By selecting a pH intermediate between pK_{H2Ox} (1.13) and pK_{HOx^-} (3.38), spectra can be obtained under conditions where HOx^- is the predominant uncomplexed form of the ligand. At this pH (~ 2.25), the reaction HB + HOx^- $\leftrightarrow$ BOx^- + H_2O (K_1') can be studied directly by ^{11}B NMR spectroscopy. The data analysis, therefore, conforms exactly to the determination of K_1, $\Delta H_1°$ and $\Delta S_1°$ for borate / α-hydroxy carboxylic acids at near neutral pH. The relatively small concentrations of H_2X and X^{2-} are explicitly taken into account in the relevant mass balance equations.

Perhaps the most surprising result in this system is that there is no evidence for 1:2 complex (BOx_2^-) formation at any pH, even at ligand concentrations as high as 1.0 M. This result is consistent with the literature [51]. Table 4.4 gives the stability constant and thermodynamic parameters for the

borate / oxalic acid system. Figure 4.8 shows the distribution diagram for the boric acid (HB) / oxalic acid system calculated with both reactant concentrations equal to 0.10M. Fig. 4.8 shows that the maximum in complex formation (BOx^-) coincides with the maximum in HOx^- concentration.

Table 4.4 : Stability constants and thermodynamic parameters for the 1:1 complexation reaction between borate ion (B^-) and oxalic acid (H_2Ox).

$$H_2X + B^- \leftrightarrow BX^- + 2\,H_2O \qquad K_1$$

Reaction	K (298K)	$\Delta H°$ (kJ / mol)	$\Delta S°$ (J / mol K)
$H_2Ox + B^-$	1.6×10^8	-46 (±2)	4 (±5)

The error associated with the stability constant K_1 is ± 10%. Numbers in parentheses denote the standard deviation (±s).

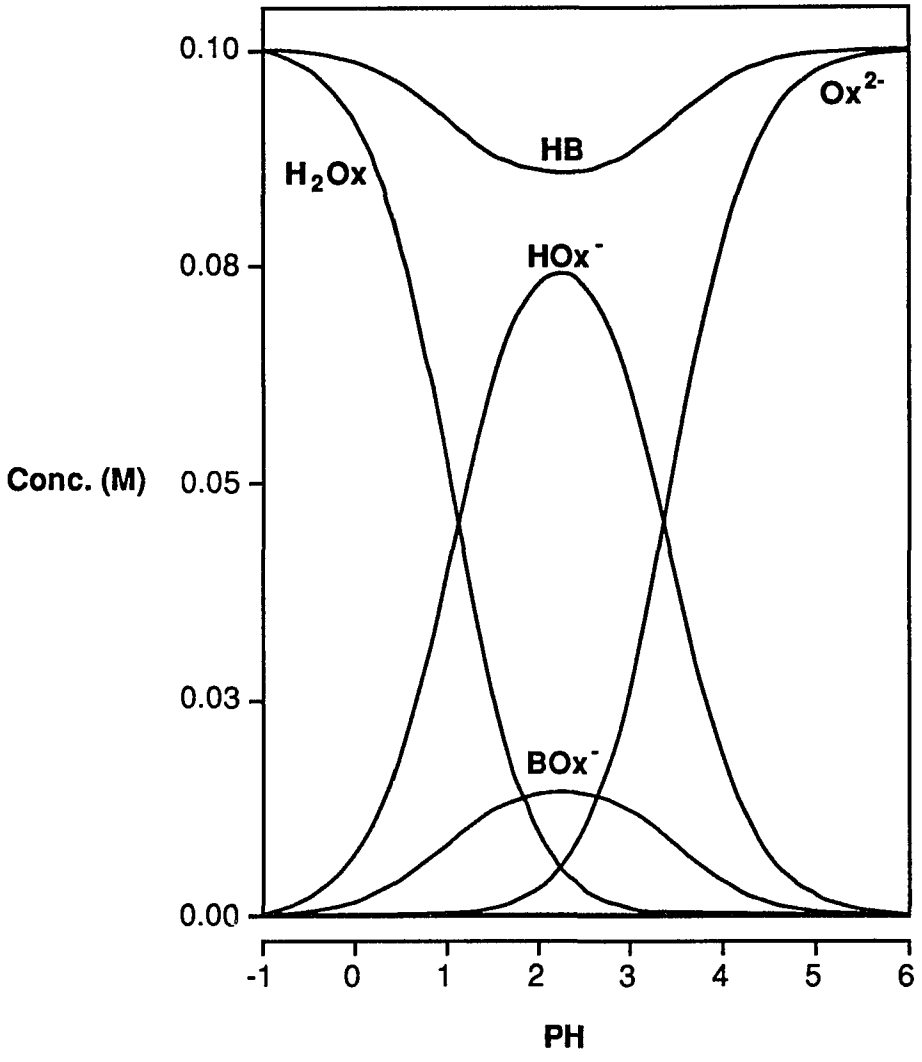

Figure 4.8: Distribution diagram for the boric acid (HB) / oxalic acid (H_2Ox) system, calculated with 0.10M concentration for each reactant (using the K_1 value given in Table 4.4 and $K_2 = 0$).

Mixed Ligand Systems. At pH ~ 7 there is no measurable concentration of 1:1 borate complexes with diols even at quite high diol concentrations (~0.8M). There are, however, significant concentrations of BX^- at reactant concentrations ≤ 0.10M if X is an α-hydroxy carboxylic acid. By adding a diol to a solution which contains boric acid and an α-hydroxy carboxylic acid near neutral pH, an ^{11}B NMR peak for a mixed ligand complex (BXY^-) can easily be assigned (δ = ~-9 ppm) and integrated with respect to the free boric acid peak (δ = 0 ppm) and the BX^- (X = α-hydroxy carboxylate) peak at (δ = ~ -13). Stability constants and thermodynamic parameters for the formation of a mixed ligand complex (BXY^-) from the reaction of a 1:1 α-hydroxy carboxylic acid complex (BX^-) with a polyol (H_2Y) can be calculated directly from the ^{11}B NMR

$$H_2Y + BX^- \leftrightarrow BXY^- + 2\,H_2O$$

integration and mass balance by conducting a series of such experiments over an appropriate temperature range.

Stability constants and thermodynamic parameters were determined in this way for both the boric acid (HB) / lactic acid (H_2L) / 1,2-ethanediol (H_2E) system and the HB / H_2L / 1,2-propanediol (H_2P) system.

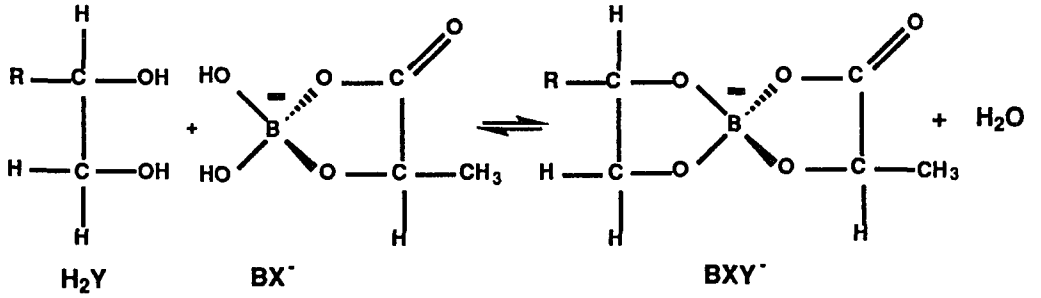

where R = H (1,2-ethanediol) or R = CH_3 (1,2-propanediol).

The results for these reactions and the results calculated for the related reaction $H_2X + BY^- \leftrightarrow BXY^- + 2\ H_2O$ are contained in Table 4.5 (p 122). The stability constants and thermodynamic parameters for the related reactions were calculated using the appropriate values from Tables 4.2, 4.3 and 4.5 in the following Hess's Law scheme:

$$\begin{aligned} H_2Y + BX^- &\leftrightarrow BXY^- + 2\,H_2O \\ H_2X + B^- &\leftrightarrow BX^- + 2\,H_2O \\ 2\,H_2O + BY^- &\leftrightarrow B^- + H_2Y \\ \hline H_2X + BY^- &\leftrightarrow BXY^- + 2\,H_2O \end{aligned}$$

where $H_2X = H_2L$ and $H_2Y = H_2E$ or H_2P.

Fig. 4.9(c) shows the ^{11}B NMR spectrum of the mixed ligand system $B(OH)_3$ / H_2L / H_2P at pH = 7.1. Fig. 4.9(a) shows the spectrum of the binary system $[HB]_o = 0.05M$, $[H_2P]_o = 0.70M$ at pH(D) = 7.1. Under these conditions no complexation occurs and the HB / B^- peak ($\delta = 0$) is the lone resonance in the spectrum. Fig. 4.9(b) shows the spectrum of the binary system $[HB]_o = 0.05M$, $[H_2L]_o = 0.10M$ at the same pH. Under these conditions only 1:1 complexation occurs. The two peaks in the spectrum are the free boric acid (HB / B^-) peak (δ = 0 ppm) and the 1:1 complex (BL^-) peak (δ = -12.5 ppm). Figure 4.9(c) shows the spectrum of the ternary system under the same reactant conditions and pH as (a) and (b). The new peak at -9.6 ppm with its characteristic bis complex chemical shift can, therefore, only be assigned to the mixed ligand species BLP^-. This series of spectra shows H_2P to be relatively reactive with the

four coordinate borate complex BL^- (Fig. 4.9(c)). It is quite unreactive with trigonal boric acid (HB) under the same experimental conditions (Fig 4.9(a)).

The spectra of this mixed ligand system (4.9(c)) after the pH(D) of the solution had been adjusted to 8.2 and 9.1 are given in Figs. 4.10 and 4.11, respectively. At pH = 8.2 (Fig. 4.10), the HB / B^- peak (δ = -1) has just started its migration across the spectrum (δ =0 to -18 ppm). The 1:1 peak (δ = -13.2 ppm) has shifted slightly up field and has become substantially broadened. This resonance can be assigned as the composite peak for the two 1:1 complexes, BL^- (δ = -12.5 ppm) and BP^- (δ = -13.7 ppm). The bis complex region of the spectrum (δ = -8.5 ppm) now contains two overlapping peaks. The peak at -9.6 ppm is still assigned to the mixed ligand complex BLP^- while the peak at -10.1 ppm can only be assigned to BP_2^- at this pH. The spectrum of this system at pH =9.1 (Fig. 4.11) shows dramatic changes compared with spectra recorded at lower pH. The HB / B^- peak has now migrated all the way to -7.0 ppm. The 1:1 complex peak (δ = -13.7 ppm) is dominated by the BP^- resonance with the BL^- resonance only appearing as a shoulder at δ = -12.5 ppm. The sharp resonance at -10.1 ppm is assigned to BP_2^-. Any BLP^- (δ = -9.6 ppm) remaining at this pH can no longer be resolved due to the migration of the HB / B^- peak. By further increasing the pH of this solution to the pH previously employed in the diol studies (pH = 11.5), all traces of complex formation with H_2L disappear. The spectrum reduces to the sharp three line pattern (δ (B^-) = -17.6 ppm, δ (BP^-) = -13.6 ppm and δ (BP_2^-) = -10.1 ppm) typical of borate / diol systems at high pH.

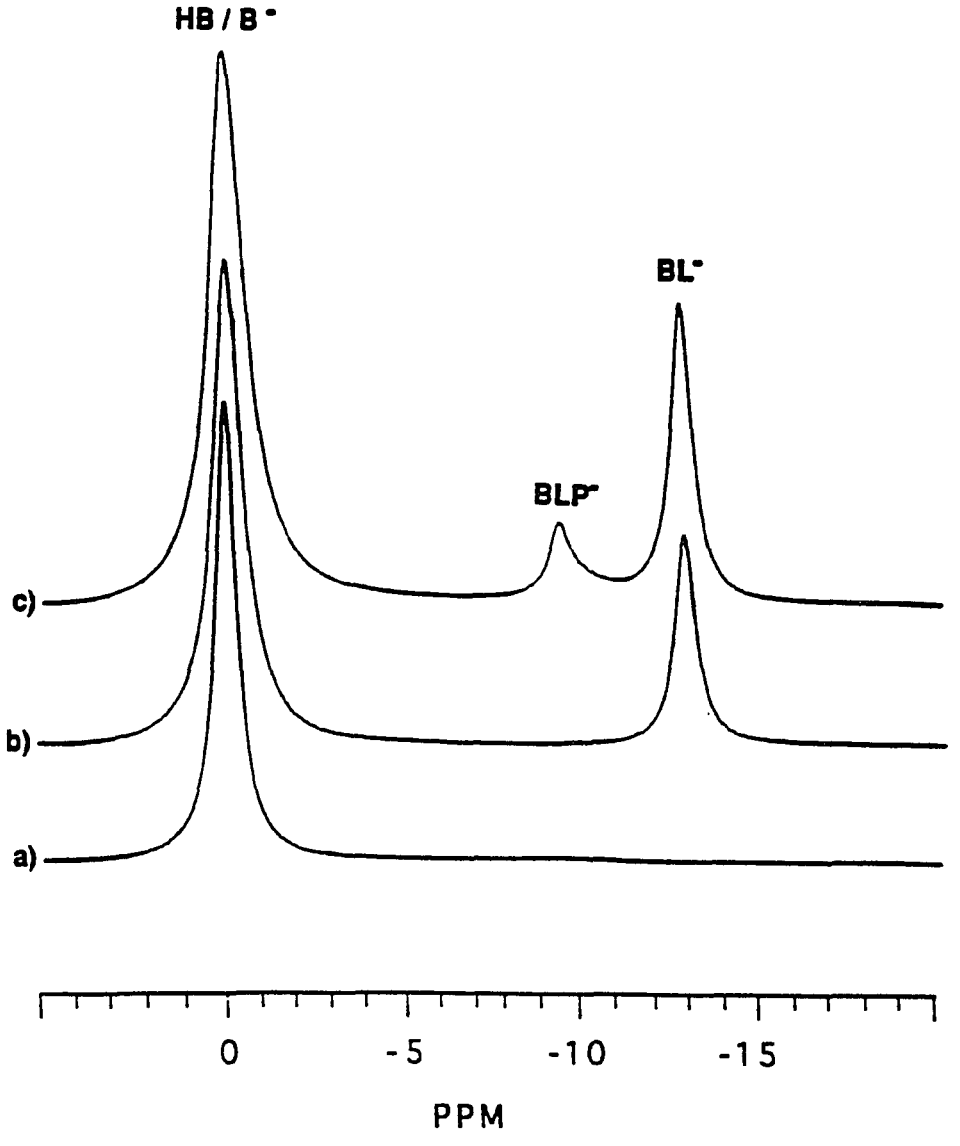

Figure 4.9 : ^{11}B NMR spectra for the mixed ligand system of boric acid (HB) / lactic acid (H_2L) / 1,2-propanediol (H_2P): (**a**) $(HB)_o$ = 0.05M, $(H_2P)_o$ =0.70M, pH(D) = 7.1, (**b**) $(HB)_o$ = 0.05M, $(H_2L)_o$ = 0.10M, pH(D) = 7.1, (**c**) $(HB)_o$ = 0.05M, $(H_2P)_o$ =0.70M, $(H_2L)_o$ =0.10M, pH(D) = 7.1. All solutions were prepared in 20% D_2O / H_2O (v/v). T = 298K . Chemical shifts are relative to external 0.15M boric acid in 20% D_2O / H_2O (v / v) at pH(D) = 2.0 .

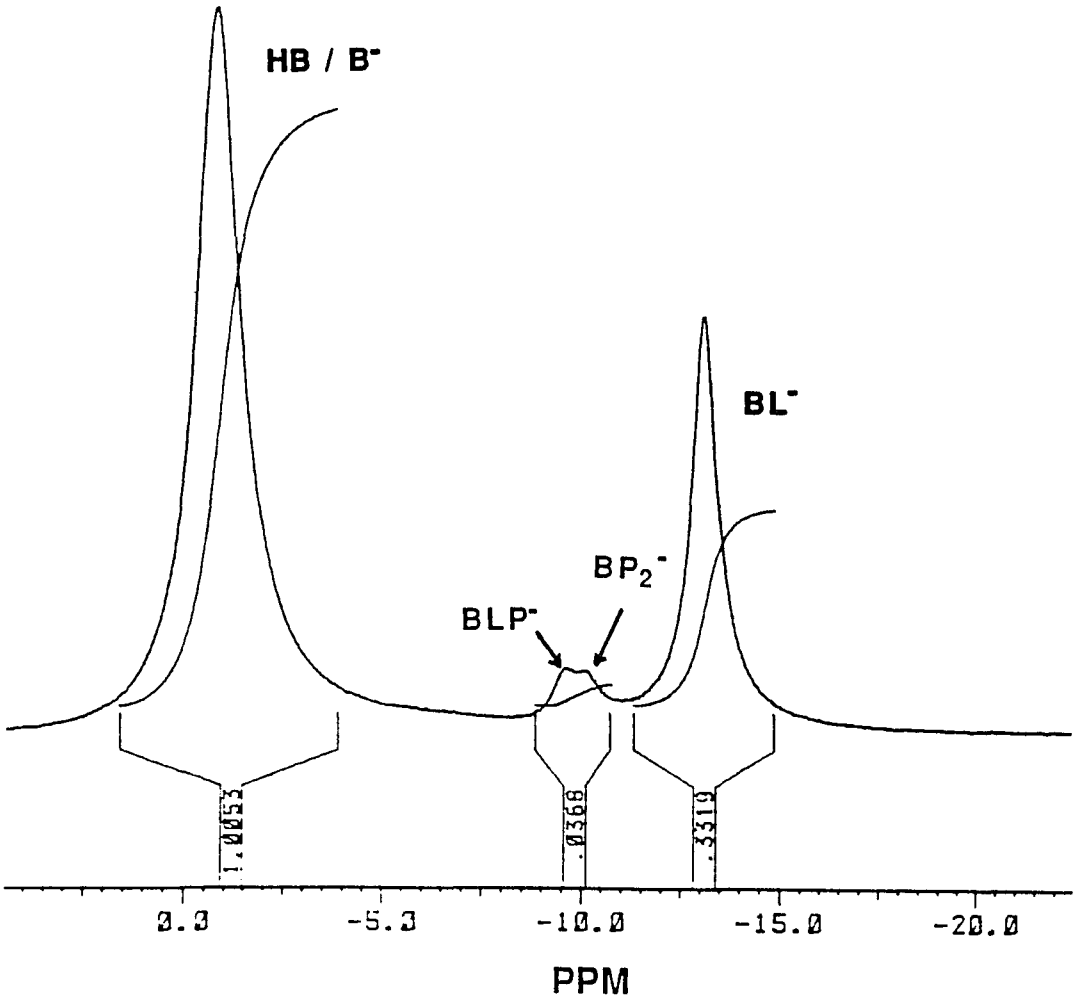

Figure 4.10 : ^{11}B NMR spectrum for the mixed ligand system of boric acid $\{(HB)_o = 0.05M)\}$ / lactic acid $\{(H_2L)_o = 0.10M)\}$ / 1,2-propanediol $\{(H_2P)_o = 0.70M\}$ at pH(D) = 8.2. All solutions were prepared in 20% D_2O / H_2O (v/v). T = 298K . Chemical shifts are relative to external 0.15M boric acid in 20% D_2O / H_2O (v / v) at pH(D) = 2.0 .

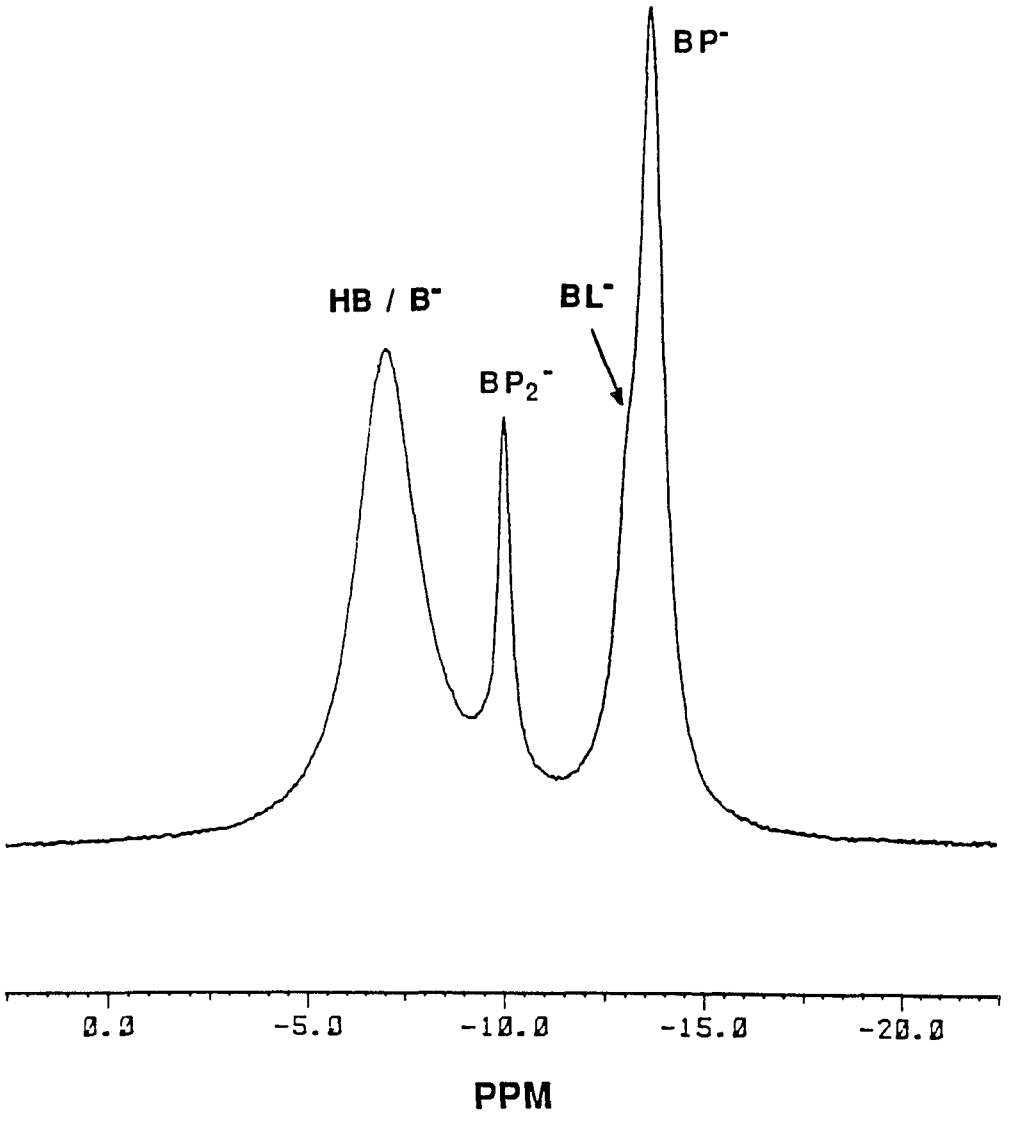

Figure 4.11 : ^{11}B NMR spectrum for the mixed ligand system of boric acid $\{(HB)_o = 0.05M)\}$ / lactic acid $\{(H_2L)_o = 0.10M)\}$ / 1,2-propanediol $\{(H_2P)_o = 0.70M\}$ at pH(D) = 9.1. All solutions were prepared in 20% D_2O / H_2O (v/v). T = 298K . Chemical shifts are relative to external 0.15M boric acid in 20% D_2O / H_2O (v / v) at pH(D) = 2.0 .

Table 4.5 : Stability constants and thermodynamic parameters for the formation of mixed ligand complexes.

$$H_2X + BY^- \leftrightarrow BXY^- + 2\,H_2O$$

Reaction	K (298K)	ΔH° (kJ / mol)	ΔS° (J / mol K)
$H_2E + BL^-$	6.5×10^{-2}	-12 (±3)	-63 (±7)
$H_2L + BE^-$	3.1×10^{4}	-45 (±3)	-65 (±7)
$H_2P + BL^-$	0.32	-5 (±3)	-27 (±8)
$H_2L + BP^-$	7.8×10^{4}	-39 (±3)	-37 (±8)

where H_2L = lactic acid, H_2E = 1,2-ethanediol and H_2P = 1,2-propanediol. The error associated with the stability constants is ± 10%. Numbers in parentheses denote the standard deviation (±s).

4.4 Summary of results

Table 4.6 is a compilation of the results presented in this chapter. The results are presented in a format in which the thermodynamics of the reactions of a particular ligand with a series of tetrahedral boron centers can be easily compared. By viewing the results in this way, the enormous effects of both boron acid and ligand acidity can be factored out. An evaluation of the effect of first ligand coordination on subsequent bis complex formation is then possible.

Disproportionation Reactions. It is useful to look at the thermodynamic data also in terms of disproportionation reactions which can be written as $2BX^- \leftrightarrow BX_2^- + B^-$. The necessary data can be obtained from Table 4.6. Table 4.7 contains results for each system.

Table 4.6: Thermodynamic parameters for particular ligands reacting with different tetrahedral boron centers. { $H_2X + BY_n^- \leftrightarrow BXY_n^- + 2\ H_2O$; where n = 0 ,1 and X = Y or $X \neq Y$ }.

Reaction	K (298K)	ΔH ° (kJ / mol)	ΔS° (J / mol K)
$H_2E + B^-$	1.4	-18 (±2)	-58 (±8)
BE^-	0.18	-3 (±3)	-24 (±10)
BL^-	6.5×10^{-2}	-12 (±3)	-63 (±7)
$H_2P + B^-$	2.8	-17 (±1)	-50 (±2)
BP^-	0.82	-15 (±3)	-49 (±7)
BL^-	0.32	-5 (±3)	-27 (±8)
$H_2G + B^-$	1.3×10^5	-43 (±2)	-46 (±6)
BG^-	10	8 (±3)	45 (±10)
$H_2L + B^-$	7.2×10^5	-51 (±2)	-60 (±5)
BL^-	61	11 (±4)	74 (±10)
BE^-	3.1×10^4	-45 (±3)	-65 (±7)
BP^-	7.8×10^4	-39 (±3)	-37 (±8)
$H_2Ox + B^-$	1.6×10^8	-46 (±2)	4 (±5)
BOx^-	0	---	---
$H_2P + \phi B^-$	2.4	-20(±3)	-60 (±9)

B^- = $B(OH)_4^-$, ϕB^- = $\phi B(OH)_3^-$, H_2E = 1,2-ethanediol ,H_2P = 1,2-propanediol, H_2G = glycolic acid, H_2L = lactic acid and H_2Ox = oxalic acid. The error associated with the stability constants is ± 10%. Numbers in parentheses denote the standard deviation (±**s**).

Table 4.7 : Thermodynamics of disproportionation.

$$2\,BX^- \leftrightarrow BX_2^- + B^-$$

REACTION	K (298K)	$\Delta H°$ (KJ/mol)	$\Delta S°$ (J/mol K)
$2\,BE^- \leftrightarrow BE_2^- + B^-$	0.13	15	34
$2\,BP^- \leftrightarrow BP_2^- + B^-$	0.29	2	1
$2\,BG^- \leftrightarrow BG_2^- + B^-$	7.7×10^{-5}	51	91
$2\,BL^- \leftrightarrow BL_2^- + B^-$	8.5×10^{-5}	62	134
$2\,BOx^- \leftrightarrow BOx_2^- + B^-$	~ 0	----	----

4.5 Discussion

In all systems, but by very different amounts, formation of BX_2^- from BX^- is characterized by a less favorable enthalpy change and a more favorable entropy change. The differences are relatively small in the case of the 1,2-diols, but remarkably large for α-hydroxy carboxylic acids. K_1/K_2 increases dramatically as the ligand becomes more acidic, and a limit is reached in the oxalic acid system in which case a 1:2 complex could not even be observed. It is clear that 1,2-diols, α-hydroxy carboxylic acids and oxalic acid represent three distinct classes of ligand and discussion of each class is presented here.

1,2-Diols. The thermodynamics of formation of 1:1 borate complexes (BX^-) were determined for the following systems: B^- / H_2P, B^- / H_2E and ϕB^- / H_2P. The principal result (Table 4.6) is that the thermodynamic parameters for the reaction of aliphatic diols with the various borate ions are quite similar. The results of a previous thermodynamic study conducted in this laboratory [36,39] show that the methylboronate ($CH_3B(OH)_3^-$) / H_2P system should also be included in this class. All four reactions are exothermic with an average value of $\Delta H° \sim -20$ kJ / mol. All the entropy changes are quite negative ($\Delta S° \sim -60$ J / mol K). This result can be attributed to a loss of ligand configurational entropy on complexation. This assertion is supported by a previous thermodynamic investigation conducted by Tihal [36,39]. In that study a comparison of the reactions of $CH_3B(OH)_3^-$ with H_2P and 1,2-dihydroxybenzene (H_2Cat), a rigid ligand, was made. H_2Cat is much more acidic than H_2P and the reaction stability

constant for this system exceeds that for the H_2P by four orders of magnitude. Surprisingly, this difference in stability constants turns out to be entirely related to a much more positive value of $\Delta S°$ and not at all to any real differences in $\Delta H°$ [39].

It is interesting to note that previous kinetic studies conducted in this laboratory [32,33] concluded that the complexation reactions of H_2Cat are likely to be characterized by a much more positive entropy of activation in the forward direction as compared with less rigid ligands. The thermodynamic results presented here are entirely in accord with the consequences of that idea. A recent thermodynamic analysis conducted by Searle and Williams [130] has estimated the "entropic cost of restricting a rotor within a hydrocarbon chain". The results for the $CH_3B(OH)_3^-$ / H_2P and $CH_3B(OH)_3^-$ / H_2Cat systems [39] yield a similar numerical value, if the difference in $\Delta S°$ between the two systems is attributed solely to the configurational entropy loss which accompanies H_2P coordination. Although this comparison is certainly not exact, it is important to acknowledge the quantitative similarity between the two results. The wide variation in previously reported thermodynamic parameters of BX^- formation for systems involving aliphatic 1,2-diols has obscured the fact that these reactions are all very similar thermodynamically [39].

There is also a tremendous variation in the literature in reported thermodynamic parameters for BX_2^- complex formation in systems involving aliphatic 1,2-diols. To cite one example, the entropy change for the reaction $BP^- + H_2P \leftrightarrow BP_2^- + 2\ H_2O$ has been independently measured by three groups. The values of $\Delta S°$ are -61.5 J / mol K [43], - 92 J / mol K [41] and

-138 J / mol K [53]. Although the ionic strength is not the same in these studies, we have shown [39] that there is essentially no effect of ionic strength at least to μ = 0.6M on either stability constants or thermodynamic parameters for formation of BP^-. Furthermore, all these studies show substantial differences between the thermodynamics of the first and second complexation steps. In contrast to the literature, our results (Table 4.2) show that thermodynamic parameters for the second complexation step are quite similar to those for the first step. Both steps are exothermic and entropy changes for all reactions are negative. Using a similar rationale as that employed in the discussion of the 1:1 complexation reactions, we can attribute the negative entropy change for the second complexation step to a loss of configurational entropy in the ligand on complexation.

On a purely statistical basis, K_1 / K_2 for bidentate chelating ligands coordinated to a tetrahedral center can be easily calculated [122] by considering boron at the center of a tetrahedron, as it is in B^-, BX^- and BX_2^-. Each of six edges of the tetrahedron represent six possible bidentate coordination sites, so there are six unique ways for primary ligand coordination. The coordinated ligand in the BX^- complex, on the other hand, has only one way of coming off, making $K_1 \propto 6 / 1$. Once one of the edges is occupied, as in BX^-, only one edge remains open for subsequent ligand coordination to form BX_2^-, but either of the ligands on BX_2^- can dissociate, making $K_2 \propto 1 / 2$. Therefore, the overall statistical ratio K_1 / K_2 for bidentate chelating ligands coordinated to a tetrahedral center is equal to 12.

The 1,2-diols have K_1 / K_2 values which are only slightly less than that

value. It is interesting to note, however, that while the assumptions of a purely statistical argument attribute the decrease in successive stability constants entirely to a less favorable entropy factor, that is not the case for either diol studied here (Table 4.6). For H_2E in particular, addition of a second ligand is considerably more favorable entropically than first ligand addition. The decrease in K_2 relative to K_1 is due to a less favorable standard enthalpy in both cases. Numerically, the ratio of 12 corresponds to an expected entropy decrease caused only by statistical effects of 19.1 J/mol K for second ligand addition compared with first ligand addition. The entropy changes observed here (ΔS_2° - ΔS_1°) are either close to zero (H_2P) or positive (H_2E). This means that there must be a compensating positive contribution to the entropy change which could possibly be related to the release of water of solvation on complexation. Since both complexation reactions involve the condensation of two hydroxyl groups on the ligand with two hydroxyl groups on boron, not only are two water molecules formed on each reaction, but any solvent associated with the four reactant hydroxyl groups is also released.

It is useful to reconsider the reaction thermodynamics from the perspective of a disproportionation reaction : $2\ BX^- \leftrightarrow BX_2^- + B^-$ (Table 4.7). Since there is no uncomplexed ligand in the disproportionation reaction, effects caused by ligand solvation and / or a loss of ligand configurational entropy are relatively unimportant. Similarly, the total number of uncoordinated -OH groups available for solvation is the same for reactants and products. Differences in solvation of B^- , BX^- and BX_2^- are expected and it is reasonable to suggest that B^- is better solvated than BX^- which, in turn, is better solvated

than BX_2^- . The small entropy change argues against any significant overall change in solvation on disproportionation. Similarly, the small enthalpy change means that there is no great difference in the B-O bond strength among B^- , BX^- and BX_2^- for diols.

α-Hydroxy Carboxylic Acids. Compared with the diols, K_1 is much greater for α-hydroxy carboxylic acids and this increase is entirely the result of a much more favorable ΔH° (Table 4.6). Entropy changes remain quite negative and this may again be attributed to a loss of configurational entropy in the ligand on complexation. In marked contrast to the diols, the second complexation reaction here is emphatically different from the first. K_2 is much smaller than K_1 and extremely large differences in both ΔH° and ΔS° are observed. The second complexation steps for H_2L and H_2G are the only endothermic reactions in the entire set and the entropy changes are the most positive (Table 4.6). For H_2L, the difference in enthalpy change ($\Delta H_2° - \Delta H_1° = +62$ KJ/mol) corresponds to a decrease in stability constant by 11 orders of magnitude. The more favorable entropy change ($\Delta S_2° - \Delta S_1° = +134$ J / mol K) corresponds to an increase in stability constant by 7 orders of magnitude. The more favorable entropy change only partially compensates for the much less favorable enthalpy change and, as a consequence, K_2 is four orders of magnitude smaller than K_1.

These results can be discussed in terms of the disproportionation reactions (Table 4.7). Compared with the diols, equilibrium constants are quite small and both ΔH° and ΔS° are much more positive. Extending the discussion

of the diol disproportionation reactions, it seems that solvation effects cannot explain these data. For example, H_2E differs from H_2G (and H_2P differs from H_2L) only by replacement of two methylene hydrogens by one carbonyl oxygen. While this difference is chemically significant, in terms of the disproportionation reaction the total number of carbonyl groups on each side of the chemical equation is the same and little net effect on overall solvation is expected. If solvation effects are not important, then the endothermic enthalpy value may be interpreted in terms of significant differences in B-O bond strengths in B^-, BX^- and BX_2^-. In these systems, the strongest B-O bonds may be found in BX^- with longer, weaker bonds being characteristic of B^- and BX_2^-. This is consistent with the thermodynamics of successive ligand addition (Table 4.6) and disproportionation (Table 4.7). Such structural differences would also contribute to the positive entropy of disproportionation. The thermodynamics of bimolecular association reactions have recently been studied in detail and factors which contribute to compensating enthalpy / entropy relations are discussed [130,131].

This argument attributes the very different thermodynamic parameters for formation of 1:2 borate / α-hydroxy carboxylic acid complexes to structural differences among the various borate complexes and not to any particular effect of solvation on the reactions. The fact that there may be significant differences in boron-oxygen bonds in various borate complex ions is supported by a recent crystal structure determination [132] of both 1:1 and 1:2 borate complexes of a substituted 1,2-dihydroxybenzene in which there are B-O bond length differences of almost 0.1 Å among the various complexes. When the donor atoms are non-equivalent as in α-hydroxy carboxylic acids, these differences

may be even more substantial.

Oxalic Acid. Oxalic acid is unique among the systems studied in having a much more positive $\Delta S°$ for the first complexation step and not forming a second complex at all. This entropy change is comparable to that of the 1:1 complexation reaction in the methylboronate / 1,2-dihydroxybenzene system [36,39]. The unexpectedly large entropy change for the oxalic acid reaction is not without precedent. We have previously used a comparison between the reactions of oxalic acid and 1,2-dihydroxybenzene with Cu^{2+} ($Cu^{2+} + H_2L \leftrightarrow CuL + 2H^+$) to elucidate this point [40].

The absence of observable BOx_2^- has been noted previously [51]. It is of particular interest here because it further supports our contention that there are significant differences in the B-O bond in the various borate species. The hydroxyl groups in BOx^- do not react with H_2Ox to form BOx_2^- whereas B^- reacts easily with H_2Ox. We did several experiments to see if any mixed ligand complexes could be formed with BOx^-. H_2P at high concentration (~1M) forms a complex with BOx^- which appears in the ^{11}B NMR spectrum only slightly downfield from BOx^-. It is of small amplitude and not well enough separated from BOx^- to be integrated. It is clear, however, that the equilibrium constant for the reaction is much less than that for the addition of H_2P to any other borate species. Similar experiments were carried out with H_2G and H_2L. The mixed ligand complex $BLOx^-$ appears in the NMR as a shoulder on BL_2^-, but $BGOx^-$ is well enough separated from other complex ions in the system to permit integration. The approximate value for the equilibrium constant for the reaction

$BOx^- + H_2G \leftrightarrow BGOx^- + 2H_2O$ is $4x10^{-2}$. This value is less than 1% of the equilibrium constant for the addition of H_2G to BG^-.

It is possible to look at this question from one other point of view. Figure 4.12 shows the plot of log K_1 and log K_2 vs. pK_a (ligand) for all of the systems studied. The plot of log K_1 vs. pK_a is linear with a large negative slope. The plot of log K_2 vs. pK_a (ligand) is also linear with a much smaller negative slope. Extrapolation of the second plot (log K_2) to pK_a ~1 allows a prediction to be made for K_2 for the H_2Ox reaction. That value is approximately 100. Using K_1 (Table 4.6) and this value for K_2, a distribution diagram (Figure 4.13(b)) with initial concentrations of H_2Ox and $B(OH)_3$ both being equal to 0.10M shows a large excess of BOx_2^- at low pH. This result is similar to that for the lactic acid system (Fig.4.7). But no such complex can be seen in the NMR at any pH or reactant concentration and the experimental value of K_2 is taken to be zero.The distribution diagram using the experimentally determined stability constants under the same conditions is shown in Figure 4.13(a) for comparison. It is clear from these results that BOx^- behaves very differently from any other BX^- species and that ligand addition to BOx^- is quite difficult.

Interestingly enough, our ability to detect a small amount of the mixed ligand complexes $BGOx^-$, $BPOx^-$ and $BLOx^-$, shows that the relatively inert BOx^- complex is much more reactive with diols or α-hydroxyl carboxylates than it is with a second oxalate ligand. The potential application of this result to the molecular recognition of carbohydrates at low pH will be discussed in Chapter 7.

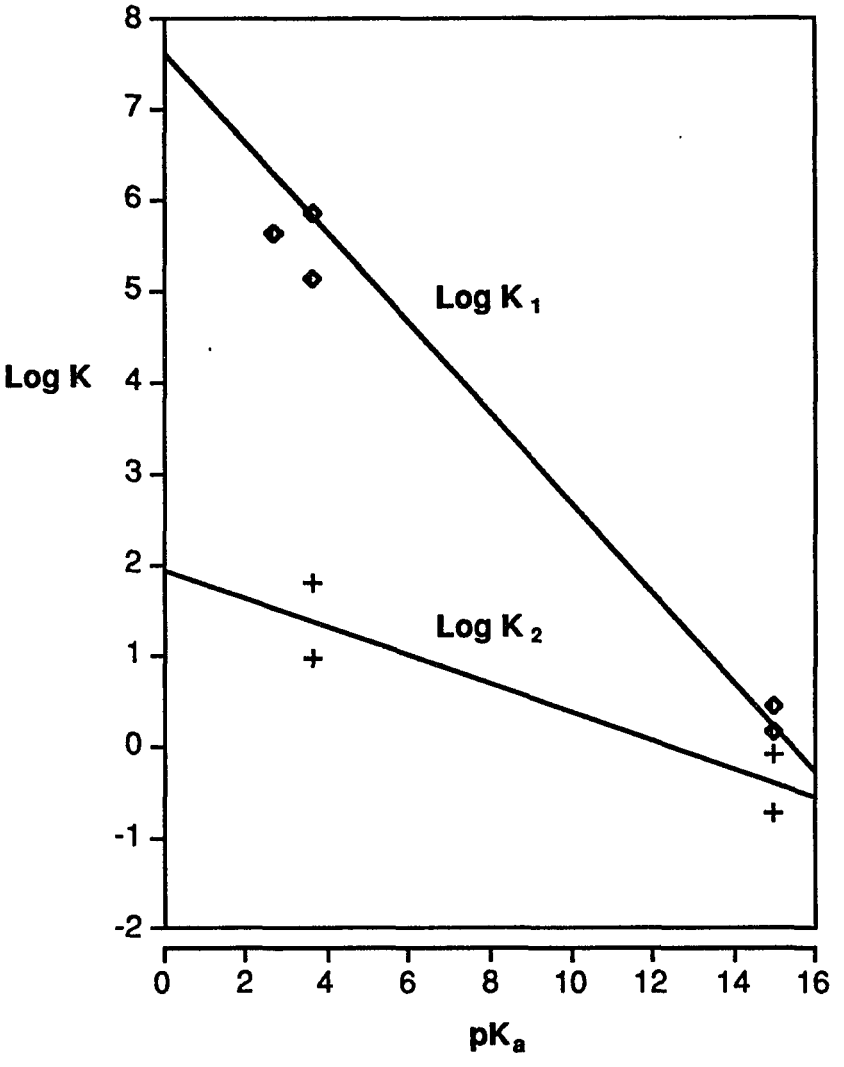

Figure 4.12 : Plot of log K_1 and log K_2 vs. ligand pK_a for the various borate complexation reactions studied.

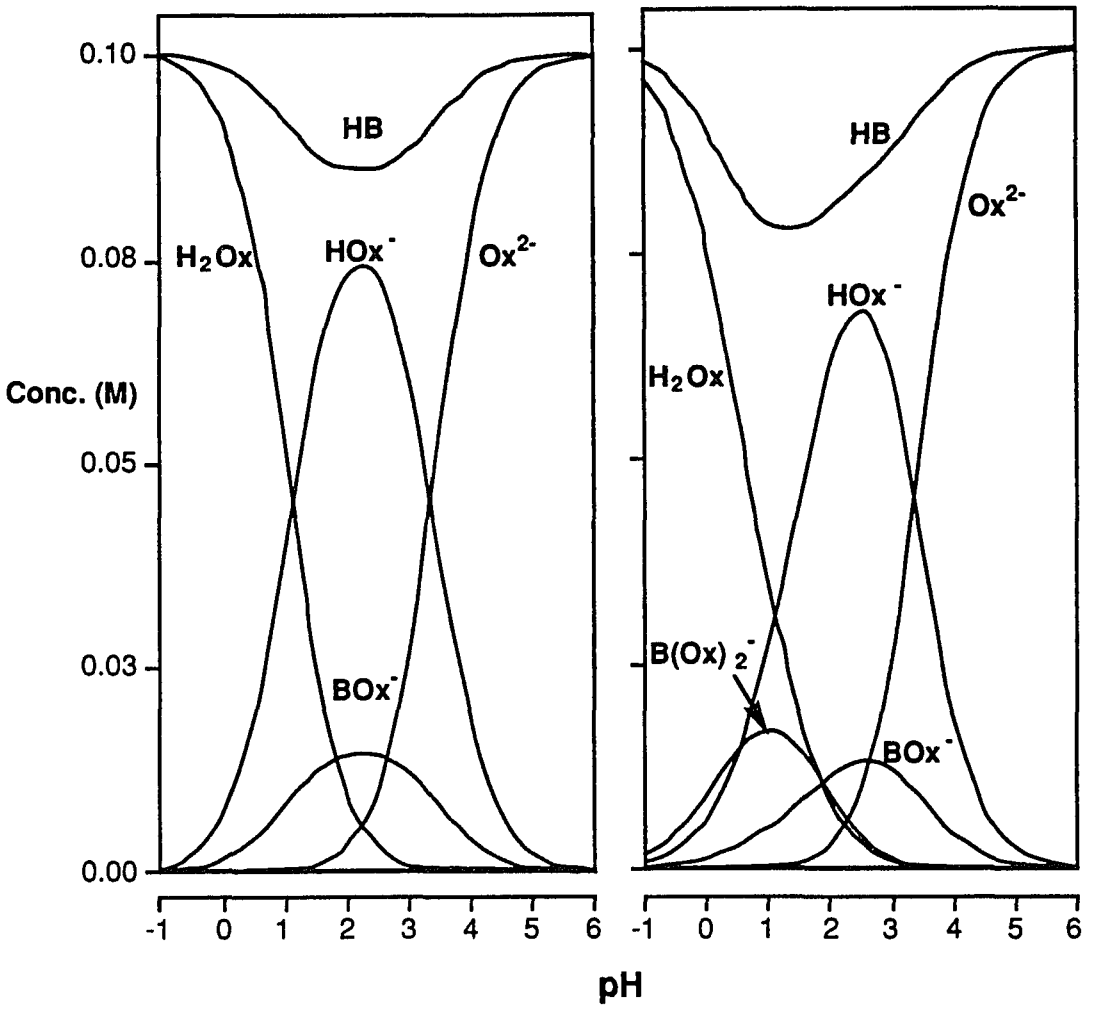

Figure 4.13: Distribution diagram for the boric acid ($(HB)_o$ = 0.10M) / oxalic acid ($(H_2Ox)_o$ = 0.10M) system. **(a)** *left)* Calculated using the K_1 value given in Table 4.4 and K_2 = 0 (experimental). **(b)** *right)* Calculated using the K_1 value given in Table 4.4 and K_2 = 100 (extrapolated from Fig. 4.12).

Mixed ligand systems. The results for the mixed ligand systems can be used to answer the following questions: What effect does primary ligand coordination have on the stability constant and thermodynamic parameters of subsequent bis complex formation? and, Is the effect a function of ligand type and is the effect steric or electronic in origin? A comparison of the reaction of H_2L with the following series of tetrahedral boron centers : B^-, BL^-, BE^- and BP^- can be used to answer these questions (Table 4.6). Of the four reactions, three of them (H_2L + B^-, BE^- and BP^-) are very similar. In fact, the effect of diol coordination on the subsequent reaction is close to statistical. $\Delta H°$ is ~ 10 kJ / mol less exothermic and $\Delta S°$ is about the same for H_2L coordination to BE^- or BP^- as compared with H_2L coordination to B^-. These results show that primary diol coordination probably involves at most a slight bond length decrease of the uncoordinated B-O bonds in BE^- and BP^- compared with those in B^-. On the other hand, primary lactate coordination has a dramatic effect on the stability constant (lower by three orders of magnitude), $\Delta H°$ (more endothermic by 60 kJ / mol) and $\Delta S°$ (more positive by ~ 130 J / mol K) for subsequent BL_2^- formation. Essentially, H_2L coordination by B^- deactivates the boron center. This deactivation of BL^- must take place through an electronic rather that a steric effect to account for the large positive enthalpy change and the fact that it is not seen in BE^- or BP^-. The uncoordinated B-O bonds in BL^- must be shorter, stronger and that much harder to break than they are in any other complex except BOx^-. The large positive entropy for the reaction of H_2L with BL^-, which

is not seen in the reactions of H_2L with B^-, BE^- or BP^-, is much harder to account for and we offer no explanation at this time. It seems then that only BX^- complexes formed from ligands with electron withdrawing carbonyl groups (H_2G, H_2L and H_2Ox) are significantly deactivated toward bis complex (BX_2^- or BXY^-) formation. The reactions of any other ligand with a series of tetrahedral boron centers (Table 4.6) can be compared in a similar way.

Figure 4.14 shows a plot of $\Delta H_1°$ and $\Delta H_2°$ vs. pK_a (ligand). The plot of $\Delta H_1°$ vs. pK_a is linear with a positive slope. The plot of $\Delta H_2°$vs. pK_a (ligand) is also linear but with a negative slope. If the two lines were extrapolated to pK_a ~ 15 they would converge, just as in the plot of log K_1 and log K_2 vs. pK_a (Fig. 4.12). A similar plot of $\Delta S_1°$ and $\Delta S_2°$ vs. pK_a (ligand) shows no correlation between the two parameters.

Throughout this discussion we have alluded to the relationship between reaction thermodynamics and complex structure. These ideas are further addressed in Chapter 5.

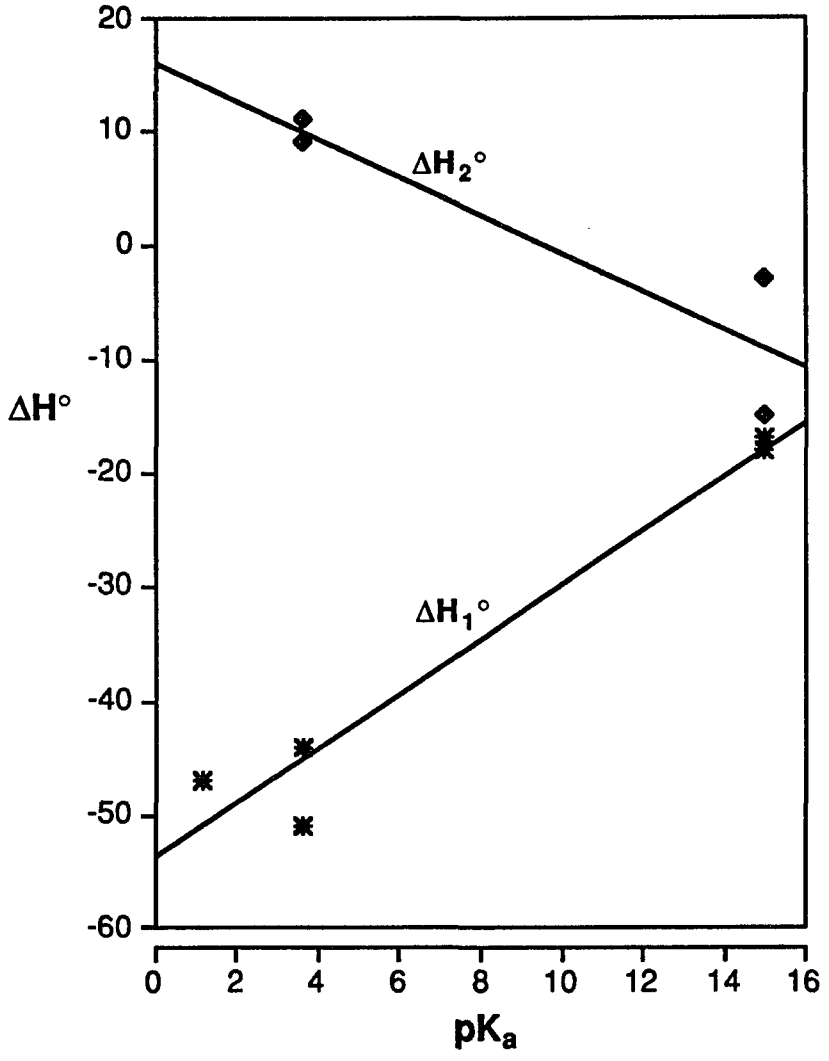

Figure 4.14 : Plot of $\Delta H_1°$ and $\Delta H_2°$ vs. ligand pK_a for the various borate complexation reactions studied.

CHAPTER 5

Computational Studies of the Structure and Energetics of Borate Complex Ions

5.1 Introduction

The results of our experimental studies on the thermodynamics of formation of 1:1 and 1:2 borate complex ions with bidentate chelating ligands [39,40] were presented in Chapter 4. One of the conclusions drawn from that work [40] is that there may be "significant differences in boron - oxygen bonds in the various borate complex ions." In a further investigation of this point, a computational study of borate complex ions was conducted. Jacobson and Pizer have prevously shown [82a] that AM1 is a useful and accurate technique for both structural and thermodynamic studies of anion addition to boron acids in the gas phase and that method was used again here.

General structures of the 1:1 and 1:2 borate complex ions are given below. An atom numbering scheme is included in the figures. Results are

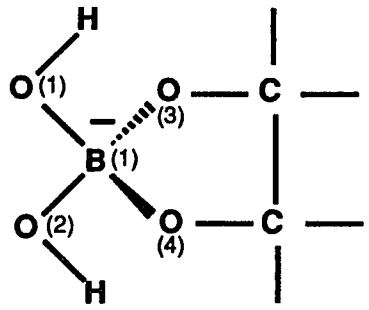

BX^-

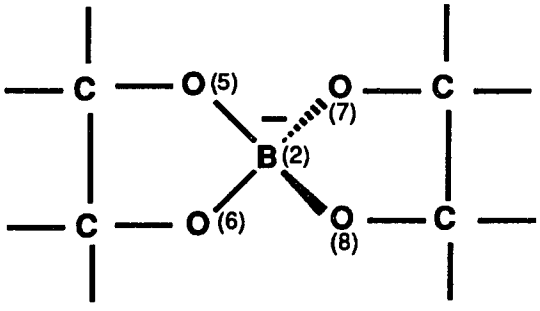

BX_2^-

reported for the following ligand systems: 1,2-ethanediol (H_2E), 1,2-dihydroxybenzene (H_2Cat), glycolic acid (H_2G), oxalic acid (H_2Ox) and squaric acid (H_2Sq). Calculations on $B(OH)_3$, $(HO)_2BOH_2^+$, $(HO)_2BO^-$ and $B(OH)_4^-$ are also presented as these structures are well represented in both the crystallographic and theoretical literature.

5.2 Computational Method

AM1 Calculations. AM1 is a semi-empirical, SCF method for chemical calculations which has been shown to give reliable structural parameters and gas-phase standard enthalpies of formation for normal valent compounds. The required parameters for all of the systems studied here can be found in the literature [133]. A recent review [134] of various computational methods summarized the results of a critical examination of the absolute errors assocated with AM1 calculations. Errors of ±0.050Å for bond length and ±3.3° for bond angle were found to be typical of AM1 [135], while the errors associated with gas phase standard enthalpies of formation were found to be ± 9 kcal / mol [136] for normal valent compounds.

Calculations were conducted using two different commercially available AM1 software packages. Both MOPAC [82b], which was used before [82a],and HyperChem [82c] gave essentially identical results.

Modeling Scheme. Molecular graphics and force field calculations contained within each of the AM1 software applications were used to obtain initial molecular geometries. The resulting structures were then optimized using the AM1 semi-empirical method contained within that particular application.

One important point should be made regarding the 1:1 complex ions studied here. The orientation of the hydroxyl hydrogens is a matter of some concern. Bond lengths and angles in the complex ions are functions of the orientation of these protons and, to a lesser extent, so is the standard enthalpy of formation. In order to make direct comparisons of the various 1:1 complex ions, these protons were always initially oriented above and below the plane of

the chelate ring and final minimizations retained this orientation in all cases. For the borate complex of 1,2-dihydroxybenzene ($BCat^-$, Fig.5.1) initial rotation of one hydroxyl proton by 180° produces a minimized structure in which the initial orientation of the protons is retained. This structure is measurably less symmetric than $BCat^-$ with the two protons oriented above and below the plane of the chelate ring, but it is only 0.5 kcal / mol higher in energy. Initial rotation of both protons away from the chelate ring results in a final minimized structure in which one proton is rotated back toward the chelate ring. In structures of complex borates, these protons are almost always oriented away from the boron atom in order to participate in intermolecular hydrogen bonding.

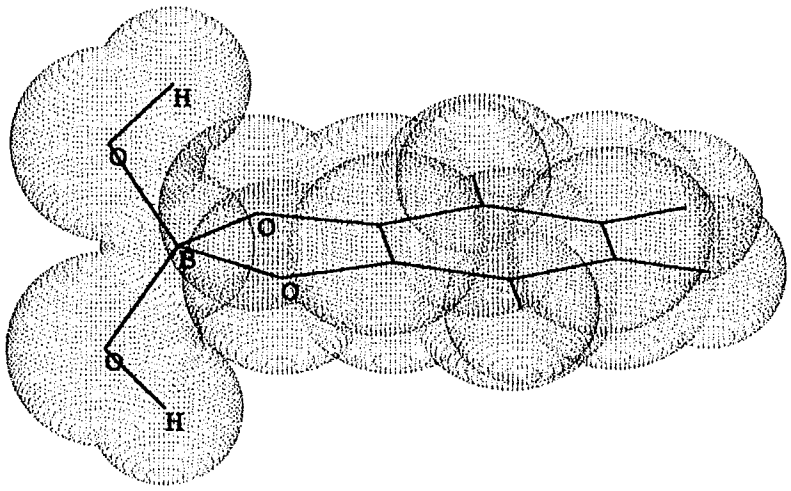

Figure 5.1: Final Minimized Structure of $BCat^-$ calculated using HyperChem.

5.3 Results and Discussion

Boric Acid and Borate Ions. Calculations were carried out on $B(OH)_3$, $(HO)_2BO^-$, $(HO)_2BOH_2^+$ and $B(OH)_4^-$. Some of the structural results of these calculations are included in Fig. 5.2. Results on $B(OH)_3$ and $(HO)_2BOH_2^+$ can be directly compared with other recent quantum mechanical calculations and agreement is excellent [137]. Similarly, results on $B(OH)_3$ and $B(OH)_4^-$ are supported by structural studies [138] which show an increase of ~ 0.1Å in B - O bond length on addition of hydroxide ion to $B(OH)_3$. Calculations were also done on $(HO)_2BO^-$ which is the conjugate base of $B(OH)_3$ acting as a Bronsted acid as it does in the gas phase [139]. The considerably shortened B - O bond is in agreement with a crystal structure determination [140] of the sodium salt of a doubly deprotonated cyclic borate trimer. Calculated boron - oxygen bond lengths in these species vary from 1.25 Å to 1.52 Å. The agreement between our AM1 results and other quantum mechanical calculations [137] as well as structural determinations [138,140] supports the validity of AM1 as an appropriate molecular orbital method for describing B - O bonds in borate complex ions.

BX^- and BX_2^-. Representative boron - oxygen bond lengths and O - B - O bond angles are given in Table 5.1 for both BX^- and BX_2^-. In all cases the structures are quite symmetrical and bond lengths and angles are effectively identical for all equivalent bonds.

In 1:1 complex ions, the O(3) - B(1) - O(4) bond angle in the chelate ring

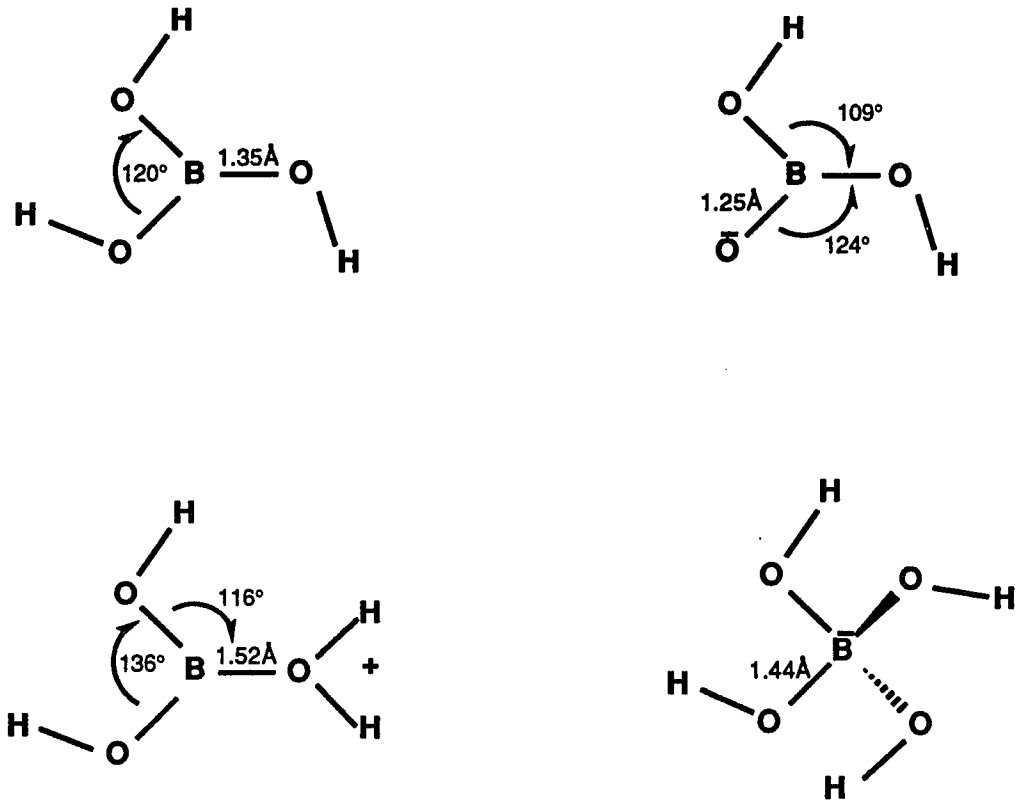

Figure 5.2: Structural Parameters for $B(OH)_3$, $(HO)_2BO^-$, $(HO)_2BOH_2^+$, and $B(OH)_4^-$.

Table 5.1. Structural Parameters for 1:1 and 1:2 Borate Complex Ions.[a]

Ligand	O(1)-B(1)-O(2)	B(1)-O(1) Å	O(3)-B(1)-O(4)	B(1)-O(3) Å	O(5)-B(2)-O(6)	B(2)-O(5) Å
H_2E	110°	1.40	104°	1.51	108°	1.46
H_2Cat	113°	1.39	102°	1.57	108°	1.49
H_2G	112°	1.39	102°	1.50[b] 1.58[c]	108°	1.45[b] 1.49[c]
H_2Ox	114°	1.38	101°	1.56	108°	1.47
H_2Sq	117°	1.37	103°	1.64	109°	1.53

[a] The B-O bond distance in trigonal $B(OH)_3$ is 1.35Å. The B-O bond distance in tetrahedral $B(OH)_4^-$ is 1.44Å.

[b] B-O (hydroxyl oxygen) bond length

[c] B-O (carboxyl oxygen) bond length

is always quite a bit less than 109.5° and the O(1) - B(1) - O(2) bond angle is increased relative to $B(OH)_4^-$. The B - OH bond in BX^- is shorter and stronger than the B - OH bond in $B(OH)_4^-$ and this shortening is marginally greater as ligand acidity increases. B - O bond lengths in the chelate ring are always greater than B - OH bond lengths and these bonds generally increase in length as ligand acidity increases. The unsymmetrical ligand, glycolic acid, clearly shows this bond length difference as the boron - hydroxyl oxygen bond is 0.08 Å shorter than the boron - carboxyl oxygen bond. This result is in agreement with a crystal structure determination of potassium boromalate [101]. Similarly, a crystal structure determination [132] of a 1:1 complex of a substituted 1,2-dihydroxybenzene shows shorter B - OH bonds relative to B - O chelate ring bonds by ~ 0.08 Å. Although a calculation on squaric acid is included, workers in this laboratory have shown experimentally [141] that BSq^- does not exist in aqueous solution and the very long calculated B - O chelate ring bond distance supports this result. Squaric acid is known to act as a bridging ligand [142] rather than a chelate because of the long O····O distance.

The results of these calculations support the idea that there are significant differences in B - O bonds in the various borate species. Considering just the B - OH bond on going from $B(OH)_4^-$ to BOx^-, a shortening of the bond by 0.06 Å occurs along with an increase in O - B - O angle of almost 5°. Given that the B - O bond length in the chelate rings may be as long as 1.58 Å, there is a surprisingly large difference of 0.2 Å in B - O bond length among the various tetrahedral borates. The strong, short B - OH bond in BOx^- may account for the experimental result [40,51] presented in Chapter 4, which

showed that $B(Ox)_2^-$ is not formed in solution. Similarly, compared with the thermodynamics of formation of the 1:1 complex [40], addition of H_2E to BE^- is less favorable enthalpically by 15 kJ / mol and addition of H_2G to BG^- is less favorable by 51 kJ / mol. In the series $B(OH)_4^-$, BX^- and BX_2^-, the shortest, strongest B - O bonds are always the B - OH bonds in BX^-.

On addition of a second ligand to BX^- to give BX_2^-, structures which are quite symmetrical are formed. O - B - O chelate ring bond angles increase and B - O chelate ring bond lengths decrease in BX_2^- relative to BX^-. Shorter and stronger B - OH bonds in BX^- are replaced by longer B - O bonds in the chelate ring of BX_2^-. The calculated $B(Cat)_2^-$ structure (Table 1) is in agreement with two separate crystal structure determinations [132,143].

Reaction Thermodynamics. From calculated standard enthalpies of formation for the various species, it is possible to calculate in a straightforward way the enthalpies of various borate complexation reactions in the gas phase. We have argued [40] that the disproportionation reaction ($2BX^- \leftrightarrow BX_2^- + B^-$) is influenced by solvation to only a small extent and comparisons of experimental [40] and calculated enthalpies of disproportionation can be made for the H_2E, H_2G and H_2Ox systems. The results are presented in Table 5.2. Agreement between the experimental and calculated $\Delta H°$ for the diols (H_2E and H_2P) is remarkable. The disproportionation reactions for the α-hydroxy carboxylic acids (H_2G and H_2L) also model very well. The highly endothermic

Table 5.2: Thermodynamics of Disproportionation. Experimental and Calculated Values.

$$2BX^- \leftrightarrow BX_2^- + B^-$$

System	$\Delta H°$ {exp.} (kJ / mol)	$\Delta H°$ {calc.} (kJ / mol)
H_2E	15	16
H_2P	2	5
H_2G	53	40
H_2L	62	48
H_2Ox	-----	89
$H_2Cat.$	-----	55

calculated enthalpy of disproportionation for BOx^- provides further evidence to account for the lack of observable $B(Ox)_2^-$ in solution. The fact that all three of these disproportionation reactions are endothermic is explained in part by the relatively strong B - OH bonds in BX^-.

Despite the surprising agreement between calculated and experimental enthalpies of disproportionation, the entropies for this reaction model very poorly as do enthalpies for other processes like ligand exchange reactions ($2\ BXY^- \leftrightarrow BX_2^- + BY_2^-$). Clearly, effects of solvation are almost always important and it is not unexpected that gas phase calculations generally do not agree with thermodynamic parameters measured in solution. Accurate modeling of thermodynamic parameters in solution requires not only the inclusion of effects of solvation, but also the effects of counterions and ionic atmosphere. This is an area of of active, current investigation [144].

Chelation. If glycolic acid is treated as an ambident, unidentate ligand, the boron oxygen bond in $(HO)_3BG^-$ when glycolic acid bonds via the hydroxyl oxygen is calculated to be 1.52 Å and the average B - OH bond length is 1.42 Å. Coordinated via the carboxyl oxygen, the B - O bond is calculated to be 1.64 Å long [145] and the average B - OH bond is 1.39 Å. The quite long boron - carboxyl oxygen bond is also reflected in the small stability constant for the addition of acetate ion to boric acid [146]. On ring closure, both B - O bonds to the chelated ligand decrease in length (Table 5.1) and so, to a lesser extent, do the B - OH bonds. Chelation in these systems is, then, enhanced by enthalpic as well as entropic factors.

CHAPTER 6

Ternary Alkaline Earth Complex Ions in the M^{2+} / Borate / Tartrate System

6.1 Introduction

In aqueous alkaline solution, borate ion ($B(OH)_4^-$) is capable of forming both 1:1 and 1:2 complexes with polyhydroxycarboxylate ligands such as *l* - (2R,3R) tartrate or *meso* -(2R,3S) tartrate (T^{2-}). The mode of coordination is pH dependent and has been shown in base to be exclusively via the 2,3 diol linkage on the ligand. The borate complexation reactions are

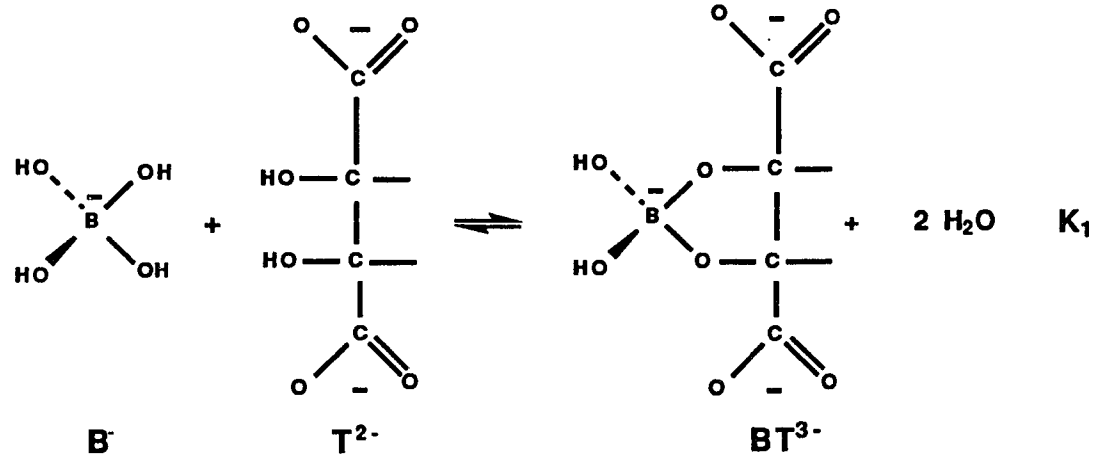

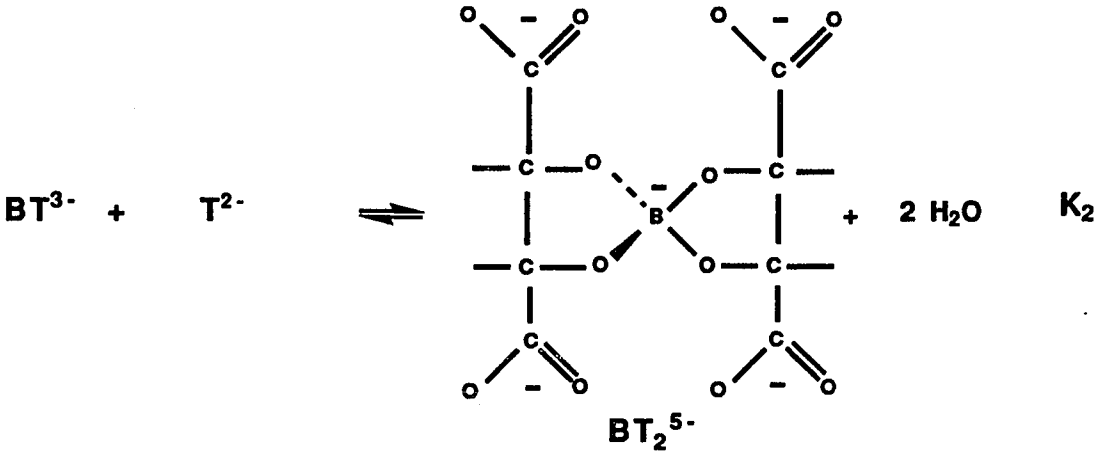

where $K_1 = [BT^{3-}] / [B^-] [T^{2-}]$ and $K_2 = [BT_2^{5-}] / [BT^{3-}] [T^{2-}]$. The complexation reactions of M^{2+} with each of the four anions in this reaction sequence are considered.

We present here the first determination of stability constants for ternary M^{2+} / borate / tartrate complexation reactions. ^{11}B NMR was used to study borate complexation reactions and the binding of alkaline earth ions by borotartrate complex ions. A spectrophotometric competitive binding technique was used to determine the stability constants for simple metal tartrate complexes (Sect. 3.7). A detailed discussion of the mathematical analysis used in these studies was presented in Sections 3.7 and 3.8.

Mg^{2+}, Ca^{2+} and Sr^{2+} coordination to *l* - tartrate complexes was studied in order to see whether these systems display any selectivity with respect to metal ion. The effect of ligand stereochemistry on the metal ion binding process was studied by comparing *l* - tartrate and *meso* - tartrate complexes in the Ca^{2+} binding study.

6.2 Results and Treatment of Data

Determination of stability constants for borotartrate complex formation (K_1 and K_2) by ^{11}B NMR

At high pH (11.5) and in the absence of any divalent cation, it is possible to keep the concentrations of borate (~0.10M) and tartrate (~0.10 M) low enough so that only the 1:1 complex (BT^{3-}, -12.6 ppm) and the free borate (B^-, -17.6 ppm) resonances are observed [39]. Under these conditions direct integration of the spectrum along with mass balance affords the calculation of K_1 values for the *l* - tartrate and *meso* - tartrate systems (Sect. 3.2). Extending the technique to measure K_2 is simply a matter of decreasing the concentration of borate (~0.05M) and increasing the tartrate concentration (~0.40M) under the same experimental conditions of pH and ionic strength [40]. Under these conditions, ^{11}B NMR spectra (Figure 6.3a) are well resolved and can be easily integrated for B^-, BT^{3-} and BT_2^{5-} (-8.5 ppm). The stability constant, K_2, for the *l* - tartrate and *meso* - tartrate systems can therefore be calculated from the ^{11}B integration as described in Sect. 3-2. K_1 and K_2 values for both the *l* - and *meso* - tartrate systems are presented in Table 6.1 (p 161).

The ratio of stability constants, K_2 / K_1, is equal to $\{ [BT_2^{5-}] [B^-] / [BT^{3-}]^2 \}$. This ratio is independent of tartrate concentration and can be calculated using ^{11}B NMR integration alone. Calculated in this manner, K_2 / K_1 values for both systems studied agree with the ratio of K_2 to K_1 calculated independently as described above. This agreement is a critical validation of the accuracy of the K_1 and K_2 values.

Metal tartrate complex formation

The conditional indicator constants ($K_{In'}$) as defined in the literature [116] for the M^{2+} / calmagite systems were determined at pH = 11.5, μ = 1.5 M ($(CH_3)_4NCl$) and T = 298K over the range of concentrations described in Section 3.7. $K_{In'}$ was calculated for each equilibrium experiment at two independent wavelengths (525nm and 615nm). Identical results were obtained at each wavelength. $K_{In'}$ for Ca^{2+} and Sr^{2+} binding to calmagite are 9.9 ($\pm$0.6) x10^3 M^{-1} and 1.02 ($\pm$0.05) x10^2 M^{-1}, respectively. Ca^{2+} and Sr^{2+} binding to *l* - tartrate and Ca^{2+} binding to *meso* - tartrate were determined via competitive binding with calmagite and K_{MT} values (Scheme 6.1, eqn. 6-3) for these systems are given in Table 6.1 (p 161). Under our experimental conditions of high ionic strength, values of K_{MT} are lower than those reported in the literature at lower ionic strength [147].

Fig. 6.1 shows the visible spectra of calmagite at various $(Ca^{2+})_o$ concentrations. Fig. 6.2 shows the visible spectra of the calmagite / *l* - tartrate system at various $(Ca^{2+})_o$ concentrations under competitive binding conditions. All spectra for either binary systems (M^{2+} / calmagite) or ternary systems (M^{2+} / calmagite / tartrate) have a common isosbestic point at 555nm. Competitive binding conditions could not be established for the Mg^{2+} / calmagite / tartrate system at high pH due to the very large conditional indicator constant ($K_{In'}$) compared with Mg^{2+} binding by *l*- or *meso* - tartrate.

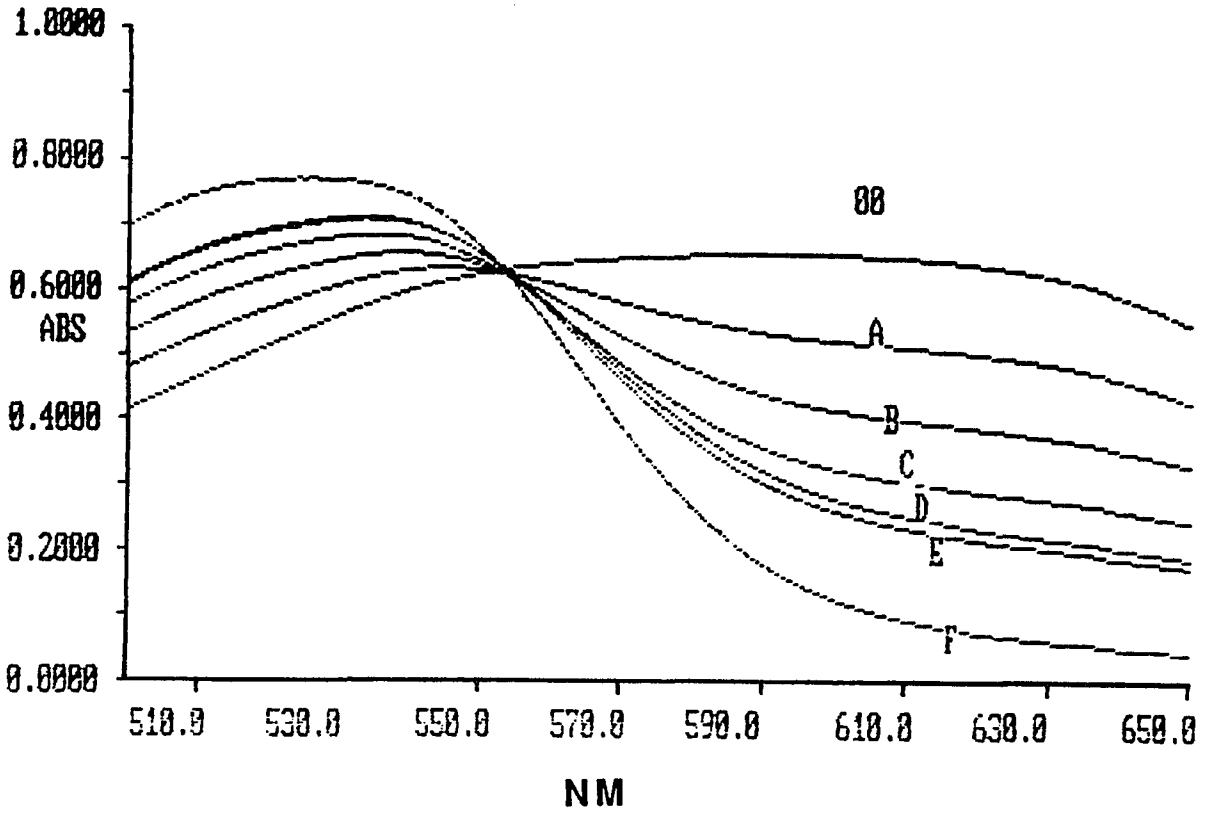

Figure 6.1: Visible spectra of the binary Ca^{2+} / calmagite system at various Ca^{2+} concentrations; $(calmagite)_o$ = 6.6×10^{-5}M, pH = 11.5, μ = 1.5M ($(CH_3)_4NCl$) and T = 298K. **00)** $(Ca^{2+})_o = 0$, **A)** $(Ca^{2+})_o = 5.0 \times 10^{-5}$ M, **B)** $(Ca^{2+})_o = 1.0 \times 10^{-4}$ M, **C)** $(Ca^{2+})_o = 2.0 \times 10^{-4}$ M, **D)** $(Ca^{2+})_o = 3.0 \times 10^{-4}$ M, **E)** $(Ca^{2+})_o = 4.0 \times 10^{-4}$ M, **F)** $(Ca^{2+})_o = 8.0 \times 10^{-3}$ M.

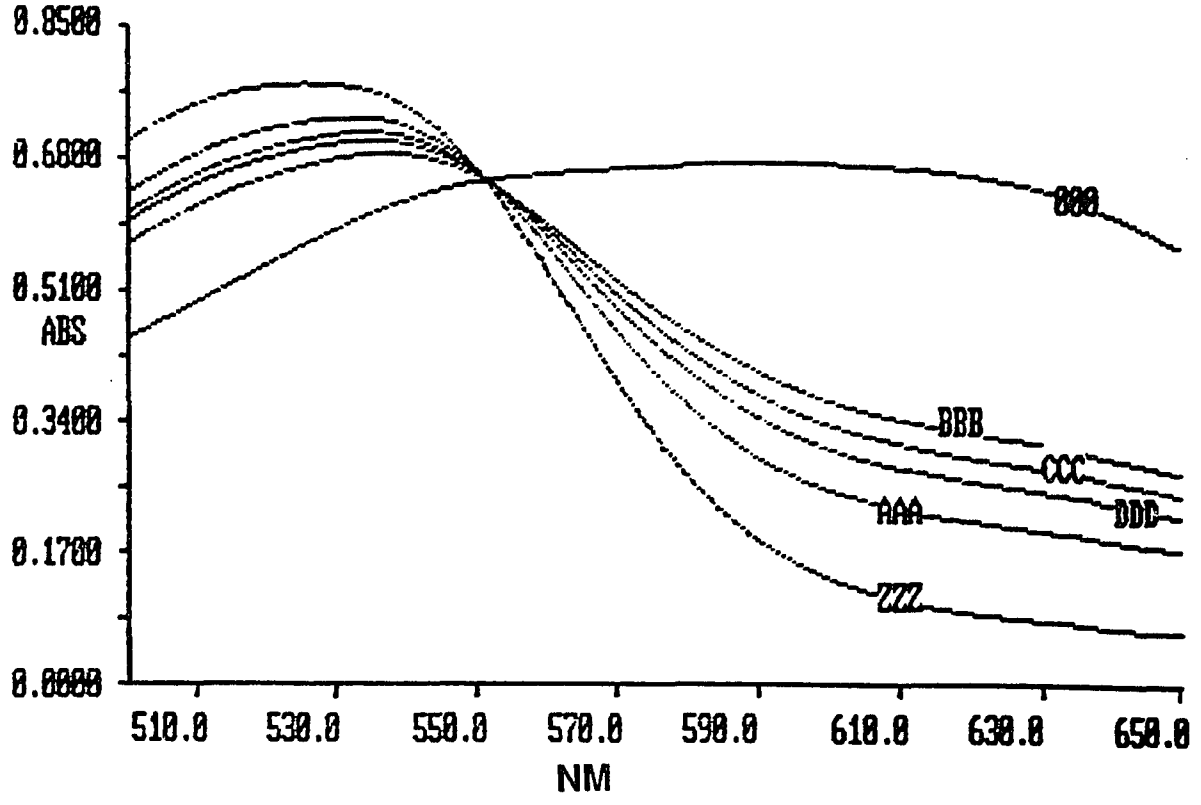

Figure 6.2: Visible spectra of the ternary Ca^{2+} / calmagite / / - tartrate system at various concentrations; $(calmagite)_o$ = $6.6x10^{-5}$M, pH = 11.5, μ = 1.5M ($(CH_3)_4NCl$) and T = 298K; **000)** $(Ca^{2+})_o$ = 0, $(T^{2-})_o$= 0, **AAA)** $(Ca^{2+})_o$ = 4.0×10^{-4} M, $(T^{2-})_o$= 0, **BBB)** $(Ca^{2+})_o$ = 4.0×10^{-4} M, $(T^{2-})_o$= 0.050M, **CCC)** $(Ca^{2+})_o$ = 4.0×10^{-4}M, $(T^{2-})_o$= 0.025M, **DDD)** $(Ca^{2+})_o$ = 4.0×10^{-4}M, $(T^{2-})_o$= 0.013 M, **ZZZ)** $(Ca^{2+})_o$= 8.0×10^{-3} M, $(T^{2-})_o$= 0.

Metal ion binding by borotartrate complex ions as determined by ^{11}B NMR

The addition of millimolar quantities of Ca^{2+} or Sr^{2+} to solutions of borate with *l* - or *meso* - tartrate causes a dramatic increase in the relative integration of the 1:2 peak with respect to the 1:1 peak (BT^{3-}) and the free borate peak (B^-). The 1:2 peak also shows a substantial metal ion induced shift [69] from -8.5 ppm in the blank spectrum (Figure 6.3a) to -7.9 ppm in the $(Ca^{2+})_o$ = 20 mM spectrum (Figure 6.3e) as well as increased broadening with increased concentrations of Ca^{2+} or Sr^{2+}. Neither the 1:1 peak (BT^{3-}) nor the free borate peak (B^-) show appreciable changes in relative integration, chemical shift or line width as a function of M^{2+} concentration. Metal ion exchange between the various borotartrate complexes and the corresponding ternary M^{2+} / borotartrate complexes is fast on the ^{11}B NMR time scale as no separate ^{11}B signals are observed for the ternary complexes. The 1:2 peak, which is dramatically affected by the addition of Ca^{2+} or Sr^{2+}, is therefore assigned to be the composite of the MBT_2^{3-} and BT_2^{5-} resonances exchanging rapidly on the ^{11}B NMR time scale as described by previous workers [69].

The Ca^{2+} / borate / *l*- tartrate, Sr^{2+} / borate / *l* - tartrate and Ca^{2+} / borate / *meso* - tartrate systems have been quantitatively modeled by considering the set of coupled equilibria given in Scheme 6.1. K_1, K_2, and K_{MT} (eqns. 6-1 to 6-3) have been determined as described previously.

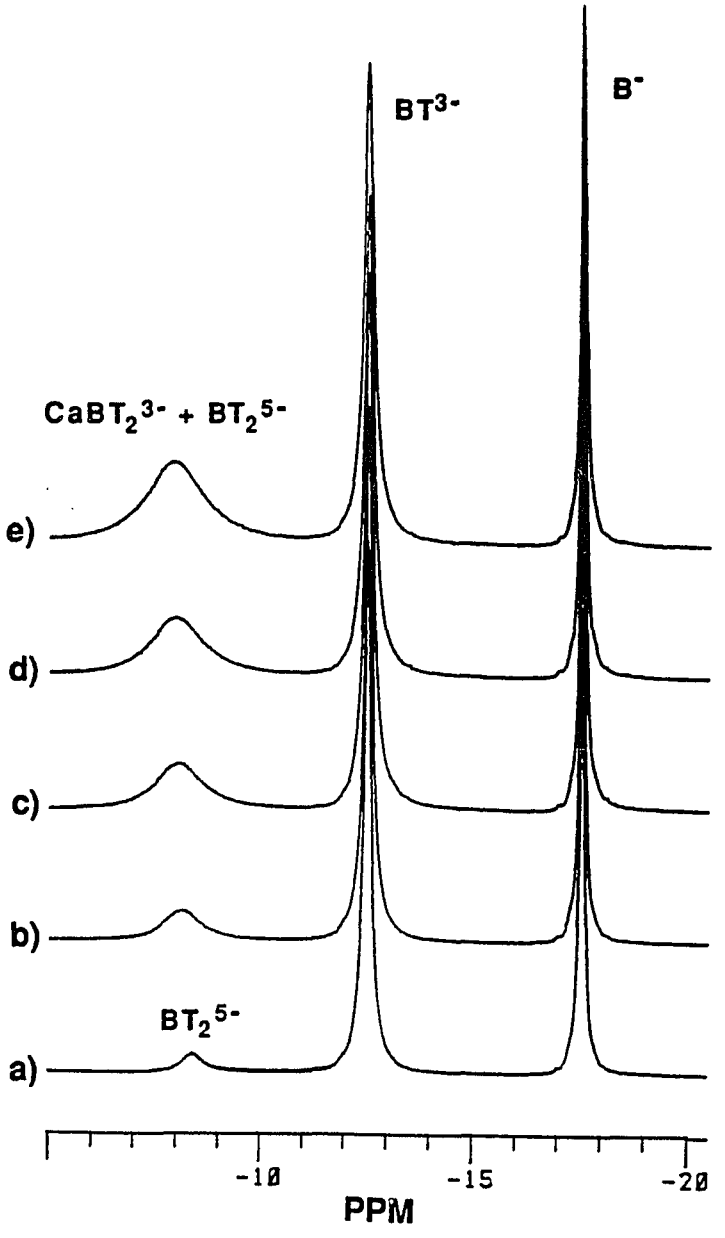

Figure 6.3: ^{11}B NMR spectra for the Ca^{2+} / borate ($(B^-)_o$= 0.050M) // - tartrate ($(T^{2-})_o$ = 0.40M) system as a function of total Ca^{2+} concentration: (**a**) $(Ca^{2+})_o$ = 0.0, (**b**) $(Ca^{2+})_o$ = 5.0 mM, (**c**) $(Ca^{2+})_o$ = 10.0 mM, (**d**) $(Ca^{2+})_o$ = 15.0 mM, (**e**) $(Ca^{2+})_o$ = 20.0 mM. All solutions were prepared in 20% D_2O / H_2O (v / v). pH = 11.5, T = 298K, μ = 1.5M (KNO_3). Chemical shifts are relative to external 0.15M boric acid in 20% D_2O / H_2O (v / v) at pH(D) = 2.0 .

Scheme 6.1:

$B^- + T^{2-} \leftrightarrow BT^{3-} + 2\,H_2O$ K_1 (6-1)

$BT^{3-} + T^{2-} \leftrightarrow BT_2^{5-} + 2\,H_2O$ K_2 (6-2)

$M^{2+} + T^{2-} \leftrightarrow MT$ K_{MT} (6-3)

$M^{2+} + B^- \leftrightarrow MB^+$ K_{MB} (6-4)

$M^{2+} + BT^{3-} \leftrightarrow MBT^-$ K_{MBT} (6-5)

$M^{2+} + BT_2^{5-} \leftrightarrow MBT_2^{3-}$ K_{MBT2} (6-6)

$MT + BT_2^{5-} \leftrightarrow MBT_2^{3-} + T^{2-}$ K_{ex} (6-7)

$K_{ex} = K_{MBT2} / K_{MT}$ (6-8)

Eqn. 6-4 which represents M^{2+} coordination to borate (B^-) can be ignored because of the low stability constants for CaB^+ [117] and SrB^+ complex formation. In our mathematical analysis, K_{MBT} (eqn. 6-5) was set equal to K_{MT} in each system. The validity of this assumption was discussed previously (Sect. 3-8).

Stability constants for eqns. 6-1 through 6-5, along with ^{11}B NMR integration and mass balance, allow the calculation of the stability constant for eqn. 6-6 (K_{MBT2}) and eqn. 6-7 (K_{ex}) using the mathematical model presented in Section 3.8. All the results are presented in Table 6.1.

Experiments were carried out over a wide range of reactant concentrations in order to establish the reaction stoichiometry of the ternary complex. Only one metal ion is bound per *bis* borotartrate complex ion under our experimental conditions. The distribution of species for the Ca^{2+} / $B(OH)_4^-$ / *l* - tartrate system as a function of total calcium ion concentration is shown in Figure 6.4.

The stability constant K_{MBT2} (eqn. 6-6) represents metal ion binding by the *bis* borotartrate ionophore and K_{ex} (eqn. 6-7) is a measure of the synergic effect observed in this chemistry. A large K_{ex} value represents the enhanced binding of M^{2+} to BT_2^{5-} rather than T^{2-}. K_{ex} is as large as 10^3 in the Ca^{2+} / $B(OH)_4^-$ / *l* - tartrate system.

The ^{11}B NMR results for the addition of Mg^{2+} to the borate / *l* - tartrate system are dramatically different (Fig. 6.5) compared with addition of Ca^{2+} and Sr^{2+}. Instead of the 1:2 peak (BT_2^{5-}) growing relative to the other other two

TABLE 6.1: Stability constants for the M^{2+} / borate / x-tartrate system.

{ pH =11.5, 298 K, μ = 1.5 M }

Stabilty Constant *ionic radius* (Å)[a]	Mg^{2+} (0.78)	Ca^{2+} (1.06)		Sr^{2+} (1.27)
Ligand	*l - tartrate*	*l - tartrate*	*meso - tartrate*	*l - tartrate*
K_1 (M^{-1})	5.0 (±0.29)[b]	5.0 (±0.29)	1.4 (±0.10)	5.0 (±0.29)
K_2 (M^{-1})	0.12 (±0.01)	0.12 (±0.01)	0.11 (±0.02)	0.12 (±0.01)
K_{MT} (M^{-1})	~11[c]	37(±2)	53(±2)	18(±3)
K_{MBT2} (M^{-1})	<11	$3.7(\pm0.3)\times10^4$	$4.5(\pm0.3)\times10^4$	$8.0(\pm0.4)\times10^3$
K_{ex}[d]	<1	$1.0(\pm0.08)\times10^3$	$8.5(\pm0.6)\times10^2$	$4.5(\pm0.2)\times10^2$

a) Reference [58].

b) The numbers in parentheses are the standard deviation (± **s**).These values were estimated using at least eight independent determinations over the reported concentration range.

c) Extrapolated from the value given at μ = 0.2M, 25°C. Reference [146] p 127.

d) Although $K_{ex} = K_{MBT2} / K_{MT}$, the values of K_{ex} presented here were calculated directly from experimental data and standard deviations were calculated as described in b).

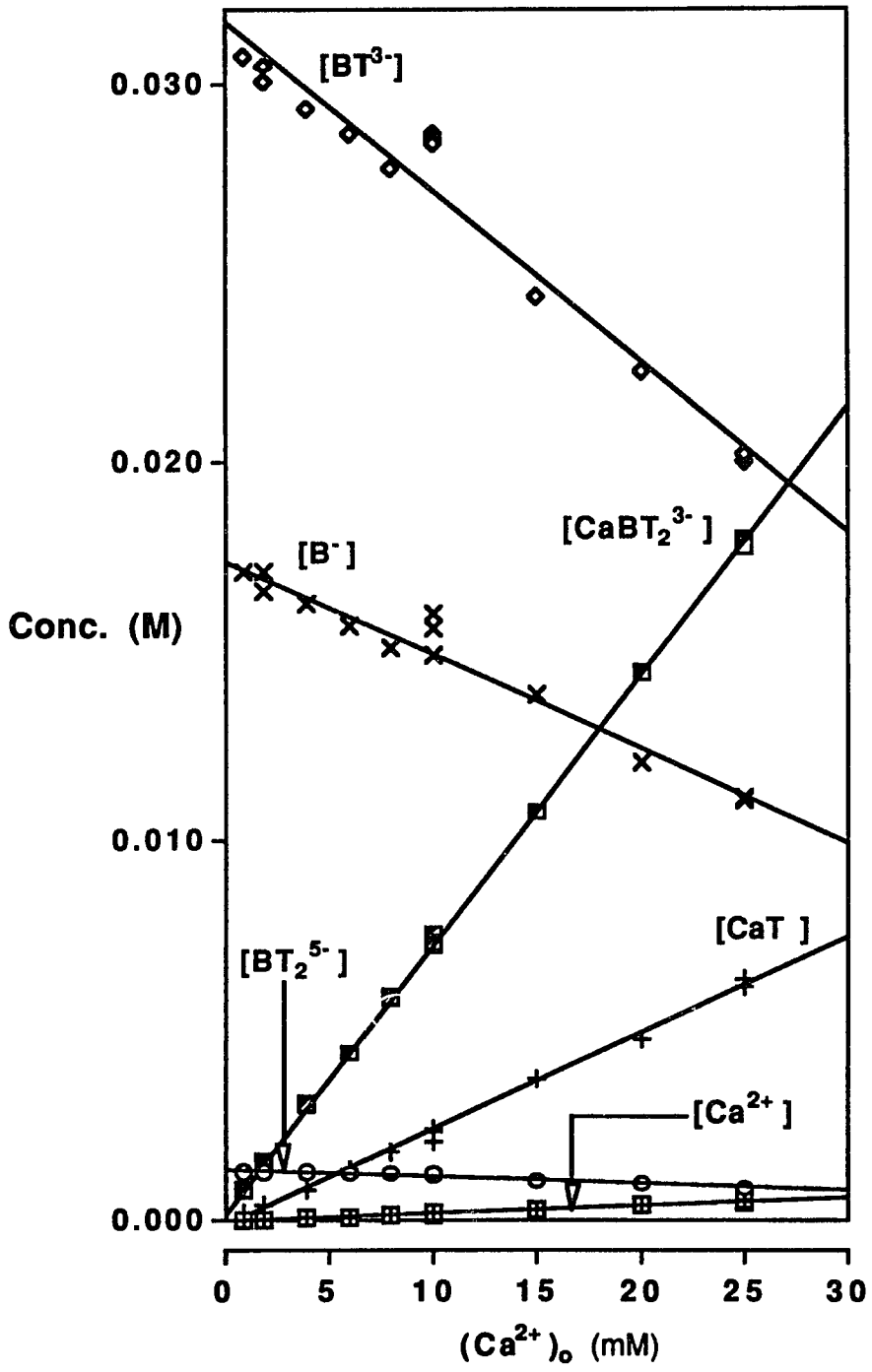

Figure 6.4: Distribution of equilibrium species for the Ca^{2+} / borate (0.050M) / / - tartrate (0.40M) system as a function of total calcium concentration $(Ca^{2+})_o$. pH = 11.5, μ = 1.5M (KNO_3), 298K. $[T^{2-}]$ and $[CaBT^-]$ are omitted for clarity.

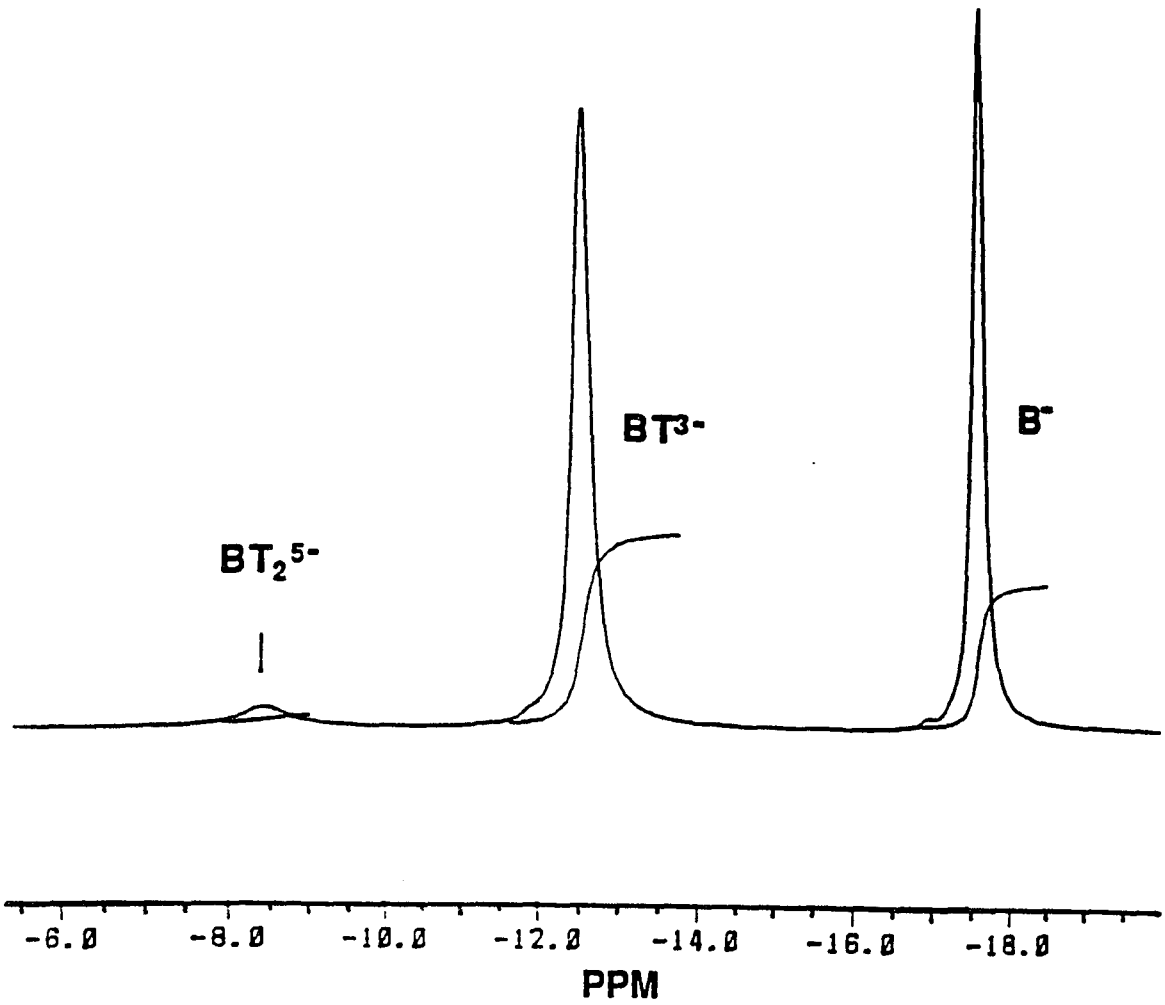

Figure 6.5: ^{11}B NMR spectrum for the ternary Mg^{2+} / borate / *l*- tartrate system; $(B^-)_o$= 0.050M, $(T^{2-})_o$ = 0.40M and $(Mg^{2+})_o$ = 82 mM. All solutions were prepared in 20% D_2O / H_2O (v / v), pH = 11.5, T = 298K and μ = 1.5M (KNO_3). Chemical shifts are relative to external 0.15M boric acid in 20% D_2O / H_2O (v / v) at pH(D) = 2.0 .

peaks in the spectrum with increased Mg^{2+} concentration, both complex peaks, 1:1 (BT^{3-}) and 1:2 (BT_2^{5-}), shrink relative to the free borate peak (B^-). Additionally, there is no metal ion induced shift or line broadening caused by Mg^{2+} addition. These results can be interpreted by assuming that Mg^{2+} preferentally coordinates to T^{2-} over BT^{3-} and BT_2^{5-}. Therefore, K_{MBT2} and K_{MBT} must be less than K_{MT} and K_{ex} must be less than 1. Since no synergic effect was observed, no further analysis of this system was undertaken.

6.3 Discussion

MBT_2^{3-} : Metal Ion Specificity

The order of stability constants (K_{MT}) for the M^{2+} / *l*-tartrate reaction is $Mg^{2+} < Ca^{2+} > Sr^{2+}$. This order is common for α-hydroxy carboxylates and a thermodynamic explanation has been given for the result [94]. In the presence of borate, the order of stability constants is qualitatively the same, but quantitatively very different: $Mg^{2+} <<< Ca^{2+} > Sr^{2+}$. While $K_{MBT2} < K_{MT}$ for Mg^{2+}, both Ca^{2+} and Sr^{2+} have greatly enhanced binding to BT_2^{5-} relative to T^{2-}. This synergic effect is reflected in K_{ex} which reaches a value of 1.0×10^3 in the case of Ca^{2+}. These results differ from the qualitative conclusions of Peters and coworkers in just two respects: 1) While we agree that Ca^{2+} and Sr^{2+} behave very similarly to one another, we find that Mg^{2+} behaves quite differently with tartrate and can not be grouped in the same class as Ca^{2+} and Sr^{2+} (Although Peters' work [71] deals with glucarate, not tartrate, Mg^{2+}, Ca^{2+} and Sr^{2+} are grouped in the same class. That is clearly not the case here.); and 2) Tartrate clearly displays a synergic effect [69] as do other polyhydroxycarboxylates.

The magnitude of K_{MBT2} for Ca^{2+} can be compared with the binding of Ca^{2+} to other ligands. With macrobicyclic ligands such as cryptands, Ca^{2+} binds with exceptionally high stability constants when there is a best fit of Ca^{2+} to the ligand cavity. For Ca^{2+} this occurs with the {221} cryptand and the equilibrium constant for Ca^{2+} / 221 cryptate formation is slightly less [148] than 10^7. Stability constants are often much less with multidentate, but not

macrocyclic, ligands. Of course, certain multidentate ligands such as EDTA have quite high stability constants with Ca^{2+} [149]. The Ca^{2+} / citrate stability constant [150], for example, is 4.3×10^3 and this is one order of magnitude less than K_{CaBT2}. The binding of Ca^{2+} with the BT_2^{5-} complex is, in fact, only slightly less than the recently reported "unusually strong binding of Ca^{2+} ions by the novel antibiotic squalestatin -1" [95].

The binding of Ca^{2+} (and Sr^{2+}) to BT_2^{5-} is exceptional and one other aspect of the chemistry should be mentioned. Since BT_2^{5-} complex formation is pH dependent, metal ion binding is clearly a strong function of pH. BT_2^{5-} is formed in alkaline media. As the pH is lowered, dissociation of BT_2^{5-} occurs and synergic metal ion binding is no longer possible. The pH dependence of borate complex ion formation has been investigated [40,121] in this laboratory (Chapter 4) and an extensive discussion of the coordination chemistry of polyhydroxycarboxylates has also been presented by Peters and coworkers [67]. In the latter work, Peters explicitly discusses the linkage isomerism of polyhydroxycarboxylates with borate ion. Coordination is shown to occur only via the diol functionality in base, but in acidic solution coordination to boron occurs via one carboxylate oxygen and one hydroxyl oxygen. Therefore, by lowering the pH, the synergic metal ion binding properties of these systems can be essentially turned off. Potential environmental and industrial applications of these systems will be discussed in Chapter 7.

The relative behavior of Mg^{2+} with BT_2^{5-} is similar to its behavior with the {221} cyptand. The stability constant for Mg^{2+} / 221 cryptate formation is at least five orders of magnitude less than those for Ca^{2+} and Sr^{2+} with 221 [148]. Since metal ion cryptate chemistry is generally so clearly related to the

complementarity of cation radius with cryptand cavity size, a molecular mechanics study of BT_2^{5-} was carried out to gain some understanding of the metal ion binding site.

Metal Ion Binding Site in MBT_2^{5-}

Molecular mechanics (MM2) calculations [151] were performed on BT_2^{5-} (*l* -tartrate) in order to understand possible reasons for the metal ion specificity. The energy minimized structure is shown in Fig. 6.6a. The two carboxylate groups in each tartrate moiety are necessarily oriented on opposite sides of each borate ester ring. Simply placing a metal ion in this structure in such a way as to give the largest number oxygen donor atoms with acceptable metal - oxygen distances provides the structure shown in Fig. 6.6b for $CaBT_2^{3-}$. BT_2^{5-} functions as a terdentate ligand with Ca^{2+} being bound to two carboxylate oxygens and one borate oxygen. The Ca^{2+} - carboxylate oxygen distances are each 2.55 Å and the Ca^{2+} - borate oxygen distance is 2.43Å. Additional coordination sites on Ca^{2+} are occupied by water molecules (not shown). All other potential oxygen donor atoms are much too far away for effective coordination to Ca^{2+}.

The binding of Ca^{2+} to carboxylate groups is a subject of continuing structural investigation and several types of coordination have been described [90,152]. The Ca^{2+} / tartrate crystal structure [92] shows an eight coordinate Ca^{2+} and an average Ca^{2+} - oxygen distance of 2.47Å. Ca^{2+} - oxygen distances in the structure range from 2.39Å to 2.54Å. The proposed $CaBT_2^{3-}$ structure (Fig. 6.6b) is entirely consistent with these results. The participation

(a)

(b)

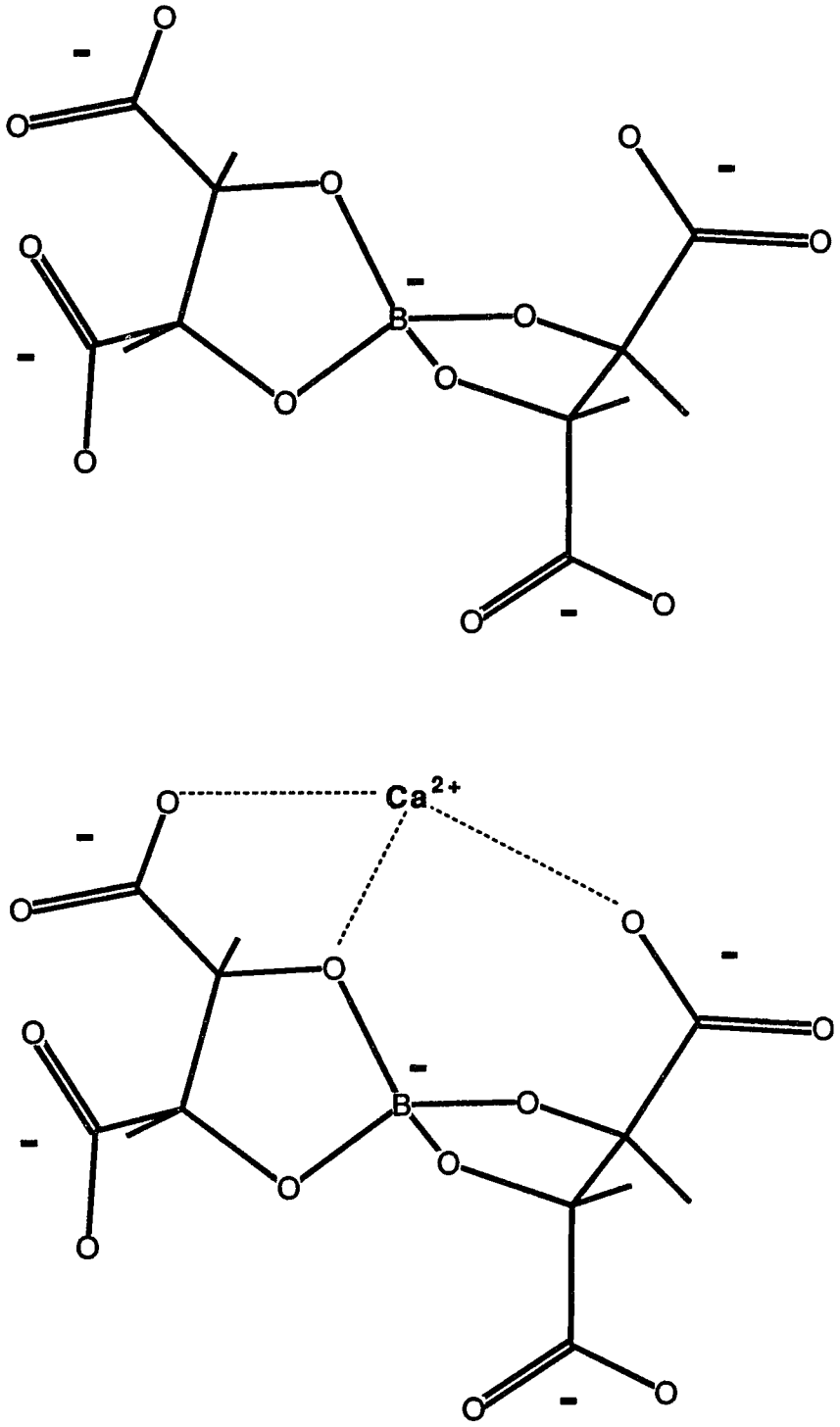

Figure 6.6: (**a**) MM2 energy minimized structure for the BT_2^{5-} (*l* - tartrate) ionophore. (**b**) Proposed terdentate Ca^{2+} binding site of BT_2^{5-} (*l* - tartrate).

of borate oxygens in metal ion coordination (Fig. 2.5a) has been shown in the crystal structure of a K^+ / boromalate complex [101]. A similar structure has been previously proposed for Na^+ / borotartrate (Fig. 2.5b) by Peters and coworkers [102]. Fig. 6.7 shows the space filling model of $CaBT_2^{3-}$ (*l* - tartrate), showing the almost ideal fit of the Ca^{2+} ion into the proposed binding cavity.

The $SrBT_2^{3-}$ complex has essentially the same structure as $CaBT_2^{3-}$, but the Sr^{2+} must be moved away slightly to accommodate its larger radius compared with Ca^{2+}. In the Sr^{2+} / tartrate crystal structure [150] the average Sr^{2+} - oxygen distance is 2.65Å. The decreased electrostatic interaction may account in part for the slight preference for Ca^{2+} over Sr^{2+} shown by BT_2^{5-}.

Given the structure of BT_2^{5-} (Fig. 6.6a) there is no way to accommodate the much smaller Mg^{2+} ion and maintain coordination to three oxygen donor atoms in BT_2^{5-}. While Ca^{2+} - oxygen distances in various carboxylate complexes show a substantial range [90] with many examples between 2.3Å and 2.6Å, the great majority of Mg^{2+} - oxygen distances fall in a much narrower range [90] between 2.0Å and 2.1Å. At these distances, Mg^{2+} coordination can occur with at most two oxygen donor atoms in BT_2^{5-} and, as a result, $MgBT_2^{3-}$ is much less stable than its Ca^{2+} and Sr^{2+} analogs. Similarly, since BT^{3-} provides only one carboxylate oxygen donor atom which is available for metal ion coordination, the various MBT^- complex ions are much less stable than the MBT_2^{3-} ternary complexes.

MM2 calculations [151] were also done on BT_2^{5-} (*meso* - tartrate). The major structural difference is that both carboxylates in each tartrate are

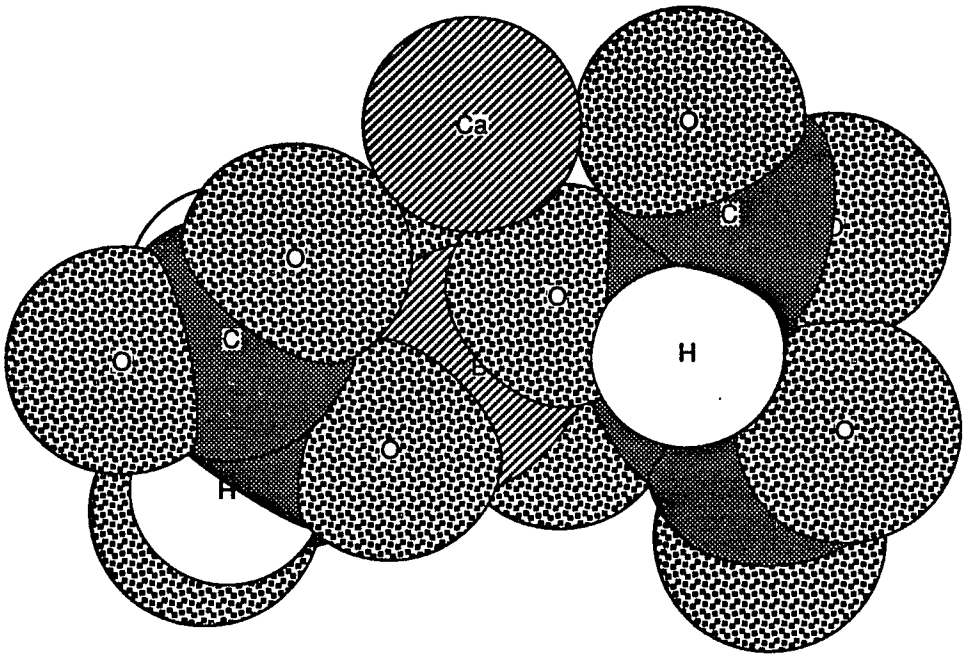

Figure 6.7: Space filling model of the $CaBT_2^{3-}$ (*l* - tartrate) ternary complex ion.

necessarily oriented on the same side of each borate ester ring. This does not change the metal ion binding site in any substantial way nor does it bring the pendant (uncoordinated) carboxylate groups appreciably closer to the metal ion. As a result there is not much difference in K_{CaBT2} for the two tartrate isomers.

Borotartrate Equilibrium Constants

Although K_2 is almost the same for *l* - tartrate and *meso* - tartrate, there is a measurable difference in K_1 with *l* - tartrate being favored by a factor of three over *meso* - tartrate. An explanation for the difference in K_2 has been presented [47] in which it is noted that greater repulsion is experienced by pendant carboxylate groups which are in a *gauche* conformation in *meso* - tartrate as opposed to an *anti* conformation in *l* - tartrate.

On the other hand, models show that interligand repulsions in BT_2^{5-} are greater in the bis *l* - tartrate complex than they are in the bis *meso* - tartrate complex. This is because the pendant carboxylates on the two tartrate ligands are necessarily quite far from one another in BT_2^{5-} (*meso* - tartrate), but there is at least one close approach of carboxylate groups on different tartrates in BT_2^{5-} (*l* - tartrate). The greater interligand repulsion in BT_2^{5-} (*l* - tartrate) may account for the fact that K_2 values for *l* - tartrate and *meso* - tartrate are quite similar.

Complex Stoichiometry

Over the range of concentrations we have used, only one metal ion is bound per BT_2^{5-} complex ion. This is supported directly by the results for Ca^{2+}

presented in Fig. 6.4. The solid lines are calculated based on the stability constants determined in this study (Table 6.1). The various points shown are experimental results. [B^-], [BT^{3-}], [BT_2^{5-}] and [$CaBT_2^{3-}$] are determined from the ^{11}B NMR integration and mass balance as described previously. K_{MT} and mass balance are used to determine [CaT] and [Ca^{2+}]. The excellent agreement between calculation and experiment validates the reaction scheme and the stability constants.

NMR Chemical Shifts

At low pH (~2) the borotartrate complex ion has tartrate ligands which are coordinated to the boron center via one carboxylate oxygen and one α-hydroxyl oxygen [28,67]. This complex ion has a chemical shift of -9.4 ppm. In this species the boron nucleus experiences a more shielded environment (upfield shift) compared with the BT_2^{5-} complex in base which is coordinated exclusively via the 2,3 diol linkage (-8.5 ppm). This shows that the ^{11}B NMR chemical shift of the 1:2 (BT_2^{5-}) complex is sensitive to changes in the electronic environment of the boron nucleus. The observed downfield metal ion induced shift found in Fig. 6.3 is in accord with these ideas. Coordination of M^{2+} by BT_2^{5-} removes electron density from the boron center, leaving it more deshielded in MBT_2^{3-} relative to BT_2^{5-}. In general the ^{11}B NMR chemical shift gives an accurate picture of the electronic environment of the boron center in these systems, with upfield shifts corresponding to a more shielded environment. An experimental correlation between ^{11}B NMR chemical shift and apparent charge density at the boron center has been documented [57].

6.4 Conclusion

In this work, the first quantitative analysis of metal ion binding by borotartrate complexes is presented. The conclusions of this study are: 1) Mg^{2+} binds preferentially to free tartrate, T^{2-}, and shows little if any interaction with the borotartrate complex ions (BT^{3-} and BT_2^{5-}); 2) Both Ca^{2+} and Sr^{2+} bind preferentially to BT_2^{5-} with Ca^{2+} binding slightly better than Sr^{2+}; 3) The proposed Ca^{2+} and Sr^{2+} binding site on BT_2^{5-} is one in which M^{2+} is coordinated to two carboxylate oxygens (one from each of the tartrate ligands) and one borate ester ring oxygen; 4) The observed metal ion specificity of the BT_2^{5-} complex ($Mg^{2+} <<< Ca^{2+} > Sr^{2+}$) is consistent with such a binding site; and, 5) The absolute configuration of the ligand (*l* - tartrate vs. *meso* - tartrate) does not significantly alter the binding properties of BT_2^{5-}.

CHAPTER 7

Conclusions, Areas of Further Work and Selected Applications

7.1 Conclusions

Throughout this thesis, the application of both ^{1}H and ^{11}B NMR to the study of boron acid complexation reactions has been demonstrated. We have shown variable temperature FTNMR to be a reliable technique for the determination of thermodynamic parameters ($\Delta H°$ and $\Delta S°$) for the complexation reactions of borate with a wide range of ligands [39,40]. These thermodynamic studies have led to certain conclusions regarding boron acid complexation reactions that were not previously contained in the literature. Our results for the reactions of aliphatic diols with various borate ions (B^-, ϕB^-, CH_3B^- and BD^-) show that all of these reactions are quite similar. The reactions are all exothermic with an average value of $\Delta H° \sim -20$ kJ / mol. All of the entropy changes are quite negative ($\Delta S° \sim -60$ J / mol K) and this can be attributed to the loss of ligand configurational entropy on complexation overriding the positive contribution to the entropy provided by the chelate effect [153]. It seems as though the wide variation in the previously reported thermodynamic parameters for borate / aliphatic 1,2 diol reactions has obscured the fact that these reactions are all very similar thermodynamically.

The thermodynamic parameters for borate complexation reactions with α-hydroxy carboxylic acids and dicarboxylic acids have not been previously reported in the literature. Our results [40] show that the large increase in K_1 for

α-hydroxy carboxylic acids compared with K_1 for the reaction of borate with diols is entirely due to a much more favorable $\Delta H°$. In marked contrast to that of the diols, the second complexation reaction here is emphatically different from the first. K_2 is much smaller than K_1 and extremely large differences in both $\Delta H°$ and $\Delta S°$ are observed.

The borate / oxalic acid system is the only system which has a much more positive $\Delta S°$ for the first complexation step and does not form a second complex at all. The results of all of these thermodynamic studies as well as those presented for the formation of mixed ligand complexes show the important effect the first ligand can have on subsequent bis complex formation. The deactivating potential of the first ligand on the reactivity of the boron center increases with the number of electron withdrawing carboxylate groups coordinated in the 1:1 complex. This effect reaches a maximum in the case of oxalic acid where BOx^- is completely unreactive with H_2Ox and only slightly reactive with other ligands. Many of these thermodynamic results can be explained by the significant differences found in boron - oxygen bonds of the various borates as determined by (AM1) calculations [82].

Since both variable temperature ^1H and ^{11}B NMR spectroscopy have now been shown to be accurate and reliable methods for the determination of thermodynamic parameters for these simple complexation reactions, the technique could be easily extended to more complicated ligands as well as biochemically important systems involving borate ions [154].

The metal ion binding study conducted for the ternary M^{2+} / borate / tartrate system proved to be very successful. We have shown that Mg^{2+} binds preferentially to free tartrate, T^{2-}, and shows little if any interaction with the

borotartrate complex ions (BT^{3-} and BT_2^{5-}). Ca^{2+} and Sr^{2+}, on the other hand, show a large preference for coordination to BT_2^{5-} compared to BT^{3-} or free tartrate (T^{2-}). We were able to quantitatively model both the Ca^{2+} and Sr^{2+} systems with *l* - tartrate and the Ca^{2+} system with *meso* - tartrate to determine the stability constants for metal ion binding by the BT_2^{5-} ionophore. Ca^{2+} binding is slightly preferred to Sr^{2+} binding by BT_2^{5-} (*l* - tartrate). Ca^{2+} binding to BT_2^{5-} (*l* - tartrate) and BT_2^{5-} (*meso* - tartrate) are almost identical.

A Ca^{2+} and Sr^{2+} binding site on the BT_2^{5-} complex is proposed in which the metal ion is coordinated to two carboxylate oxygens (one from each of the tartrate ligands and one borate ester ring oxygen). Both the observed metal ion specificity of the BT_2^{5-} complex ($Mg^{2+} <<< Ca^{2+} > Sr^{2+}$) and the fact that the absolute configuration of the ligand does not significantly alter the binding properties of BT_2^{5-} are consistent with this proposed binding site.

7.2 Areas of Further Research

A quantitative study of the interaction between borate and bifunctional ligands such as *d, l* - glyceric acid (shown below) as a function of pH would be a logical next step to the thermodynamic studies presented in this thesis. In

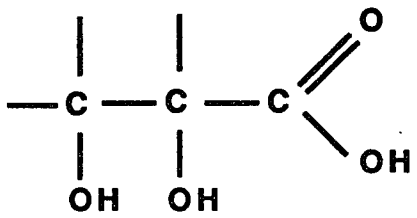

d, l - glyceric acid

acidic solution, *d, l* - glyceric acid has been shown [51] to coordinate to borate predominately via the α-hydroxy carboxylate linkage. The stability constants and thermodynamic parameters for both the 1:1 and 1:2 complexation reactions under these conditions are expected to be very similar to those of the borate / lactic acid system already studied. At high pH, *d, l* - glycerate is known [51] to coordinate to borate exclusively via the diol linkage. The stability constants and thermodynamic parameters under these conditions are expected to be very similar to those of the borate / 1,2-propanediol system.

It is at intermediate pH where these systems really become interesting from a kinetic as well as thermodynamic perspective. As the solution pH is increased in this intermediate region, a pH sensitive isomerization takes place for both the 1:1 and 1:2 complexes (shown below) in which the borate either slides or rotates one carbon down the ligand chain, from a hydroyxl / carboxyl linkage to a hydroxyl / hydroxyl linkage displacing either one or two protons

(H^+) as shown below. Since these isomerization reactions are accompanied by

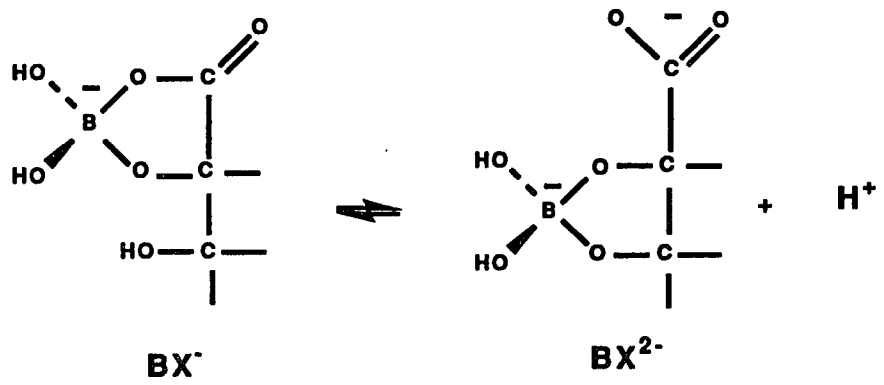

BX^- BX^{2-}

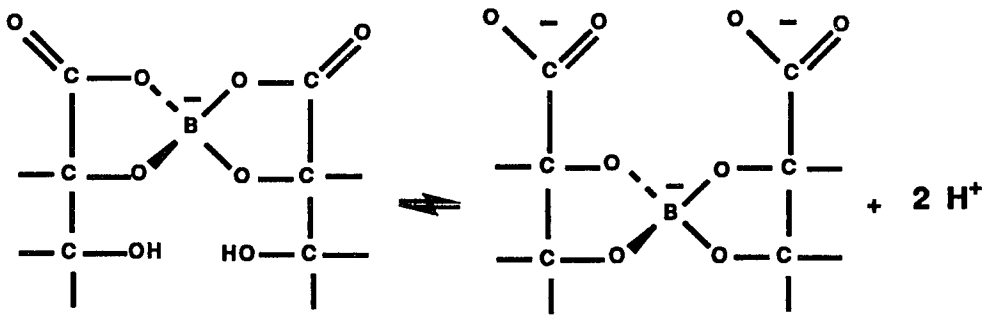

BX_2^- BX_2^{3-}

loss of H^+, the complexes in their low pH form (left hand side) can be considered weak acids with measurable pK_a's. In the case of the isomerization of the bis complex (BX_2^-) it would be quite interesting to see if the solution pH could be fine tuned to detect the half isomerization species BX_2^{2-}. BX_2^{2-} can be

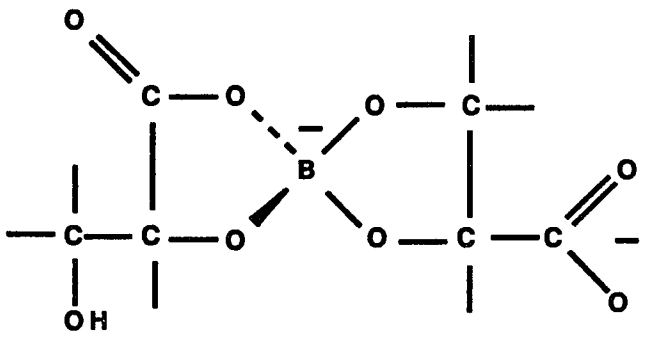

BX_2^{2-}

described as an intramolecular mixed ligand complex. This complex, which is expected to be similar in stability to the mixed ligand complex BLP^- already studied, may not be easy to detect in aqueous solution depending on the spectral resolution and the rate of isomerization. The stability constants and thermodynamic parameters for such a system could be studied by ^{11}B NMR spectroscopy, while the kinetics would probably be best studied using a relaxation method such as temperature-Jump.

A second area of research currently under investigation in this laboratory is a kinetic study of the borate / 1,2 propanediol system at high pH. This work is important because it would be the first kinetic study to include bis complex formation in alkaline media. Although much kinetic data have already been acquired for this system using the T-jump technique [155], no complete mathematical analysis of the system has been conducted yet.

One of the problems associated with this analysis is that it may be necessary to treat the boric acid / borate interconversion (shown below) as being non-diffusion controlled, as was the case in the kinetic analysis of the

$$B(OH)_3 + OH^- \leftrightarrow B(OH)_4^-$$

phenylboronic acid / 1,2 ethanediol system studied by Tihal[36]. In that work, a rate constant approximately three orders of magnitude lower (10^4 $M^{-1}s^{-1}$) than that proposed in the literature (1.1×10^7 $M^{-1}s^{-1}$) [156] was necessarily used for the trigonal / tetrahedral interconversion on phenylboronic acid. This lower value was required in order to obtain a reasonable fit of the proposed mechanism to the experimentally determined relaxation times.

Since an accurate determination of the rate constant for the trigonal / tetrahedral interconversion of boron acids is so important to any boron acid complexation study at high pH, a critical experiment which must be conducted in the future is to independently measure the addition of hydroxide to boron acids under the same experimental conditions used for the overall kinetic analysis. It may be possible to study this interconversion directly using substituted boron acids which absorb or emit in the UV using either UV or fluorescence T-jump. We have already shown that both phenylboronic acid and *meta* -nitrophenylboronic acid have large shifts in the wavelengths of absorbance and emission (>50nm) associated with the trigonal / tetrahedral interconversion on the boron center. It may also be possible to study this reaction in the absence of any indicator using the pressure-jump method.

Another area of interest which follows directly from the metal ion binding studies described in this thesis would be to conduct a kinetic study of metal ion binding by bis borotartrate (BT_2^{5-}) complexes. It may be possible to study these reactions directly by conducting a ^{11}B NMR line width analysis of the 1:2 peak in ternary M^{2+} / borate / tartrate systems (Fig. 6.3 p 158) in order to determine the metal ion exchange rate between MBT_2^{3-} and BT_2^{5-}.

$$MBT_2^{3-} + BT_2^{5-} \leftrightarrow BT_2^{5-} + MBT_2^{3-}$$

It may be possible to study the kinetics of these metal ion complexation reactions using the T-jump technique with calmagite as the metal ion indicator.

$$M^{2+} + BT_2^{5-} \leftrightarrow MBT_2^{3-}$$

$$M^{2+} + In' \leftrightarrow MIn^{-}$$

7.3 Selected Applications

Molecular recognition of carbohydrates and other polyhydroxy compounds by boron acids has been the subject of much recent interest [157-160]. The basis of the recognition is the formation of covalent bonds between the boron acid and appropriately oriented hydroxyl groups on the ligand. One problem associated with the use of boron acids for this purpose is that they interact with diol functions only at high pH (>9). This can be a problem in studies which involve pH sensitive ligands or studies which must be conducted at physiological pH (pH =7.2). We have shown that borate forms only 1:1 complexes with oxalic acid regardless of ligand concentration. We have also shown that the 1:1 complex (BOx^-) reacts with diols (H_2D) to form the mixed ligand complex $BDOx^-$ at near neutral pH.

$$BOx^- + H_2D \leftrightarrow BDOx^- + 2\,H_2O$$

The mixed ligand complex ($BDOx^-$) is easily detected by ^{11}B NMR and can be used qualitatively to detect appropriately oriented diol functions on the ligand of interest. The combination of the simplicity of the technique with its greater pH range may lead to the application of this technique to the study of certain pH sensitive ligands.

Recently, the allosteric interaction of metal ions with 1:1 diboronic acid - saccharide complexes was studied using circular dichroism spectrophotometry [161]. This study shows the powerful effect borate coordination can have on the binding properties of a particular ligand. Borate coordination could induce a conformational change in the ligand which either activates or deactivates a

non-overlapping binding site. Ca^{2+} and Sr^{2+} binding by BT_2^{5-} could be viewed as a positive allosteric interaction in which the borate acts to greatly enhance the metal ion binding properties of tartrate. There are many macromolecular ligands containing polyhydroxyl groups whose binding properties may be dramatically affected by borate coordination. In fact, the role of trace amounts of boron in the body is usually associated with the allosteric effect of borate on biologically important molecules. Many of these systems could be easily studied using the ^{11}B NMR techniques discussed in this thesis.

The application of synergic metal ion binding by borate-polyhydroxycarboxylate systems to biochemical, environmental and industrial problems has been discussed in the literature for some time [69, 96, 99-100]. Two of the possible applications of these systems are included here.

Calcium supplements. The tremendous increase in public awareness of the importance of calcium to the skeletal system in the prevention of such debilitating diseases as osteoporosis [162] has led to an huge influx of calcium supplements on the market. While there is general agreement concerning the importance of calcium metabolism in the body, the most effective method of calcium absorption and retention is far from undisputed.

Calcium compounds typically used in supplements fall into two categories. The first one is inorganic salts, such as calcium carbonate, calcium phosphate and calcium silicate. In the second category, calcium is chelated to organic ligands such as citrate, gluconate, pantothenate and stearate which all contain oxygen donor groups. Typically, these organic ligands also have an affinity for other biologically important divalent cations such as Mg^{2+} and Zn^{2+}. Therefore, the absorption of calcium complexes affects the delicate balance of

Ca^{2+} with other minerals in the body.

Ca^{2+} supplements which contain calcium salts of polyhydroxy carboxylates such as glucarate or tartrate in conjunction with small amounts of either calcium or potassium borate may allow for an increased absorption of calcium by the body. A formulation such as this may increase Ca^{2+} intake without greatly affecting the Mg^{2+} and Zn^{2+} levels in the body due to the selective interaction of Ca^{2+} with 1:2 borate complexes. The application of calcium borogluconate solutions in the treatment of acute hypocalcaemia has been known in veterinary science for over fifty years [96]. It is interesting to note that there are several boron supplements on the market. One such supplement, *Triboron*, manufactured by Twin Laboratories contains boron citrate, boron asparate and boron glycinate. The deficiency of trace amounts of boron in the diet has recently been correlated to the loss of Ca^{2+} and Mg^{2+} in the urine [163]. This condition can lead to the onset of osteoporosis. Although the exact function of boron in Ca^{2+} and Mg^{2+} metabolism is unknown at this time, it is quite possible that borate synergically enhances the binding and transport of Ca^{2+} by biological ligands in much the same way that it enhances the binding properties of simple tartrate ligands.

Sequestering agents. The application of the synergic metal ion coordinating ability of borate complexes of polyhdroxy carboxylates to water treatment and detergent formulations is evident in the patent literature [99, 100]. The borate ion in these systems can be envisioned as a pH sensitive template

which forms highly ionophoric species like BT_2^{5-} in basic solution. Under these conditions BT_2^{5-} acts as a powerful sequestering agent allowing the desired amount of water softening to take place so that cleaning can take place more efficiently. The sequestered metal ions can be released by the BT_2^{5-} complex at any time during the process simply by lowering the pH or diluting the solution.

In formulations of powdered laundry detergents salts of borate and polyhydroxy carboxylates could be used as builders replacing the phosphate builders of the past. These co-builders may provide the water-softening and alkalinity required without the negative environmental side effects. It is also interesting to note that the recent ban on chlorine bleach in certain products has led to the use of sodium perborate as an environmentally safer bleach substitute. Sodium perborate is hydrolyzed to borate and hydrogen peroxide in aqueous solution [164]. It is quite possible that certain products currently on the market may be inadvertently benefiting from the synergic metal ion binding properties associated with borate / polyhydroxy carboxylate systems.

References

[1] Biot, M. *Compt. Rend.* **1842**, *14*, 49.

[2] Thomson, *J. Soc. Chem. Ind.* **1893**, *12*, 432.

[3] Magnanini, G. *Z. Physik. Chem.* **1890**, *6*, 58.

[4] Magnanini, G. *Z. Physik. Chem.* **1892**, *9*, 230

[5] Magnanini, G. *Z. Physik. Chem.* **1893**, *11*, 281.

[6] van't Hoff, J.H. *The Arrangement of Atoms in Space,* **1898**, p.151.

[7] Boeseken, J.; van Rossem, A. *Rec. Trav. Chim.* **1912**, *30,* 392.

[8] Boeseken, J. *Ber.* **1913**, *46,* 2612.

[9] Boeseken, J. *Rec. Trav. Chim.* **1921**, *40,* 553.

[10] Boeseken, J. *Ber.* **1923**, *56,* 2411.

[11] Boeseken, J.; Vermaas, N. *J. Phys. Chem.* **1931**, *35,* 1477.

[12] Boeseken, J. *J. Bull. Soc. Chim.* **1933**, *53,* 1332.

[13] Boeseken, J.; Vermaas, N. *Rec. Trav. Chim.* **1935**, *54,* 853.

[14] Boeseken, J. *Rec. Trav. Chim.* **1942**, *61,* 82.

[15] Hermans, P.H. *Z. Anorg. Allgem. Chem.* **1925**, *142,* 83.

[16] Meulenhoff, J. *Z. Anorg. Allgem. Chem.* **1925**, *142,* 373.

[17] Edwards, J.O.; Morrison, G.C.; Ross, V.F.; Schultz, J.W. *J. Am. Chem. Soc.* **1955**, *77,* 266.

[18] Larson, R.; Nunziata, G. *Acta Chem. Scand.* **1970**, *24,* 2165.

[19] Larson, R.; Nunziata, G. *Acta Chem. Scand.* **1972**, *26,* 1503.

[20] Oertel, R.P. *Inorg. Chem.* **1972**,*11,* 544.

[21] Arrhenius, S.A. *Theories of Solutions,* Yale University Press: New Haven, 1912.

[22] Manov, G; Delollis, N.; Acree, S. *J. Research National Bur. Standards* **1944**, *33,* 287.

[23] Edwards, J.O.; Sederstrom, R.J. *J. Phys. Chem.* **1961**, *65,* 862.

[24] Pitzer, K.S. *J. Am. Chem. Soc.* **1937**, *59,* 2365.

[25] Coyle, T.D.; Stone, F.G. *Progress in Boron Chemistry* **1964**, *1*, 83.

[26] Lanthier, G.F.; Graham, W.A.G. *Chem. Commun.* **1968**, 715.

[27] Cotton, F.; Wilkinson, G. *Basic Inorganic Chemistry;* Wiley: New York; 1976, p.233.

[28] Kustin, K.; Pizer, R. *J. Am. Chem. Soc.* **1969**, *91,* 317.

[29] Freidman, S.; Pizer, R. *J. Am. Chem. Soc.* **1975**, *97,* 6059.

[30] Lorber, G.; Pizer, R. *Inorg.Chem.* **1976**, *15,* 978.

[31] Friedman, S.; Pace B.; Pizer, R. *J. Am. Chem. Soc.* **1974**, *96,* 5381.

[32] Babcock, L.; Pizer, R. *Inorg. Chem.* **1980**, *19,* 56.

[33] Babcock, L.; Pizer, R. *Inorg. Chem.* **1977**, *16,* 1677.

[34] Pizer, R.; Selzer R. *Inorg. Chem.* **1984**, *23,* 3023.

[35] Pizer, R.; Tihal, C. *Inorg. Chem.* **1992**, *31,* 3243.

[36] Tihal, C. Ph.D. Thesis; *Boron Acid Complexation Reactions in Basic Solution;* CUNY Press: New York, **1991**, Ch. 5.

[37] Antikainen, P.J. *Acta Chem. Scand.* **1955**,*9,* 1008.

[38] Roy, G.L.; Laferriere, A.L.; Edwards, J.O. *J. Inorg. Nucl. Chem.* **1957**, *4,* 106.

[39] Pizer, R.; Ricatto, P.J.; Tihal, C. *Polyhedron* **1993**, *12,* 2137.

[40] Pizer, R.; Ricatto, P.J.; *Inorg. Chem.* **1994**,*33,* 2402.

[41] Conner, J.M.; Bulgrin, V.C. *J. Inorg. Nucl. Chem.* **1967**, *29,* 1953.

[42] Paál, T.; Barcza, L. *Acta Chim. Acad.Sci.Hung.* **1975**, *85,* 147.

[43] Paál, , T. *Acta Chim. Acad. Sci. Hung.* **1977**, *95,* 31.

[44] Henderson, W.G.; How, M.J.; Kennedy, G.R.; Mooney E.F. *Carbohydr. Res.* **1973**, *28,* 1.

[45] Dawber, J.G.; Green, S.I.E. *J. Chem. Soc., Faraday Trans. 1* **1986**, *82,* 3407.

[46] Dawber, J.G.; Green, S.I.E.; Dawber, J.C.; Gabrail, S. *J. Chem. Soc., Faraday Trans. 1* **1989**, *84,* 41.

[47] van Duin, M.; Peters, J.A.; Kieboom, A.P.G.; van Bekkum, H. *Tetrahedron* **1985**, *41*, 3411.

[48] Oi,T.; Takeda, T.; Kakihana, H. *Bull. Chem. Soc. Jpn.* **1992**, *65,* 1903.

[49] Antikainen, P.J.; Kauppila, A. *Suomen Kemistilehti, B* **1959**, *32,* 141.

[50] Antikainen, P.J.; Pitkanen, I.P. *Suomen Kemistilehti, B* **1968**, *41,* 65.

[51] van Duin, M.; Peters, J.A.; Kieboom, A.P.G.; van Bekkum, H. *Tetrahedron* **1984**,*40* , 2911.

[52] Levine, I.N. *Physical Chemistry,* 2nd Ed. McGraw Hill: New York, 1983, p.178.

[53] Aruga, R. *Talanta* **1985**, *32,* 517.

[54] Antikainen, P.J. *Suomen Kemistilehti, B* **1957**, *30,* 185.

[55] Evans, W.J.; Frampton, V.L; French, A.D. *J. Phys. Chem.* **1977**, *81,* 1810.

[56] D'Silva, C.; Green, D. *J. Chem. Soc., Chem. Commun.* **1991**, 227.

[57] Schaeffer, R. In *Progress in Boron Chemistry* Steinberg, H.; McCloskey, A.L., Eds.; Macmillian: New York, 1964; Vol. 1, Ch. 10.

[58] Emsley, J.; *The Elements;* Clarendon Press: Oxford, 1989.

[59] Akitt, J.W. *NMR and Chemistry;* Chapman & Hall: London, 1992; Ch. 1.

[60] How, M.J.; Kennedy, G.R.; Mooney, E.F. *J. Chem. Soc., Chem. Commun.* **1969**, 267.

[61] How, M.J.; Kennedy, G.R. *Carbohydr. Res.* **1973**, *28,* 13.

[62] Makkee, M.; Kieboom, A.P.G.; van Bekkum, H. *Recl. Trav. Chim. Pays-Bas* **1985**,*104*, 230.

[63] van Duin, M.; Peters, J.A.; Kieboom, A.P.G.; van Bekkum, H. *Recl. Trav. Chim. Pays-Bas* **1986**,*105*, 488.

[64] van Duin, M.; Peters, J.A.; Kieboom, A.P.G.; van Bekkum, H. *Magn. Res. Chem.* **1986**,*24*, 832.

[65] van Duin, M.; Peters, J.A.; Sinnema, A.; Kieboom, A.P.G.; van Bekkum, H. *Recl. Trav. Chim. Pays-Bas* **1987**,*106*, 495.

[66] van Haveren, J.; Peters, J.A.; Batelaan, J.G.; Kieboom,A.P.G.; van Bekkum, H. *Recl.Trav.Chim. Pays-Bas* **1989**,*108*, 179.

[67] van Duin, M.; Peters, J.A.; Kieboom, A.P.G.; van Bekkum, H. *Recl. Trav. Chim. Pays - Bas.* **1989**,*108*, 57.

[68] van den Berg, R.; Peters, J.A.; van Bekkum, H. *Carbohydr. Res.* **1994**, *253*, 1.

[69] van Duin, M.; Peters, J.A.; Kieboom, A.P.G.; van Bekkum, H. *Carbohydr. Res.* **1987**,*162*, 65.

[70] van Duin, M.; Peters, J.A.; Kieboom, A.P.G.; van Bekkum, H. *J. Chem. Soc., Perkin Trans.2* **1987**, 473.

[71] van Duin, M.; Peters, J.A.; Kieboom, A.P.G.; van Bekkum, H. *J. Chem. Soc., Dalton Trans.* **1987**, 2051.

[72] van Haveren, J.; Peters, J.A.; Batelaan, J.G.; Kieboom, A.P.G.; van Bekkum, H. *J. Chem. Soc., Dalton Trans.* **1991**, 2649.

[73] van Haveren, J.; van den Burg, M.H.B. ; Peters, J.A.; Batelaan, J.G.; Kieboom, A.P.G.; van Bekkum, H. *J. Chem. Soc., Perkin Trans. 2* **1991**, 321.

[74] van Haveren, J.; Peters, J.A.; Batelaan, J.G.; van Bekkum, H. *Inorganica Chimica Acta* **1992**,*192*, 261.

[75] Venema, F.R.; Peters, J.A.; van Bekkum, H. *Recl. Trav. Chim. Pays - Bas* **1993**, *112*, 445.

[76] van Haveren, J.; Lammers, H.; Peters, J.A.; Batelaan, J.G.; van Bekkum, H. *Carbohydr. Res.* **1993**, *243*, 259.

[77] Salentine, C.G. *Inorg. Chem.* **1983**, *22*, 3920.

[78] Balz, R.; Brandle, U.; Kammerer,E.; Kohnlein, D.; Lutz, O.; Nolle, A.; Schafitel, R.; Veil, E. *Z. Naturforsch.* **1986**, *41a*, 737.

[79] Blackborow, R.J. *J. Chem. Soc., Dalton Trans.* **1973**, 2139.

[80] Adebodun, F.; Jordan, F. *J. Am. Chem. Soc.* **1988**, *110*, 309.

[81] Baldwin, J.E.; Claridge, T.D.; Derome, A.E.; Smith, B.D.; Twyman, M.; Waley, S.E. *J. Chem. Soc., Chem. Commun.* **1991**, 573.

[82] (a) Jacobson, S.; Pizer, R. *J. Am. Chem. Soc.* **1993**, *115*, 11216.

(b) QCPE program 506 by the Dewar research group and J.J.P. Stewart. Obtained from QCPE, Indiana University, Bloomington, IN.

(c) *HyperChem Reference*; Autodesk, Inc.; 1992; Ch.7.

[83] Seel, C; Vogtle, F. In *Perspectives in Coordination Chemistry;* Williams, A.F.; Floriani, C.; Merbach, A.E., Eds.; VCH: Weinheim, 1992; p.31.

[84] Raymond, K.N.; Muller, G.; Matzanke, B.F. *Top. Curr. Chem.* **1984**, *123*, 49.

[85] Seel, C. Vogtle, F. *Angew. Chem. Int. Ed. Engl.* **1992**, *31*, 528.

[86] Pizer, R.; Selzer, R. *Inorg. Chem.* **1983**, *22*, 1359.

[87] Loyola, V.M.; Wilkins, R.G.; Pizer, R. *J. Am. Chem. Soc.* **1975**, *97*, 7382.

[88] Pizer, R. *J. Am. Chem. Soc.* **1978**, *100*, 4239.

[89] Loyola, V.M.; Pizer, R.; Wilkins, R.G. *J. Am. Chem. Soc.* **1977**, *99*, 7185.

[90] Einspahr, H.; Bugg, E. In *Metals Ions in Biological Systems;* Siegel, H., Ed.; Marcel Dekker: New York, 1984, Vol. 17, Ch. 2.

[91] Reference 90; pp. 57-66.

[92] Ambady, G.K. *Acta. Cryst.* **1968**, *B24*, 1548.

[93] Doxsee, K.; Ferguson, C.M.; Walsh, P.L.; Saulsbery, R.L. *J. Org. Chem.* **1993**, *58,* 7557.

[94] Aruga,R. *Inorg. Chem.* **1980**, *19* , 2895.

[95] Bal, W.; Drake, A.F.; Malgorzata, J.; Kozlowski, H.; Pettit, L.; Sadler, P.J. *J. Chem. Soc., Chem. Commun.* **1944**, 555.

[96] Macpherson, H.T.; Stewart, J. *Biochemical Journal* **1938**, *32,* 76.

[97] Kereichuk, A.S.; Mokhnatova, N.V. *Russ. J. Inorg. Chem.* **1976**, *21,* 651.

[98] Nieuwenhuizen, M.S.; Kieboom, A.P.G.; van Bekkum, H. *J. Am. Oil Chem. Soc.* **1983**, *60,* 120.

[99] Peters, H.; Neth. P. 219949 / **1961** (*Chem. Abstr.* **1961**, *56,* 12682.)

[100] Heesen, J.G.; Neth. P. 76-15,180 / **1972** (*Chem. Abstr.* **1974**, *81*, 176040.)

[101] Mariezcurrena, R.A.; Rasmussen, S.E. *Acta Cryst.* **1973**, *B29*, 1035.

[102] van Koningsveld, M. van Duin, M.; Jansen, J.C.; "refinement of the structure in progress", as referenced in [70].

[103] Jensen, W.B. *The Lewis Acid Base Concepts;* Wiley: New York; 1980, p 251.

[104] Brown, P.L.; Sylva, R.N.; Ellis, J. *J. Chem. Soc., Dalton Trans.,* **1985**, 723.

[105] Midgley, D. *Chem. Soc. Rev.*, **1975**, *4*, 547.

[106] Shannon, R.D. *Acta Cryst. , Sect. A* **1976**, *32*, 751.

[107] Eigen, M. *Pure Appl Chem.* **1963**, *6*, 105.

[108] Venema, F.R.; Peters, J.A.; van Bekkum, H. *Inorg. Chim. Acta* **1992**, *191*, 261.

[109] Venema, F.R.; Peters, J.A.; van Bekkum, H. *Inorg. Chim. Acta* **1992**,*197*, 1.

[110] Davies, C.W. *J. Chem. Soc.* **1938**, 2093.

[111] (a) A.F. Series FT - NMR. BVT - 1000 Varible Temperature Unit Users Guide, IBM Instruments, Inc.: Danbury, CT, 1983.

(b) Bruker, BVT - 1000 - ER4111VT Instruction Manual, Bruker Instruments, Inc.: Billerica, MA, 1983.

[112] (a) van Geet, A. *Anal Chem.* **1968**, *40*, 2227.

(b) van Geet, A. *Anal. Chem.* **1970**, *42*, 679.

[113] (a) Nonweiler, T.R.F. *Computational Mathematics*; Wiley: New York, 1984; p. 164.

(b) Vandergraft, J.S. *Introduction to Numerical Computations;* Academic Press: New York, 1978; p 234.

[114] Kodama, M. Miyamoto, K. *Bull Chem. Soc. Jpn.* **1969**, *42*, 835.

[115] Nakagawa, G.; Wada, H. Fujita, Y. *Bull Chem. Soc. Jpn.* **1973**, *46*, 489.

[116] Laitinen, H.; Harris, W. *Chemical Analysis*; McGraw - Hill: New York, Second Edition; 1975; p201.

[117] Frydman, M.; Sillen, L.G.; Hogfeldt, E.; Ferri, D. *Chemica Scripta* **1976**, *10*, 152.

[118] Elmagadam, M. *M.A. Thesis*, Brooklyn College, 1994.

[119] Vermaas,N. *Recl. Trav. Chim. Pays-Bas* **1932**, *51*, 955.

[120] Yoshino, K.; Kotaka, M. ; Okamoto, M.; Kakihana, H. *Bull Chem. Soc. Jpn.* **1979**, *52*, 3005.

[121] Babcock, L.; Pizer, R. *Inorg. Chem*. **1983**, *22*, 174.

[122] Pizer, R. *Inorg. Chem.* **1984**, *23*, 3027.

[123] Ingri, N. *Acta Chem. Scand.* **1962**, *16*. 439.

[124] Reference 36, p112.

[125] Nagata, K.; Umayahara, A.; Tsuchiya, R. *Bull. Chem. Soc. Jpn.* **1965**, *38*, 1059.

[126] Vasil'ev, V.; Shekhanova, L.; Kochergina, L. J. *Chem. USSR (Engl. Transl.)* **1976**, *46*, 729 (730).

[127] Daniele, P.; Rigano, C.; Sammartano, S. *Thermochim. Acta* **1981**,*45*, 103.

[128] Young, H.D. Statistical Treatment of Experimental Data; McGraw-Hill: New York, 1962; p146.

[129] See also Reference [40], note (22).

[130] Searle, M.S.; Williams, D.H. *J. Am. Chem. Soc.* **1992**, *114*, 10690.

[131] Searle, M.S.; Williams, D.H.; Gerhard, U. *J. Am. Chem. Soc.* **1992**, *114*, 10697.

[132] Mohr, S.; Heller, G.; Timper, U.; Woller, K.-H. *Z. Naturforsch.* **1990**, *45b*, 308.

[133] (a) Dewar, M.J.S.; Zoebisch, E.G.; Healy, E.F.; Stewart, J.J.P. *J. Am. Chem. Soc.* **1985**,*107*, 3902.

(b) Dewar, M.J.S.; Jie, C.; Zoebisch, E.G. *Organometallics* **1988**,*7*, 513.

[134] Levine,I.N. *Quantum Chemistry*, 4th Ed.; Prentice-Hall: Englewood Cliffs, NJ, 1991; Chapter 17.

[135] Stewart, J.J.P. *J. Comput. Chem.* **1989**, *10*, 221.

[136] Stewart, J.J.P. *J. Comput. Chem.* **1990**, *11*, 543.

[137] Attina, M.; Cacace, F.; Ricci, A.; Grandinetti, F.; Occhiucci,G. *J. Chem. Soc.,Chem Commun.* **1991**, 66.

[138] Christ, C.L.; Clark, J.R.; Evans, H.J. *Acta Cryst*. **1958**, *11*, 761.

[139] Attina, M.; Cacace, F.; Occhiucci, G.; Ricci, A. *Inorg. Chem.* **1992**, *31*, 3114.

[140] Corazza, E.; Menchetti, S.; Sabelli, C. *Acta Cryst*. **1975**, *B31*, 1993.

[141] (a) Pizer, R.; Widroff, J. unpublished results.

(b) Dominique, A. *M.A. Thesis*, Brooklyn College, 1993.

[142] Solans, X.; Aguilo, M.; Gleizes, A.; Faus, J.; Julve, M.; Verdaguer, M. *Inorg. Chem.* **1990**, *29*, 775.

[143] Westcott, S.A.; Blom, H.P.; Marder, T.B.; Baker, R.T.; Calabrese, J.C. *Inorg. Chem.* **1993**, *32*, 2175.

[144] (a) Liotard, D.; Hawkins, G.D.; Lynch, G.C.; Giessen, D.; Storer, J.;. Cramer, C.J.; Truhlar, D.G. 207th American Chemical Society meeting, March 1994, San Diego, CA (PHYS 37).

(b) Zerner, M.C. 207th American Chemical Society meeting, March 1994, San Diego, CA (PHYS 36).

[145] Midgley, D. *J. Chem. Soc., Dalton Trans.* **1991**, 1585.

[146] Martell, A.E.; Smith, R.E. *Critical Stability Constants* ; Plenum: New York , 1977; Vol. 3.

[147] Martell, A.E.; Smith, R.E. *Critical Stability Constants*; Plenum: New York, 1989, Vol. 6, p 341.

[148] Lehn,J.M.; Sauvage, J.P. *J. Am. Chem. Soc.* **1975**, *97*, 6700.

[149] Reference [116], p194.

[150] Pearce, K. N. *Aust. J. Chem.* **1980**, *33*, 1511.

[151] (a) Burkert, U.; Allinger, N.L. *Molecular Mechanics* ; American Chemical Society: Washington, D.C. 1982.

(b) *CSC Chem3D Plus User's Guide*; Cambridge Scientific Computing, Inc.: Cambridge, MA, 1993; Ch. 7.

[152] (a) Hodgson, D.J.; Asplund, R.O. *Inorg. Chem.* **1990**, *29*, 3612.

(b) Einspahr, H.; Bugg, C.E. *Acta Crystallogr., Sect. B* **1981**, *37*, 1044.

[153] Reference [27], p 143.

[154] Beattie, J.H.; Weersink. E. *J. Inorg. Biochem.* **1992**, *46*, 153.

[155] Pizer, R.; Ricatto, P.J.; Tihal, C.A. unpublished results.

[156] Watson,G.; Mallo, P.; Candau, S.J. *J. Phys. Chem.* **1984**, *88*, 3301.

[157] Burgess, K.; Pote, A. M. *Angew. Chem. Int. Ed. Engl.* **1994**, *33*, 1182.

[158] Mori, Y.; Kohchi, Y.; Suzuki, M.; Furukawa, H. *J. Am. Chem. Soc.* **1992**, *114*, 3557.

[159] Shinkai, S.; Tsukagoshi, K.; Ishikawa, Y.; Kunitake, T. *J. Chem. Soc., Chem. Commun.,* **1991**, 1039.

[160] Soundararajan, S.; Badawi, M.; Kohlrust, C. M.; Hageman, J.H. *Analytical Biochem.* **1989**, *178*, 125.

[161] Deng, G.; James, T.D.; Shinkai, S. *J. Am. Chem. Soc.* **1994**, *116,* 4567.

[162] Aloia, J. *Osteoporosis;* Leisure press: Champaign, Illinois; 1989, p 53.

[163] Nielsen, F.H.; Hunt, C.D.; Mullen, L.M.; Hunt, J.R. *FASEB J.* **1987**, *1*, 394.

[164] Pizer,R.; Tihal, C. *Inorg. Chem.* **1987**, *28*, 3639.